Molecular Mechanisms Regulating Calretinin Expression in Malignant Pleural Mesothelioma

---

Dissertation

zur

Erlangung der naturwissenschaftlichen Doktorwürde
(Dr. sc. nat.)

vorgelegt der

Mathematisch-naturwissenschaftlichen Fakultät

der

Universität Zürich

von

Jelena Kresoja

aus

Serbien

Promotionskommission

Prof. Dr. Beat W. Schäfer (Vorsitz)

PD Dr. Emanuela Felley-Bosco (Leitung der Dissertation)

Prof. Dr. Beat Schwaller

Prof. Dr. Lukas Sommer

Prof. Dr. Rolf A. Stahel

Zürich, 2017

“The complexity of an organism is primarily determined by the variety of gene regulation mechanisms, rather than by the number of genes [1].”

TABLE OF CONTENTS

1. SUMMARY

Malignant pleural mesothelioma (MPM) is a poor-prognosis tumor that arises from mesothelial cells lining the lungs and thoracic cavity. The primary cause of MPM is inhalation of asbestos fibers, a naturally occurring mineral that was massively mined and used in industry throughout the 20th century due to its excellent heat- and acid-resistant properties. This resulted in the exposure of a substantial number of people. Mesothelioma is further categorized into three histological subtypes, and each of these types is associated with different patient survival outcome. The *epithelioid* histotype predicts better patient outcome, the *sarcomatoid* histotype prognosticates the worst patient outcome and is considered untreatable and aggressive, whereas the biphasic (mixed) contains both fractions: epithelioid and sarcomatoid. Among several antigens used to aid mesothelioma diagnosis, **calretinin** detection is considered the most specific for mesothelioma diagnosis. Calretinin is a calcium-binding protein that is physiological expressed in a subset of neuronal cell populations and e.g. Leydig cells. Calretinin is differentially expressed in the different MPM histotypes, with a strong cytosolic and nuclear immunoreactivity in the epithelioid and a weak/absent expression in the sarcomatoid histotype. In the biphasic histotype, calretinin appears in a mosaic form as it is expressed mostly in the epithelioid compartment. Furthermore, longer overall survival is associated with higher calretinin expression suggesting that calretinin expression is a prognostic marker. Despite being a mesothelioma diagnostic marker for 20 years, the mechanisms driving calretinin expression in MPM were unknown until this study. Therefore, we investigated the molecular regulation of calretinin expression in MPM at the transcriptional (4.1) and post-transcriptional (4.2) levels. Characterization of calretinin expression in a panel of mesothelioma cell lines, showed strong positive correlation between calretinin protein and mRNA expression levels, indicating that calretinin expression is regulated at the mRNA level in mesothelioma. Using the promoter-reporter system assay (pGL3-basic), we identified a minimal active calretinin promoter (*CALB2* -161bp/+80bp) in malignant pleural mesothelioma. We further revealed NRF-1 and E2F2 as two positive regulators of the calretinin promoter. Since epigenetic modifications target gene promoters we investigated and report here that DNA methylation of *CALB2* promoter does not affect calretinin expression in mesothelioma cells. In addition, we identified that calretinin is expressed in a cell-cycle dependent way.

The regulation of gene expression at the mRNA level includes post-transcriptional mechanisms mediated through the 3' untranslated region (3'UTR). Utilizing a reporter assay, we determined that calretinin 3'UTR exerts a downregulatory effect mediated by two miR-30 binding sites.

Mimic and anti-miR treatment identified miR-30e-5p as a regulator of calretinin expression. Furthermore, mutational analysis revealed a stabilizing ARE motif within the *CALB2* 3'UTR. In support of the functional ARE (AUUUA) element, a biochemical assay (REMSA) demonstrated that a 25nt RNA oligo harboring the ARE sequence specifically binds to a cytosolic protein from mesothelioma cells. For the first time, we showed the presence of alternative calretinin transcripts in mesothelioma cells, and we postulate that they play a putative role in regulating expression of protein-coding calretinin transcripts by competing for the miRNA or AU-binding protein pools. This is the first study reporting on the mechanisms regulating calretinin expression in mesothelioma. The findings from this study are important for the understanding of mesothelioma development and provide further avenues for the investigation of calretinin expression in mesothelioma.

1.1. ZUSAMMENFASSUNG

Das maligne Pleuramesotheliom (MPM) ist ein Tumor mit schlechter Prognose, der aus Mesothelzellen entsteht, die die Lunge und die Thoraxhöhle auskleiden. Primäre Ursache für MPM ist die Inhalation von Asbestfasern, ein natürlich vorkommendes Mineral, das massiv abgebaut und in der Industrie während des 20. Jahrhunderts aufgrund seiner ausgezeichneten Wärme- und Säurebeständigkeitseigenschaften verwendet wurde, was zur Exposition einer grossen Anzahl von Menschen führte. Das Mesotheliom ist in drei histologische Subtypen kategorisiert und jeder dieser Typen ist mit einem unterschiedlichen Überleben der Patienten verbunden. Der epitheloide Histotyp prognostiziert ein besseres Überleben, der sarkomatöse Histotyp das schlechteste Überleben des Patienten und gilt als unheilbar und aggressiv angesehen wird, während der biphasische (gemischte) Subtyp sowohl epitheloide und sarkomatöse Anteile enthält. Unter mehreren Antigenen, die verwendet werden, um die Mesotheliom-Diagnose zu unterstützen, gilt der Calretinin-Nachweis als der spezifischste Hinweis auf eine Mesotheliom-Diagnose. Calretinin ist ein kalziumbindendes Protein, das physiologisch in einem Teil der neuronalen Zellpopulation und z.B Leydig-Zellen exprimiert wird. Calretinin wird in den verschiedenen MPM-Histotypen mit einer starken zytosolischen und nuklearen Immunreaktivität im epitheloiden Histotyp und einer schwachen/fehlenden Expression im sarkomatösen Histotypen exprimiert, während im biphasischen Histotyp Calretinin aufgrund seiner Expression nur vorzugsweise im epitheloiden Anteil in einer Mosaikform erscheint. Darüber hinaus ist ein längeres Gesamtüberleben mit einer höheren Calretinin-Expression verbunden, was nahelegt, dass die Calretinin-Expression ein prognostischer Marker ist. Obwohl Calretinin seit 20 Jahren als diagnostischer Marker für MPM verwendet wird, waren die der Calretinin-Überexpression zugrundeliegenden Mechanismen bis zu dieser Studie unbekannt. Daher haben wir diese Studie entwickelt, um die molekulare Regulation der Calretinin-Expression im MPM auf Transkriptions- (4.1) und post-transkriptioneller Ebene (4.2) zu untersuchen. Die Charakterisierung der Calretinin-Expression in einer Gruppe von humanen Mesotheliom-Zelllinien zeigte eine starke positive Korrelation zwischen dem Calretinin-Protein- und dem mRNA-Expressionsniveau, was darauf hindeutet, dass die Calretinin-Expression im MPM auf mRNA-Ebene reguliert wird. Mit dem Promotor-Reporter-System Assay (pGL3-basic) identifizierten wir einen Minimal Calretinin Promotor (*CALB2* -161bp/+80bp) im malignen Pleuramesotheliom. Weiterhin wurden NRF-1 und E2F2 als zwei positive Regulatoren des Calretinin-Promotors identifiziert. Da epigenetische Modifikationen ebenfalls Gen-Promotoren regulieren können, untersuchten wir die DNA-

Methylierung des CALB2-Promotors und konnten zeigen, dass diese nicht die Calretinin-Expression in Mesotheliom-Zellen beeinflusst. Zusätzlich zeigten Zellzyklusanalysen, dass dieser einen der Mechanismen darstellt, die die Expression von Calretinin im MPM regulieren. Die Regulation der Genexpression auf mRNA-Ebene umfasst post-transkriptionelle Mechanismen, die durch die 3' untranslatierte Region (3'UTR) vermittelt werden. Unter Verwendung eines Reporter-Assays haben wir festgestellt, dass der Calretinin 3'UTR einen von zwei miR-30-Bindungsstellen vermittelten herabregulierenden Effekt ausübt. Mimetik und Anti-miR-Behandlung identifiziert miR-30e-5p als Regulator der Calretinin-Expression. Darüber hinaus identifiziere die Mutationsanalyse ein stabilisierendes ARE-Motiv. Zur Unterstützung des funktionellen ARE (AUUUA) -Elements zeigte der biochemische Assay (REMSA), dass das 25nt RNA Oligo, das nukleotide die ARE-Sequenz beherbergt, spezifisch ein zytosolisches Protein aus Mesotheliomzellen bindet. Zum ersten Mal zeigte diese Arbeit zudem die Anwesenheit von alternativen Calretinin-Transkripten in Mesotheliomzellen und wir postulieren ihre potentielle Rolle im Konkurrieren um den miRNA- oder AU-bindenden Proteinpool und damit eine Rolle in der Regulation der Expression des Protein-kodierenden Calretinintranskripts. Dies ist die erste Studie, die über Mechanismen der Regulierung der Calretinin-Expression im Mesotheliom berichtet. Die Ergebnisse aus dieser Studie sind wichtig für das Verständnis der Entstehung des Mesotheliom und eröffnen weitere Forschungsrichtungen für die Untersuchung der Calretinin-Expression im Mesotheliom.

2. INTRODUCTION

2.1. Mesothelioma

Malignant mesothelioma (MM) is a fatal cancer originating from mesothelial cells lining the pleural, peritoneal, pericardial cavities and the tunica vaginalis testis. The disease has very poor prognosis mainly because patients are diagnosed with an advanced cancer state. Retrospective analysis of MPM patients in the United States showed that cancer-directed surgery and tumor grade appear to have the greatest impact on overall survival (OS) [2]. MPM accounts for 90% of all mesothelioma cases [3]. Peritoneal mesothelioma patients have significantly better survival than the ones with pleural mesothelioma [4].

Malignant pleural mesothelioma arises mainly due to the inhalation of asbestos fibers. There is now a strong body of evidence, based on animal and human population studies that demonstrates causal association between asbestos and non-malignant and malignant diseases including MPM and lung cancer [5, 6]. Asbestos (from the Greek word – "inextinguishable") is a naturally-occurring fibrous silicate mineral that possesses excellent fire resistant properties, heat stability, and chemical resistance and for these properties was referred to as a "magic mineral" [7]. The National Academy of Science defined "asbestos" as "a generic term for a number of hydrated silicates that, when crushed or processed, separate into flexible fibers made up of fibrils"[8]. Many minerals (~400) can appear in a fibrous habit [9], however only six are of commercial importance and therefore regulated under the term "asbestos": 1) *serpentine* mineral chrysotile (white asbestos) and 2) the amphibole minerals actinolite, amosite (brown asbestos), anthophyllite, crocidolite (blue asbestos), and tremolite [10]. Widely commercially used forms of asbestos were chrysotile, amosite, anthophyllite, and crocidolite, [11] among which chrysotile made up more than 90 percent of total asbestos output [7]. Currently, all commercial forms of asbestos are considered and claimed as potential human carcinogens and are associated with an increased risk of lung cancer and mesothelioma [11]. Asbestos has been used in roofing, ceilings, manufacturing of household equipment, thermal and electrical insulation, cement pipe and sheets, coatings, flooring, plastics, textiles, paper, and even in hairdryers [11].

Documentation (e.g. physicians' reports) associating diseases (asbestosis, mesothelioma or "endothelioma", and lung cancer) and occupational asbestos inhalation started to appear at the beginning of the 20th century [12]. A 1924 medical report of a woman who worked in a textile plant with asbestos and died of lung fibrosis, was the first report that officially drew attention

to the hazards of asbestos [13]. Until 1950 and beyond, there was doubt that mesothelioma existed as a primary tumor, which complicates tracing back the first documented cases of mesothelioma. In the first edition of Hunter's "The Diseases of Occupations" (1955), asbestos is discussed as a cause of only asbestosis and lung carcinoma, however, there is no mentioning of mesothelioma. Even in the 1960s, skepticism remained of the existence of mesothelioma as primary and separate tumor entity [14]. In 1960, Wagner et al. clearly established the link between asbestos and mesothelioma. The work described 33 cases of pleural mesothelioma located in the north-west of the Cape Province, South Africa. All of the mesothelioma cases, except for one, most likely involved exposure to asbestos. For some of the cases the presence of asbestosis was even histologically documented [15].

2.1.1. Epidemiology

Already the early civilizations used asbestos for bucket-shaped pottery for storing and making food. For instance, the Romans wove asbestos into napkins that could be cleaned by fire [16]. With the era known as the Industrial Revolution, asbestos-use intensified as it was utilized for insulation for boilers, turbines, steam pipes, ovens, roofing, and other high-temperature equipment. Between 1870 and 1970 asbestos was widely used, advertised and viewed as an indispensable material (Figure 1).

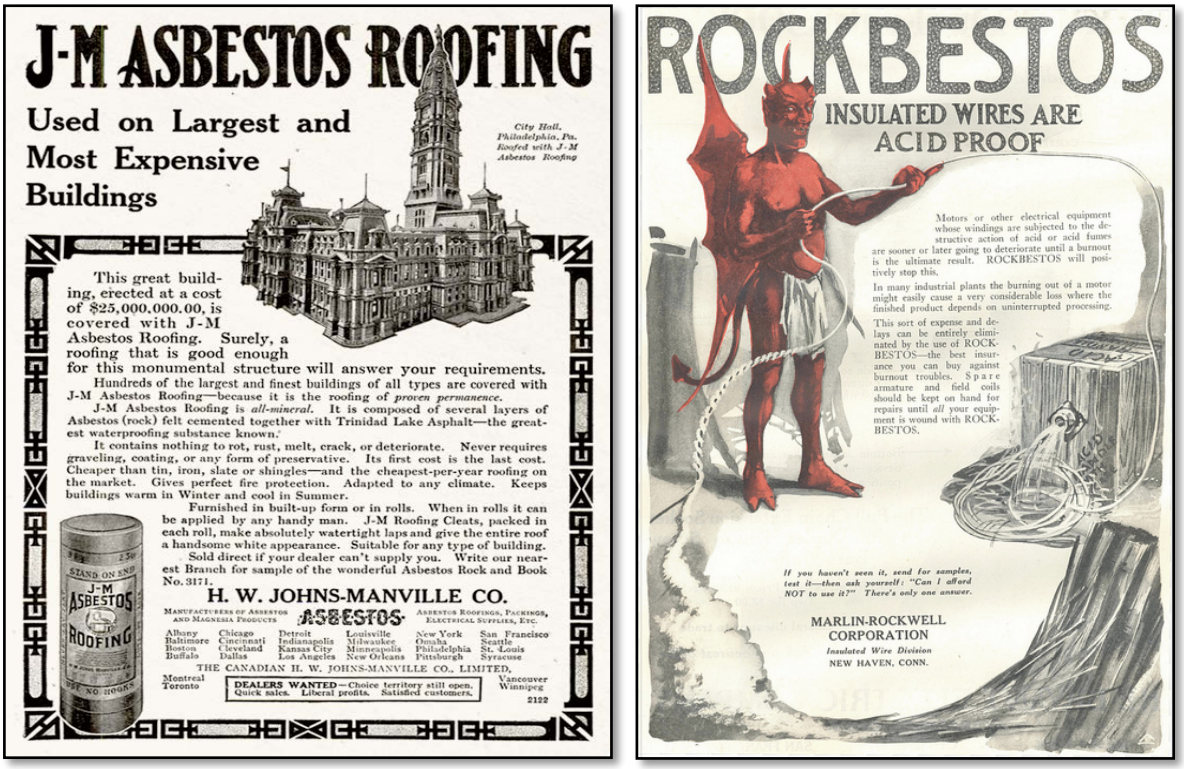

Figure 1. Asbestos advertisements from 1913 and 1920.

Mass mining and use of asbestos started at the beginning of the 20th century and peaked between the 1960s and 1980s (Figure 2) [17]. Canada was the leading world producer of asbestos (Province of Quebec), followed by Russia (Eastern slopes of the Ural Mountains, town Asbest), the Republic of South Africa (primarily the Cape Province), South Rhodesia, Swaziland, Italy, Western Australia, China and Japan [7]. Asbestos consumption started to decline after 1982 [18]. Currently, the annual incidence of mesothelioma is highest in Australia, the United Kingdom and Italy (29:29:24 per million) [19].

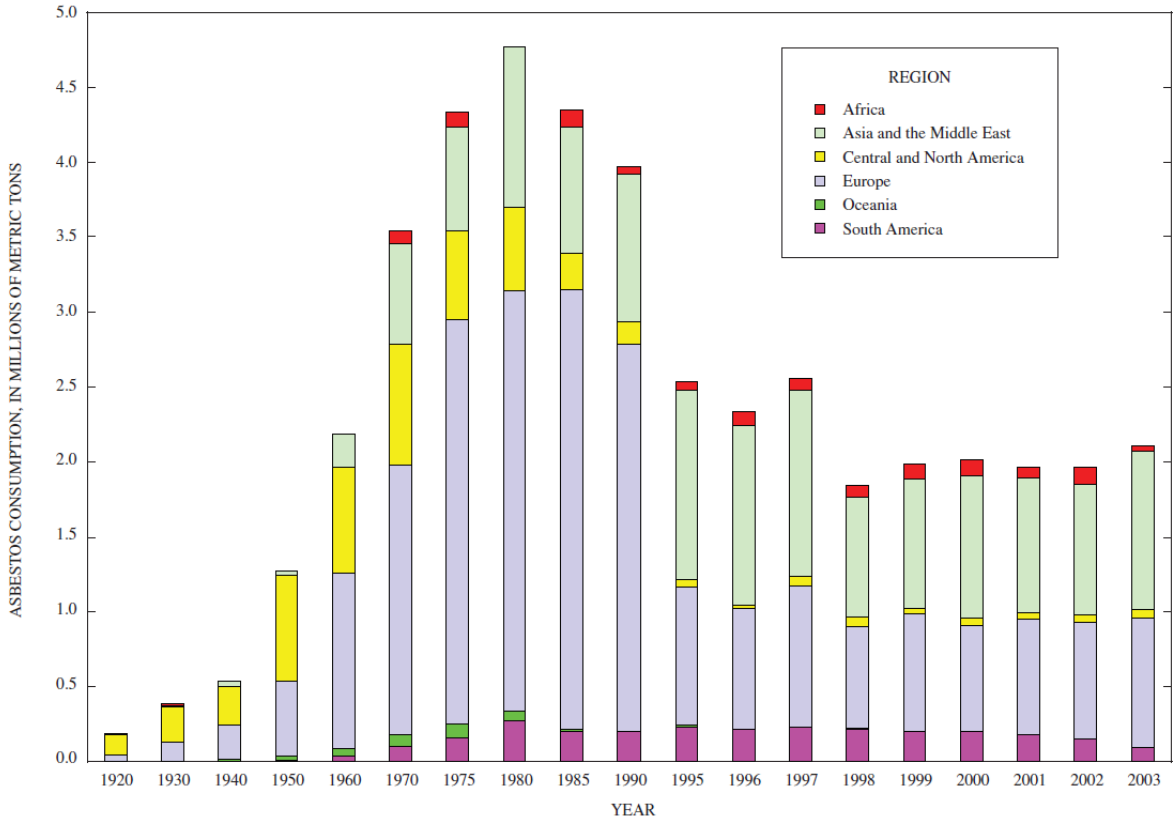

Figure 2. Bar graph of asbestos consumption by region from 1920 to 2003. Modified from [17].

Park et al. described a substantial hidden burden of mesothelioma in a total of 33 countries including Russia, Kazakhstan, China, India and Thailand, countries for which only asbestos consumption is known, but mesothelioma cases are not reported [20]. Currently, asbestos is banned in 52 countries, but asbestos mining still continues, with Russia as the leading producer followed by China [21]. Even though banned in all European Union member states, much asbestos remains in many buildings and strict control of any abatement work is required.

Exposure to mineral fibers is not only occupational or para-occupational (family members of asbestos-exposed workers), but also there is environmental exposure from natural fibrous materials disturbed by weathering or human activities. For instance, rocks containing fibrous minerals in California were indicated as a source of MPM, as the risk for MPM decreased with the distance from a natural source of minerals [22]. In addition, environmental erionite exposure in Turkey, the Cappadocian villages of Turkey [23], Karäin [24], and Tuskoy, resulted in the highest incidence of MPM world-wide. Environmental exposure to naturally occurring asbestos was linked to risk of MPM in younger populations [25]. Besides asbestos and natural occurring fibrous material, other known causes of mesothelioma are the following: ionizing radiation (in patients given Thorotrast as a radiographic contrast and in patients undergoing radiotherapy),

and chest injuries [26]. Patients with prostate cancer, that undergo external beam radiotherapy (EBRT), also have a risk of developing mesothelioma as a secondary malignancy [27]. Mesothelioma risk demonstrates dose-dependence. For example, miners and millers in the asbestos mining town Wittenoom (Western Australia) showed higher rate of disease with greater intensity of asbestos exposure [28].

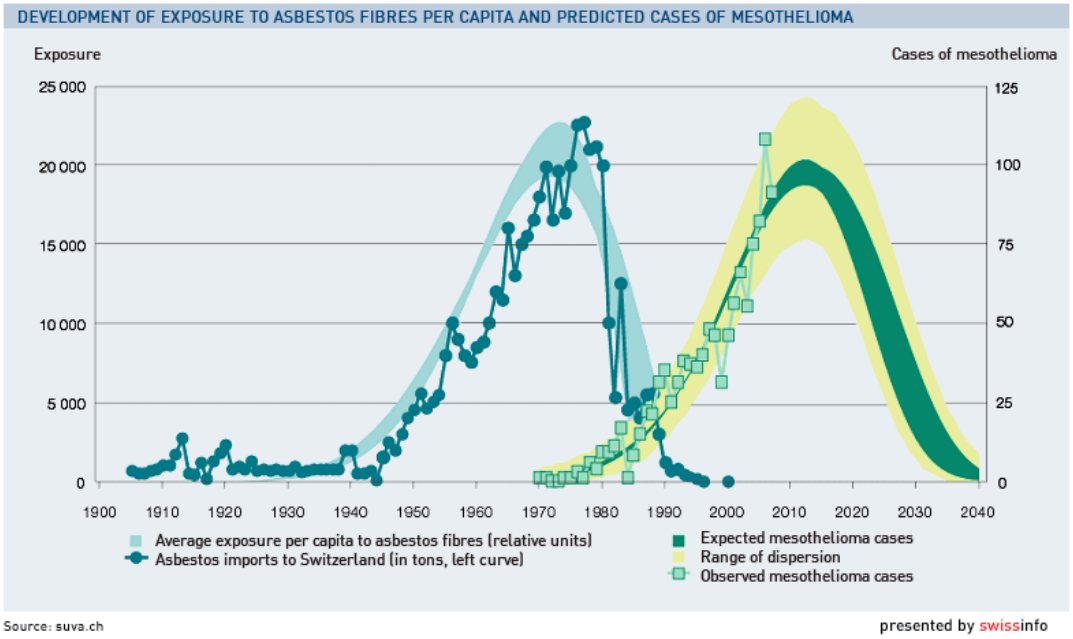

Figure 3. The peak of asbestos-boom was in 1978 in Switzerland. After a longer period of latency, the burden of diagnosed mesothelioma cases is observed in the 2010's. Modified from [29].

A higher rate of mesothelioma in many industrialized Northern and Western European countries reflects the increased asbestos production and use in the past, which suggests a long lag time between the first asbestos exposure and MM diagnosis. The latency period between the first exposure and diagnosis is relatively long, with some studies showing a mean time of 44.6 years [30] or 48.5 years [31]. For example, in Switzerland the peak of asbestos imports was in the late 1970s and 30 years later the number of mesothelioma cases is increasing with an expected peak around 2020 (Figure 3) [29]. In general, studies in which projections of the future burden of mesothelioma cases were carried out, all suggest the peak to occur over the following decade.

2.1.2. Mesothelial cells

The mesothelium is made of flattened squamous-like mesothelial cells, organized as a monolayer and covering serous cavities [32]. The mesothelium lining the internal organs and body wall is referred to as the *visceral* or *parietal* mesothelium, respectively, whereas the space in between is considered the pleural cavity/space (Figure 4). In 1827 Bichat first described a single layer of flattened cells lining serous cavities and the term “mesothelium” was later introduced in 1890 by Minot [33].

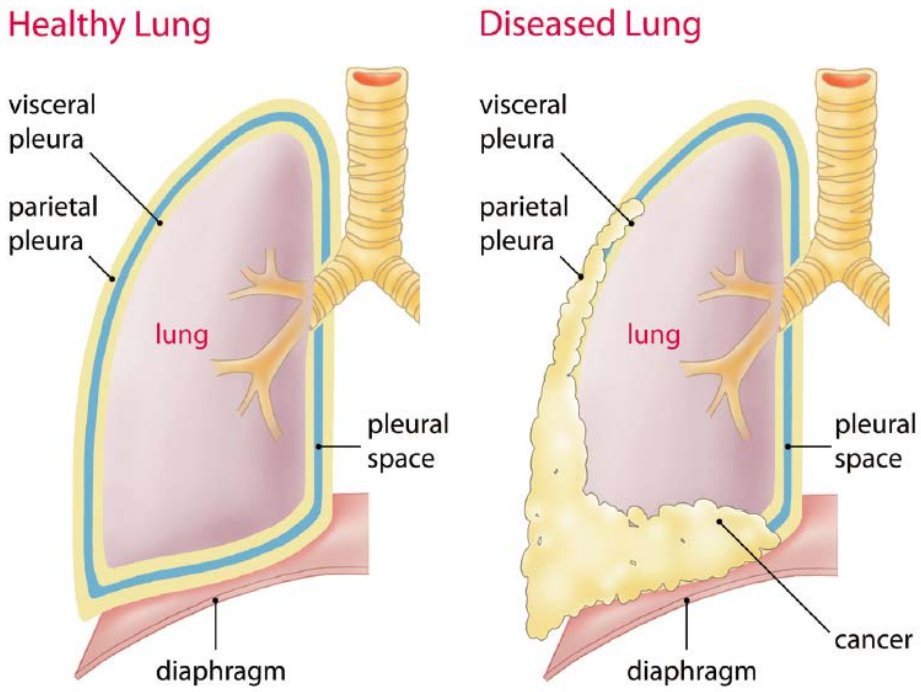

Figure 4. Anatomy of normal mesothelium and appearance of mesothelioma. Modified from [34].

The primary role of the mesothelium is to provide a slippery, protective and non-adhesive surface. Later, it became clear that mesothelial cells have additional functions since they secrete proteoglycans, glycosaminoglycans (hyaluronan), surfactant, present antigens to T cells [35, 36], secrete cytokines, growth factors, inflammatory mediators, and facilitate transport of fluid and other cells across the serosal membrane (Figure 5) [37]. They also have pro-coagulant and fibrinolytic activity [38, 39]. The mesothelium develops from the mesoderm between days 8 and 18 of gestation depending on the species [37]. However, mesothelial cells display dual epithelial/mesenchymal phenotypes because they express both epithelial characteristics such as tight, adherens and gap junctions, and desmosomes, surface microvilli, apical/basal polarity,

cytokeratins, and mesenchymal features including the cytoskeletal proteins vimentin and desmin [40, 41]. The mesothelial cells reside on a thin basement membrane below which is a connective stroma tissue that contains blood vessels, lymphatics, adipose, macrophages and subserosal mesenchymal cells [37]. Mesothelial cells have well-developed tight-junctions, gap junctions, adherent junctions, and desmosomes [42, 43]. In addition, the mesothelium contains openings called "stomata" surrounded by cuboidal mesothelial cells, which provide direct access to the submesothelial lymphatic system [44]. In the pleural mesothelium, only the parietal mesothelium contains stomata [45, 46]. Mesothelial cells also participate in serosal inflammation by producing anti- and pro-immunomodulatory mediators [44].

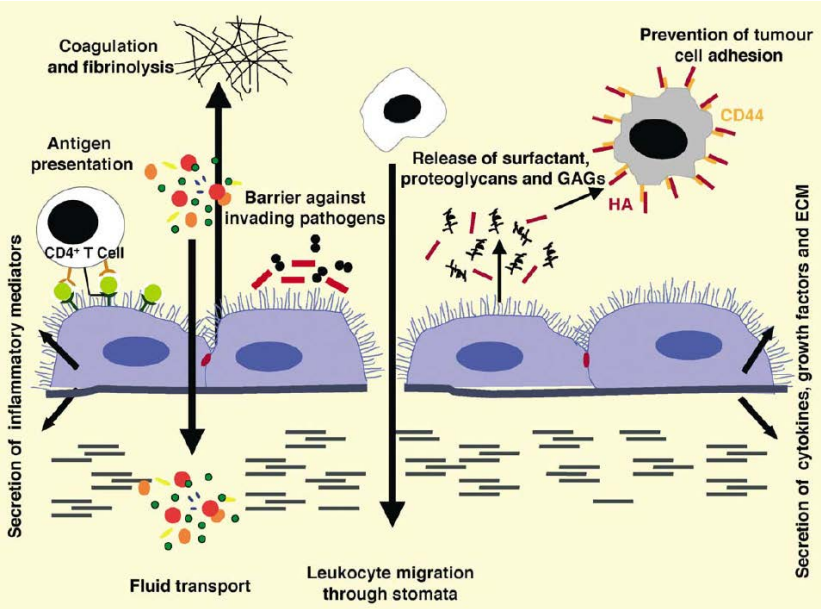

Figure 5. Different functions of mesothelial cells. Modified from [37].

The exact mechanism of mesothelium regeneration is still debated. In 1919, it was first reported that both small and large parietal peritoneal mesothelium injuries healed at the same time, and this observation was confirmed in many subsequent studies [47, 48]. It was concluded that the mesothelium could not regenerate solely by centripetal migration of proliferating cells at the wound edge as observed in true epithelia. Based on many studies, it is currently widely accepted that the healing process starts within 24h after injury, when a population of cells migrates to the wound surface, and is completed within the following 7-10 days [49-51]. The origin of the "healing cells" is still not fully understood but many studies have proposed several potential candidates [52]. The mesothelium is a slow renewing tissue with 0.16-0.25% of mesothelial cells undergoing mitosis in mice at a time [53, 54]. Upon injury of the mesothelium, 30-80%

of cells around and in close proximity of the wound edge become mitotically active as they start to replicate DNA within the following 24 to 48 hours [55, 56]. Moreover, it was demonstrated through tracking fluorescently labeled cells that the mesothelial cells, distant from the wound surface, detach from the basement membrane into the serosal fluid, proliferate and repopulate the injured mesothelium [57]. This suggested that proliferating mesothelial cells around the wound along with exfoliation of proliferating mesothelial cells from nearby or the opposite surface mesothelial cells are an important source of the cells that regenerate the mesothelium. In addition, incorporation of free-floating mesothelial cells was also proposed to aid in mesothelium healing [57, 58]. 2 days post-injury of the mesothelium, peritoneal lavage fluid was found to contain an increased number of viable free-floating mesothelial cells [55]. In another study, postoperative removal of the peritoneal lavage led to the retarded healing rate of the mesothelium probably due to the concomitant removal of free-floating serosal cells [59]. An additional possible origin of regenerating mesothelial cells that should be considered, is bone marrow-derived circulating stem cells [60]. Currently, the general model of mesothelium healing proposes that upon mesothelium injury, inflammatory cells are recruited to the wound surface and start releasing cytokines, which in turn stimulate proliferation of mesothelial cells surrounding the wound. Activated mesothelial cells break cell-to-cell contacts and migrate towards the wound surface. The origin of these free mesothelial cells is still unknown: whether they are daughter cells of proliferating mesothelium, exfoliated mesothelial cells found in proximity to the injury, or descendents from circulating precursors remains to be elucidated.

An increasing body of evidence suggests that mesothelial cells have the capacity to undergo epithelial-mesenchymal transition (EMT), or more recently referred to as mesothelium-mesenchymal transition (MMT) and differentiate into different cell types [40, 61]. Namely, several studies have shown that during development the mesothelial cells lining the heart, liver, lungs and gut can differentiate into endothelial cells, vascular smooth muscle cell, interstitial fibroblasts, hepatic stellate cells and adipocytes [62-68]. Transforming growth factor β_1 (TGF-β_1) stimulates adult mesothelial cells to acquire a myofibroblast phenotype *in vitro* [69]. Furthermore, the adult mesothelial cells also can undergo MMT and give rise to vascular smooth muscle cells [70, 71]. There have been many case reports on MM patients in which the tumor was found to contain parts with osseous and/or cartilaginous differentiation [72-75]. Based on this observation, it was demonstrated that human and rat adult mesothelial cells, when grown in osteogenic or adipogenic medium, are able to further differentiate into osteoblast- and adipocyte-like cells [76]. Importantly, a subset of mesothelioma tumors retains the potential to

differentiate into osteoblast-like cells [77]. All these studies support the concept that mesothelial-derived cells retain their multipotent nature.

2.1.3. Pathogenesis

Carcinogenic effects of asbestos on the pleura is possible because asbestos fibers reach the pleural space and accumulate on stomatal openings in the parietal pleura [78]. There are several possible scenarios how mineral fibers such as asbestos can cause malignant transformation of mesothelial cells. The first scenario is ***pleural irritation/injury,*** in which very long, thin fibers, which have the greatest carcinogenic potency [79], penetrate the lung and induce persistent mesothelium injury and local inflammation [80]. In turn, the chronic inflammation can lead to cancer development by dysregulation of tissue-repair mechanisms and stem cell self-renewal [81]. The second possible mechanism is ***interference with mitosis,*** as asbestos fibers can interfere physically with the mitotic spindle resulting in potential chromosome damage (structural rearrangements) typically seen in mesothelioma [82]. The third possible explanation is the ***generation of reactive-oxygen species (ROS)***, by asbestos, which induce different types of DNA lesions, promoting oncogenic cell transformation [83]. Comprehensive genomic analysis from 216 MPMs, found differences in mutational profiles und thus identified five distinct mutational signatures (S1-S5), among which the S1 signature was predominant [84]. The S1 signature, characterized with no predominant transition or transversion, was observed in ~50% of analyzed mesotheliomas. The rest of mesotheliomas displayed mutational signatures (S2, S4, S5) with enrichment in C>T transition.

2.1.4. Molecular pathology of mesothelioma

According to cytogenetic analysis, the majority of mesotheliomas have extensive aneuploidy and structural rearrangements and extensive loss of genetic material [85, 86] implying that a tumor suppressor loss is necessary for mesothelioma development. The most commonly affected chromosomes are 22q, 9p21, 1p, 4q, 6q, 13, and 14q.

In the catalogue of somatic mutations in cancer (COSMIC, http://www.sanger.ac.uk/cosmic) [87], the three most commonly mutated genes in malignant pleural mesothelioma are cyclin – dependent kinase activator inhibitor - *CDKN2A* (chr.9), neurofibromatosis type 2 - *NF2* (chr.22), and BRCA - associated protein - *BAP1* (chr.3) [88].

CDKN2A encodes for the proteins p16 and ARF, and it was previously reported that lack of p16/ARF expression in MPM is due to either gene deletion or methylation [89-93]. *NF2 (*Neurofibromatosis type 2, or *merlin*- product of *NF2* gene) is a part of the Hippo pathway that controls organ size by regulating cell cycle, proliferation and apoptosis [94] and is mutated at high frequency in MPM [95]. NF2 activates the Hippo pathway in normal tissue repair and upon cell-cell contact (cell-contact inhibition) [96]. The Hippo pathway is frequently disrupted in most malignant mesotheliomas, either by loss of NF2 or other regulators (e.g. *LATS2*) of the pathway [97, 98]. BAP1, a nuclear-localized deubiquitinating enzyme, has been found to be mutated in 23% of MPM specimens [99] or even up to 61% in Yoshikawa et al.'s study [100]. Additional evidence suggests that BAP1 is a bona-fide tumor suppressor [101]. In order to exhibit its tumor suppressor function, BAP1 requires deubiquitinating activity and nuclear localization [102]. Germline BAP1 mutation increases the risk of suffering from mesothelioma along with acquiring other types of tumors (cutaneous melanoma, uveal melanoma, renal cancer) [103]. Interestingly, MM patients carrying BAP1 mutations appear to have a 7-fold longer survival when compared to patients with sporadic MM [104].

Nf2 hemizygous mice develop mesothelioma at a higher rate when exposed to asbestos fibers [105]. In *Bap1* hemizygous mice, accelerated asbestos-induced mesothelioma formation was also observed [106]. Even *Bap1* (-/+) mice had a significantly higher incidence of mesothelioma development upon very low doses of asbestos exposure compared to wild type mice [107]. Double conditional knockouts of *Nf2/Ink4a/Arf* in the mesothelial lining of the thoracic cavity in mice showed accelerated mesothelioma development [108]. All together, these mouse genetic studies support essential roles for *NF2, CDKN2A*, and *BAP1* genes in mesothelioma development and explain why these genes are frequently mutated in human mesothelioma specimens.

The latest study on comprehensive genomics analysis of MPM tumors identified ten significantly mutated genes, which include *BAP1, NF2, TP53, SET2, DDX3X, ULK2, RYR2, CFAP45, SETDB1* and *DDX51* [84]. Recurrent mutations in *TRAF7*, encoding an atypical member of the tumor necrosis factor (TNF) receptor-associated factor family, and in *SF3B1*, encoding a splicing factor with a role in branch-point recognition and U2-snRNP assembly, were further identified. Mutation in *TRAF7* was mutually exclusive with mutations of *NF2*, suggesting that both could participate in a common signaling pathway.

2.1.5. Histopathology of mesothelioma

To distinguish mesothelioma from metastatic adenocarcinoma is a common diagnostic issue, since both cancers appear with similar clinical symptoms such as chest pain, pleural effusion and respiratory distress, and even similar cytomorphological features of cancer cells [109]. Hence, immunohistochemistry is widely accepted as an essential tool towards diagnosis of mesothelioma. There are three major mesothelioma histotypes: *epithelioid* characterized with epithelial square shaped cells (60%), *sarcomatoid* (fibroblastic) with predominant spindle tumor cells organized in the wavy pattern and *biphasic* (mixed) consisting of both epithelioid and sarcomatoid compartments and each of them are further subdivided [110]. This classification is important for prognosis [111] as the epithelioid type predicts the longest survival (16.3 months) than for patients with biphasic tumors (9.5 months) or sarcomatoid (6.1 months) [112]. Patients with epithelial histology appear to have a survival benefit from surgery or multimodality therapy in contrast to sarcomatoid in which therapy has no impact on survival [113].

To aid in differential mesothelioma diagnosis, a panel of immunohistochemistry markers was established comprising of: 1) Carcinoma-related markers - carcinoembryonic antigen (CEA), LeuM1 (CD15), Ber-EP4, B72.3 and BG8 and 2) markers characteristically expressed by mesothelial cells - Wilms tumor gene product (WT1), mesothelin, cytokeratin 5/6, HBME-1 antigen, thrombomodulin and podoplanin (D2-40) [3]. Of these, calretinin is the most commonly used mesothelioma marker [114]. Besides its use as a diagnostic marker, calretinin can be utilized as a prognostic marker, as low calretinin expression is associated with poor prognosis in MPM patients [115-117]. The focus of this PhD work was to study the mechanisms regulating the expression of calretinin. As a side project, I also worked on a long noncoding RNA, growth-arrested 5 (GAS5), where my contribution was to construct and study a *GAS5*-promoter reporter gene, which allowed me to familiarize myself with the promoter reporter tool that I later applied to study calretinin.

2.2. Calretinin

Calretinin (calbindin 2, CR; human gene: *CALB2*; mouse gene: *Calb2*) is a ~31kDa calcium-binding protein that was initially discovered and cloned from chick retina in 1987 (calcium + retina = calretinin) [118].

The protein sequence is highly conserved and its length varies with 269 amino acids in chicken or 271aa in human, rat, mouse, and bovine [119]. An invertebrate ortholog is found in *Drosophila melanogaster*, called calbindin 53E (*Cbp53E*) and has 42% identity with chicken calretinin [120].

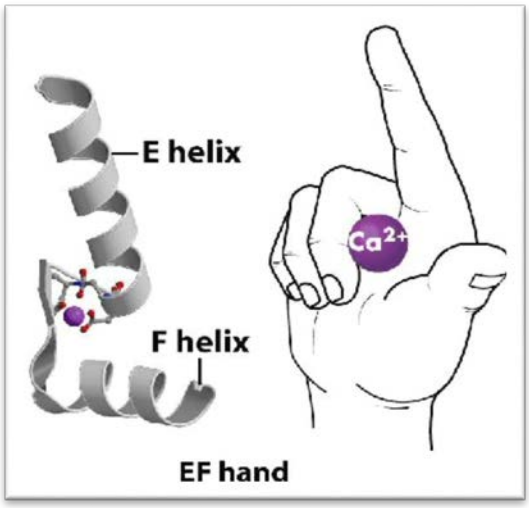

Figure 6. Schematic representation of the *EF-hand motif, described by Kretsinger and Nockolds. Modified from [119].*

Calretinin, along with calbindin D-28k and secretagogin, belongs to the hexa-EF-hand protein family, as they all contain six EF-hand domains, which bind calcium ions [121]. An EF-hand motif consists of around 30 residues and is the most common calcium-binding motif [122]. The three-dimensional structure of the EF-hand domain can be represented using a folded right hand where the index finger represents 1-10aa (E-helix), the middle finger (folded) represents 10-21aa and binds Ca^{2+}, and the thumb represents 19-29aa (the F-helix) (Figure 6).

In calretinin, five EF-hand domains are active to bind Ca^{2+} ions. The first four exert high affinity for binding Ca^{2+} ions with positive cooperativity, whereas the sixth domain is inactive [123]. The fifth EF-hand domain has very low Ca^{2+} -binding affinity (36µM) [124]. The secondary structure of calretinin has been determined for the first 100 N-terminal amino acids through nuclear magnetic resonance (NMR) spectroscopy [125].

The human *CALB2* gene is located on chromosome 16q22.2 and encodes for three transcripts: 1) calretinin isoform 1 (full length isoform) - 29kDa-protein – *CALB2* – normally spliced; 2) calretinin transcript variant - non-coding RNA – *CALB2b* (*Δ*8), and 3) calretinin isoform 22k - *CALB2c* (*Δ*8, 9), both alternatively spliced from the primary full length calretinin mRNA [126-128].

2.2.1. Calretinin expression in tissues

Calretinin expression has been mainly investigated in neuronal cells. CR is physiological strongly expressed in peripheral sensory neurons of the auditory, vestibular and visual systems, and selectively expressed in granule cells of the cerebellum [129, 130]. In non-neuronal cells, CR is detected in adipocytes, mast cells, muscle spindle, convoluted tubules of the kidney, Leydig and Sertoli cells, ovarian stromal cells, adrenal cortical cells and pancreatic islets [114, 131]. Frequent strong, positive staining for calretinin in mesothelioma but not in adenocarcinoma was reported for the first time by Doglioni et al. in 1996, suggesting that calretinin is a good mesothelioma marker [132, 133]. Immunohistochemistry staining of epithelioid, sarcomatoid and biphasic mesothelioma specimen shows strong, absent and intermediate calretinin immunoreactivity, respectively (Figure 7). The expression of calretinin in normal mesothelium is still unclear. Gotzos et al. (1996) reported that calretinin immunoreactivity was typically observed in: epithelioid mesothelioma, epithelioid component of mixed type, and reactive mesothelium (cuboidal mesothelial cell of visceral pleura), but negative in sarcomatoid mesothelioma, flattened cells of mesothelium, paratumoral tissues such as pulmonary parenchyma (bronchi, bronchioles, respiratory bronchioles, alveoli), tissue associated with lungs (cartilage, perichondrium, glands, nerves), and blood cells of the lung and pleura [133]. In contrast, Lugli et al. performed a tissue microarray analysis in 5233 tumor samples and reported calretinin expression in normal lung mesothelium [131]. Therefore, calretinin-positive staining is currently only considered to identify cells of mesothelial origin [134].

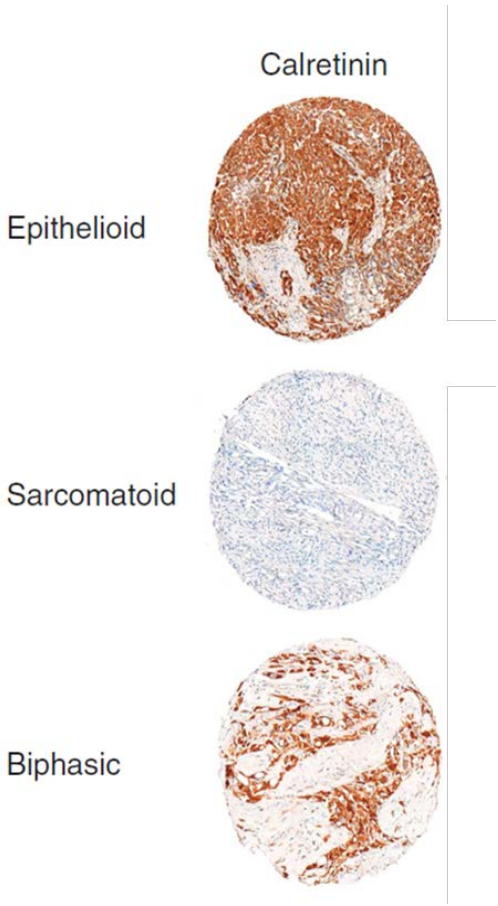

Figure 7. Calretinin expression in epithelioid, sarcomatoid and biphasic mesothelioma. Modified from [116].

2.2.2. Function of calretinin

As a calcium-binding protein, the main function of calretinin is to act as a cytosolic Ca^{2+} buffer. When the intracellular Ca^{2+} concentration is at resting level (50-100nM), upon a brief Ca^{2+} increase, calretinin acts as a typical slow-onset buffer (EGTA). If the same Ca^{2+} increase occurs while the intracellular Ca^{2+} level is elevated (1µM), in which the first pair of EF-hand domains are occupied by calcium, calretinin behaves as a fast-onset buffer (BAPTA) due to cooperativity among the calcium-binding sites. Therefore, calretinin-buffering activity depends on the initial intracellular Ca^{2+} concentration followed by a brief and limited Ca^{2+} increase [121, 135]. Additionally, *Calb2*$^{-/-}$ mice showed disturbance of motor coordination, indicating the role of calretinin in modulating neuronal excitability [136].

Calretinin is assumed to have an additional role as a Ca^{2+} sensor since purified calretinin undergoes Ca^{2+} dependent conformation changes *in vitro* [123, 137]. To date, the channel

subunit $\alpha_1$2.1 and Huntingtin (Htt) protein were shown experimentally to be interacting partners of calretinin [138, 139].

The role of calretinin in genesis of mesothelioma is unknown. Calretinin knockdown in two epithelioid MPM cell lines, using a lentiviral short-hairpin approach, led to impaired cell viability and proliferation consequently triggering apoptosis [140]. The mesothelium in *Calb2*$^{-/-}$ mice was normally formed, suggesting that calretinin is not essential for mesothelium development. Furthermore, comparing mouse derived mesothelial primary cultures from wild type (WT) and calretinin knockout (*Calb2*$^{-/-}$) mice, *Calb2*$^{-/-}$ mesothelial cells (but not lung fibroblasts) displayed significantly reduced proliferation rates, increased wound closure time and a more "giant" cells phenotype [141]. These studies suggest an important role of calretinin for cell proliferation, mobility, and its necessity in epithelioid mesothelioma; however, the molecular mechanisms that drive calretinin expression in mesothelioma remain elusive.

2.3. Regulation of gene expression

Different mechanisms and levels of control underlie tight and precise regulation of gene expression in order to adapt to the environmental changes and to respond to external cues. Genes expressed at a given time point determine what a specific cell can do and thus, different cells produce different sets of proteins. Mechanisms that control the final protein amounts are: **A)** ***Transcriptional control*** *(1)* when and how often is the gene transcribed; **B)** ***Post-transcriptional control*** (2) how the RNA transcript is spliced, (3) which transcript is exported to the nucleus, (4) if certain transcripts are degraded or stabilized; **C)** ***Translational control*** (5) selecting which transcript is translated by ribosomes; **D)** ***Post-translational control*** (6) activation or inactivation of the protein after it has been synthesized(Figure 8) [142]. For most cells, transcriptional control is the main mechanism of control as this can prevent the production of unnecessary intermediates.

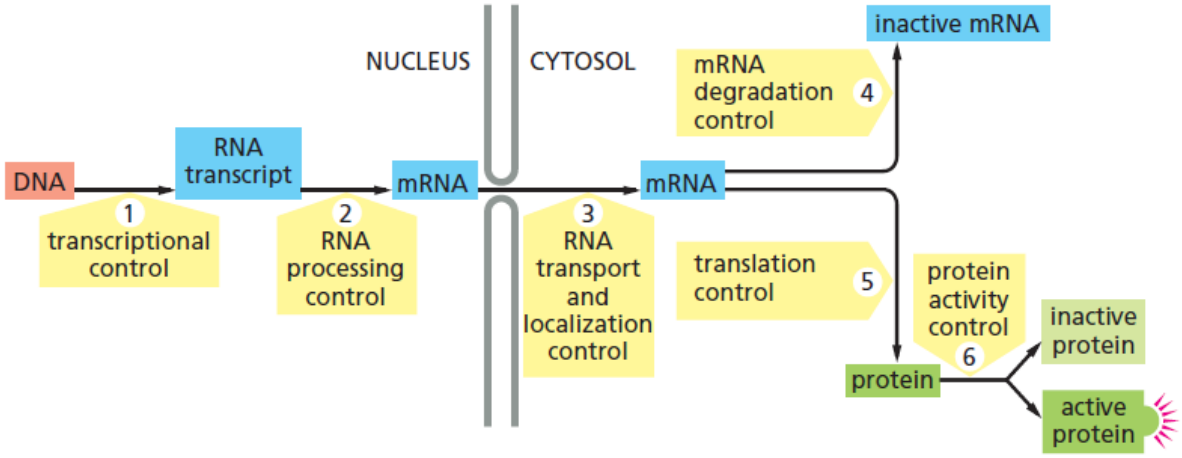

Figure 8. Gene expression in eukaryotic cells is controlled at several different levels. Modified from [142].

2.3.1. Transcriptional control

In general, several events occur before gene transcription starts. These events include decondensation of the locus, nucleosome remodeling and histone modifications, binding of transcription factors to enhancers or promoters, and recruitment of the basal transcription machinery to the core promoter. The core promoter is generally considered as the "minimal stretch of DNA sequence that is sufficient to direct accurate initiation of transcription" [143]. The DNA stretch of the core promoter includes DNA motifs spanning ~35nt upstream and/or downstream of the transcription initiation start site TSS (Figure 9) [144]. Initiation of transcription, the key event in the regulation of gene expression, starts by recruiting RNA polymerase (e.g. for protein coding and non-coding RNA – Pol II) to the core promoter region by the basal transcription machinery [145]. In general, the basal transcription machinery or preinitiation complex (PIC) is formed through association of the basal transcriptional factors in the following order: TFIID (TATA-binding protein (TBP) and TBP-associated factors (TAFs), then TFIIB, RNA Pol II, TFIIF, TFIIE, and TFIIH [144]. Nevertheless, due to the diversity of the core promoter components, different compositions of the PIC exists [146].

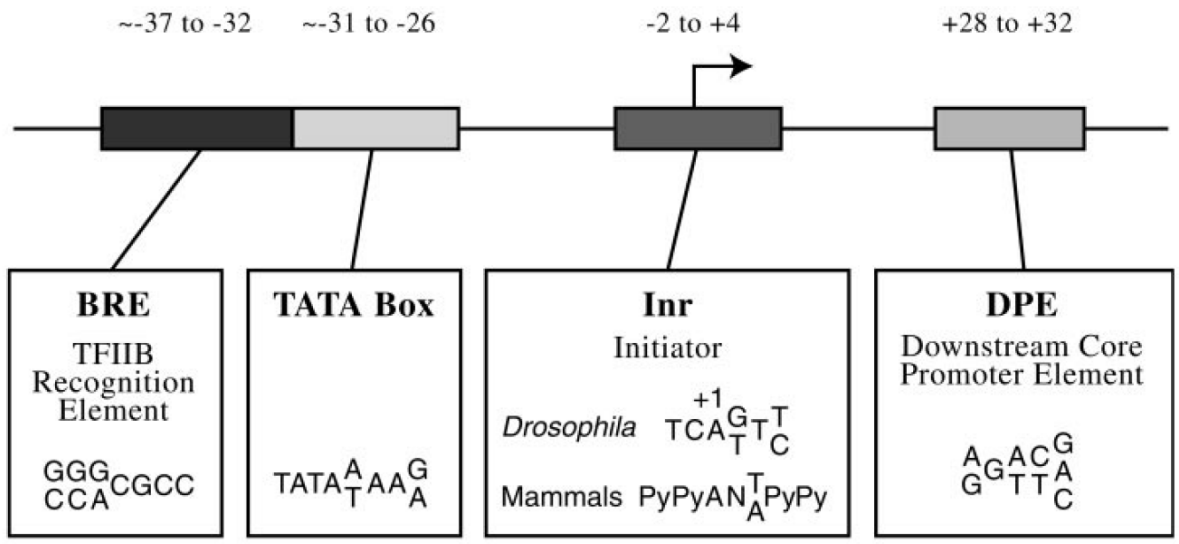

Figure 9. Core promoter elements. A core promoter consists of some or all, sometimes even none of the indicated DNA motifs. Modified from [144].

Transcription driven by the basal transcriptional complex at the promoter is low. However, it can be increased by the binding of other constitutively active or cell-specific transcription factors to the so-called upstream-promoter element (UPE) or other *cis*-regulatory elements usually located immediately upstream of the promoter (Figure 10) [147].

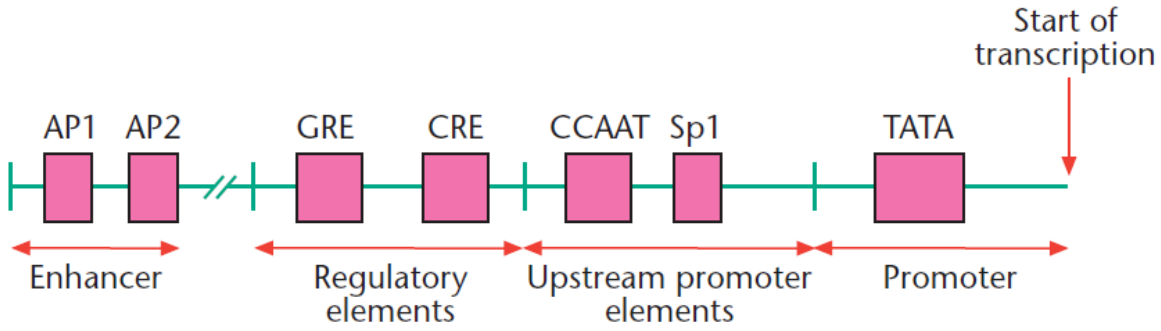

Figure 10. Structural motifs of a typical eukaryotic gene. Modified from [147].

Interestingly, different hallmarks are associated with active promoters and they include: reduced nucleosome occupancy over promoters (NDR), DNaseI hypersensitive sites (DHS) and enrichment of specific histone modifications such as tri-methylation H3K4 and acetylation of H3K4 and H3K27 [146]. There is a strong correlation between transcription initiation and CpG islands, as CpG islands coincide with many promoters. CpG islands (CGIs) are short regions of DNA that contain significantly more GC dinucleotides, and thus stand out from the average

genomic pattern. Cytosines within these CpG moieties can be subjected to methylation, which correlates with “switch-off” of the gene. This is another level for regulating transcription initiation [148].

2.3.2. Post-transcriptional control

Post-transcriptional regulation is an important mechanism of regulating gene expression through which cells can “tune” the level of the produced gene product if a rapid response to intracellular or extracellular signals is required (e.g. during stress situations). One of the critical post-transcriptional mechanisms in controlling gene expression is mRNA stability and decay which can be mediated through miRNA or regulatory proteins (e.g. AU-binding proteins) acting upon the 3’untranslated region (3’UTR) on mRNA (Figure 11). During evolution from worms to humans, it appears that genome size has dramatically increased, in particular in the noncoding part of the genome that could account for the increased organism complexity [149]. 3’UTR belongs to the noncoding portion of the genome and the number of genes producing alternative 3’UTRs doubled, and the 3’UTR length increased from a median of 140nt in worms to 1200nt in humans [150]. The 3’UTR is involved in transcript cleavage, polyadenylation, stability, localization, and mediates protein-protein interaction [151-153], hence 3’UTRs are important for determining the fate of an mRNA.

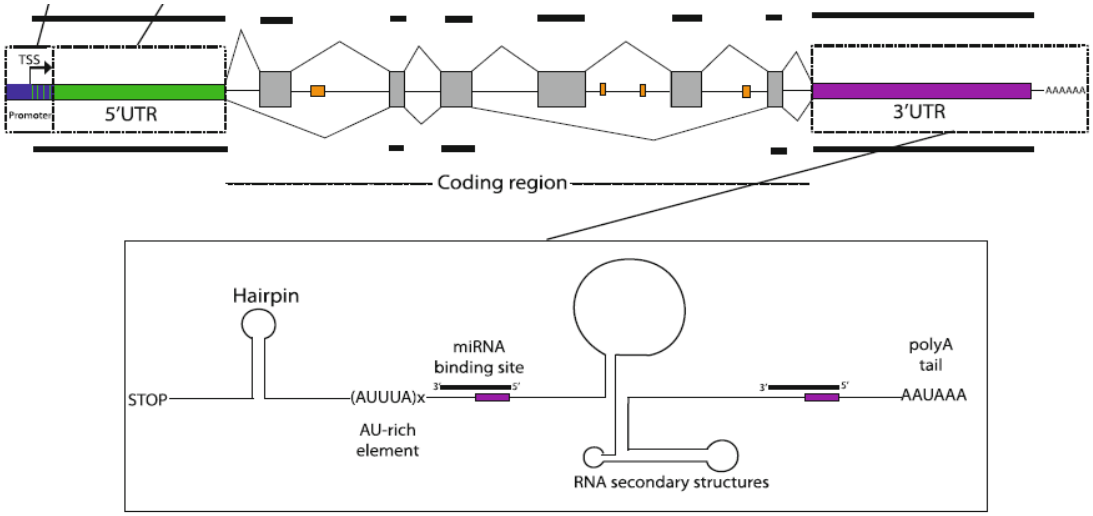

Figure 11. 3’UTR is a regulatory element in a typical mRNA. Modified from [151].

Cells can generate multiple mRNA isoforms differing only in the 3'UTR length by using a system of alternative cleavage and polyadenylation (APA) [154, 155]. The length of the 3'UTR can affect the expression of the mRNA, since the longer 3'UTR is more likely to possess miRNA binding sites, making the mRNA less stable [156]. The observation that the length of the 3'UTR affects translation efficacy was demonstrated for the first time using the 3'UTR of the luciferase reporter gene. The shorter 19 bp-3'UTR conveyed an approximate 45-fold increase in expression than the WT 156bp-3'UTR [157]. Using global analysis, the effect of 3'UTR isoforms on the gene expression program was tested during T cell activation. It was observed that 86% of changes towards decreased gene expression occurred concomitantly with an extended 3'UTR generated due to different polyadenylation sites in a terminal exon. The observed tendency was tested in the *Hip2* gene (huntingtin interacting protein 2) that uses alternative 3'UTR to control its expression. In activated T cells, expression of *Hip2* transcript with the longer 3'UTR is decreased, whereas with the shorter 3'UTR gene expression increased resulting in increased protein levels [158]. This led to the prediction that the shorter 3'UTR might escape regulation mediated by 3'UTR elements, and therefore would be more stable.
The secondary structure that arises from optimal folding of specific regions within RNA is also emerging as an important determinant of 3'UTR activity and hence the expression of mRNA [159]. The most common example of secondary structure is the hairpin stem-loop RNA structure which is recognized by many RNA-binding proteins (RBP) [160]. Furthermore, binding of the RBP can alter the local secondary structure of mRNA and allow access of miRNA to the target sites promoting miRNA-mediated repression [161].

2.3.2.1. MicroRNAs and 3'UTR

Genome-wide interspecies comparison revealed a distribution of motifs within the 3'UTR that are 8bp on average, and half of all identified motifs corresponded to miRNA target sites [162]. miRNAs are ~21-24nt single-stranded RNA noncoding molecules which interact with mRNA and regulate its translation. In 1993, the first miRNA gene *lin-4* was discovered and studied using genetic studies in the larval development of *C. elegans* [163]. In the miRBase database (Release 21), which is the most commonly used bioinformatics tool to archive and annotate miRNA sequences, there are currently 28645 hairpin precursor miRNAs registered, which express 35828 mature miRNA products in 223 species [164]. miRNA genes tend to be distributed as clusters in a genome. For example, in humans approximately 50% of miRNA

genes have a genomic distribution in the form of clusters and are transcribed as a single polycistronic primary transcript that is processed to produce several miRNAs [165]. Furthermore, many miRNAs have paralogs, based on the seed sequence, comprising a particular miRNA family. Hence, it is to be expected that there is high redundancy among them, and that mutations in a particular miRNA do not result in an abnormal phenotype but only mutations of all paralogs results in a synthetic abnormal phenotype [166].

According to the genomic location, there are four groups of miRNA: 1) intronic miRNA in noncoding transcripts; 2) exonic miRNA in noncoding transcripts; 3) intronic miRNA in protein-coding transcripts; 4) exonic miRNA in protein-coding transcripts [167].

miRNA genes are transcribed into primary pri-miRNA which can be more than 1000 nt long, containing RNA hairpins (Figure 12). Such a pri-miRNA is processed by Drosha (double-stranded RNA-specific endoribonuclease) in the nucleus and produce a 60-70nt stem-loop intermediate called precursor miRNA (pre-miRNA) [168]. The pre-miRNA is then transported from the nucleus to the cytoplasm by the exportin 5/RanGTP complex. In the cytoplasm, Dicer enzyme cleaves the pre-miRNA into 21-25nt miRNA/miRNA* duplex, which is then incorporated into the Argonaute proteins (Ago1-4) followed by RISC (RNA-induced silencing complex) assembly. After RISC assembly, the miRNA duplex is unwound and one of the miRNA strands is discarded (the “passenger” strand), whereas the other strand is retained (the “guide” strand) to exert its function on the targeted mRNA. In general, one strand is selected preferentially as a guide strand (either 5’ or 3’-arm); however, there are miRNAs in which both strands are equally used. miRNA bind to mRNA through partial/perfect base pairing between 2 – 7 nucleotides at the 5’ end of the miRNA called the "seed sequence" and miRNA-responsive element (MRE) on mRNA [169]. It should be noted that miRNA need to be assembled into the RNA-induced silencing complex (RISC) in order to regulate targeted mRNA [170, 171]. miRNA-binding sites are preferentially found within the 3’UTR rather than within the 5’UTR or the coding region of the mRNA. This is most likely because the miRNA-programmed RISC complex is required to remain attached to the target mRNA in order to effectively induce silencing, otherwise this would be counteracted by movement of the ribosome along the transcript [172].

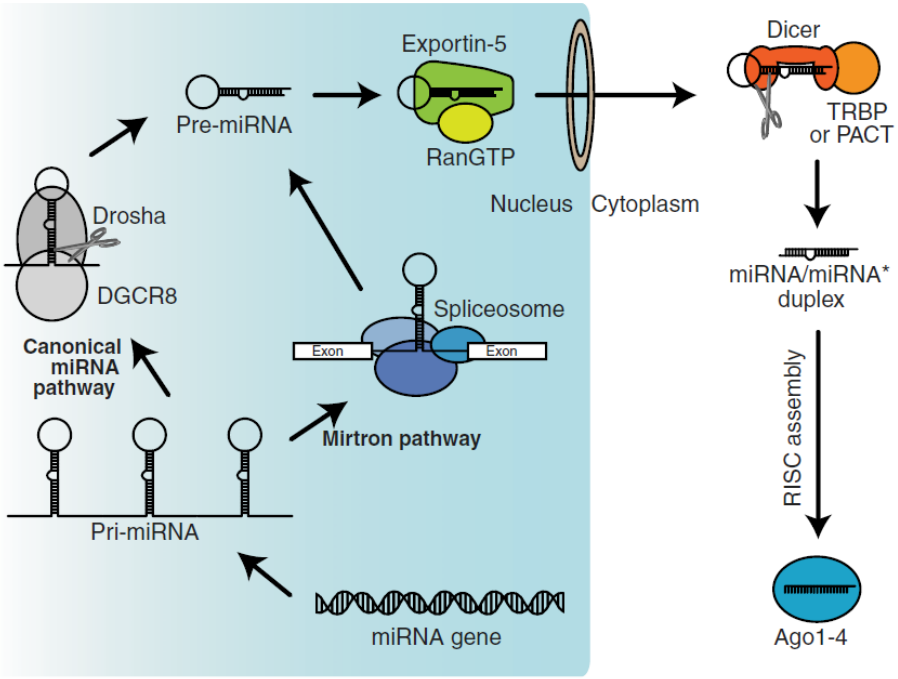

Figure 12. Biogenesis of a microRNA. Details are described in the text. *Modified form [170].*

Expression of most miRNA is regulated through developmental and tissue-specific signaling [173]. Transcription is a major level of regulation for miRNA biogenesis. miRNAs are transcribed by RNA polymerase II or polymerase III [174, 175]. Promoters of miRNA share similar characteristics to the promoters of protein-coding genes and it seems that the same mechanisms might be applied to miRNA biogenesis [176, 177]. Although miRNAs tend to be distributed in clusters, they are transcribed as a long polycistronic primary transcript, which suggests that miRNAs have cluster-specific promoters [165]. It was also shown that each miRNA in the same genomic cluster might be transcribed and regulated independently [178].
A global decrease of miRNA levels is observed in cancer [179]. There are two proposed mechanisms for the downregulation of miRNA in cancer. One postulates the genetic dysregulation of the members (Drosha, Dicer, XPO5, AGO etc.) involved in miRNA processing pathways [180-183], whereas the second mechanism suggests that binding of MYC to the miRNA promoter [184] causes impaired miRNA biogenesis.

2.3.2.2. AU-rich elements and 3´UTR

The most well characterized regulatory element is the adenine-uridine (AU)-rich element (ARE) situated at the 3'UTR of mRNAs [185]. ARE can lead to mRNA stabilization or to fast degradation through a process called ARE-mediated mRNA decay (AMD) under stress

situations. mRNA containing AU-rich elements encodes proteins such as cyclins, cytokines, growth factors and proto-oncogenes, all requiring spatial and temporal control [185, 186]. AREs are divided into three classes: Class I ARE contain1 to 3 copies of the AUUUA pentamer within U-rich regions. This class has been reported and described in mRNA encoding nuclear transcription factors c-fos and c-myc as well as cytokines IL-4 and IL-6 [185, 187, 188]. Class II AREs contain 5-8 copies of overlapping AUUUA pentamers and they are found in mRNA of GM-CSF, IL-2, tumor necrosis factor α (TNFα) and interferon α (IFNα) [187, 188]. Class III AREs lack the AUUUA motif, but contain U-rich sequences and are found in c-jun and p53 mRNA [185, 187, 188]. Although the ARE classification is based on the AUUUA pentamer, there is a tendency of categorizing them according to their biological function [185].

ARE motifs are specifically recognized by *trans*-acting factors referred to as AU-binding proteins (AUBP), which lead to either stabilization or destabilization of a target mRNA. Most AUBPs have a tissue or cell-type specific expression [189], with ARE secondary structure having an important role in ARE-BP activity. Many mRNAs (e.g. c-myc, c-fos, GM-CSF) are able to bind more than one AUBP [185]. The three most extensively studied AUBPs are AUF1, HuR and TTP.

3. AIM OF THE THESIS

Since the mid-1990´s, calretinin, a calcium-binding protein, has widely been used as a mesothelioma diagnostic marker. Several studies reported that calretinin could be used as a prognostic marker because higher calretinin expression in mesothelioma samples was associated with better prognosis.

The role of calretinin, as well as the molecular mechanisms driving calretinin expression, in mesothelioma is unknown. Calretinin appears to be essential for the epithelioid mesothelioma type, as calretinin knockdown using a lentiviral short-hairpin approach led to impaired cell viability and proliferation and triggered apoptosis [140]. In this thesis, we aimed to investigate the molecular mechanisms underlying calretinin expression in mesothelioma.

AIM 1: INVESTIGATION OF TRANSCRIPTIONAL CONTROL OF CALRETININ EXPRESSION IN MPM

AIM 2: POST-TRANSCRIPTIONAL REGULATION OF CALRETININ EXPRESSION IN MPM

4. PUBLICATIONS

4.1. Identification of *cis*- and *trans*- acting elements regulating calretinin expression in mesothelioma cells

Manuscript published in Oncotarget on February 01, 2016

Contribution: EFB designed the study. JKR carried out cloning promoter into reporter system, *in silico* analysis, introducing mutation into the construct, dual luciferase assays, hypomethylating treatment, quantification of gene expression Western blots, EMSA assay, and ChIP (1A, B, C / 2A, B, / 3A, B, C / 4A, B, C / 5A, B, C, D, E). EFB performed cell-cycle synchronization experiment; GZ and EFB performed immunofluorescence (6B) and GZ carried out Western blot (6A). EK generated two mutational constructs. DD helped with ChIP analysis. BCC and KCJ conducted the analysis of the promoter on the TCGA data (2C, Table 1). RS provided tools for ChIP analysis.

JKR and EFB drafted the manuscript. BS, JKR, RS, RAS, KCJ and BCC were involved in critically revising the manuscript.

Identification of *cis*- and *trans*-acting elements regulating calretinin expression in mesothelioma cells

Jelena Kresoja-Rakic[1], Esra Kapaklikaya[1], Gabriela Ziltener[1], Damian Dalcher[2], Raffaella Santoro[2], Brock C. Christensen[3], Kevin C. Johnson[3], Beat Schwaller[4], Walter Weder[5], Rolf A. Stahel[1], Emanuela Felley-Bosco[1]

[1]Laboratory of Molecular Oncology, Clinic of Oncology, University Hospital Zürich, Zürich, Switzerland

[2]Institute of Veterinary Biochemistry and Molecular Biology, University of Zürich, Zürich, Switzerland

[3]Departments of Epidemiology, Pharmacology and Toxicology and Community and Family Medicine, Geisel School of Medicine at Dartmouth, Hanover, NH, USA

[4]Anatomy, Department of Medicine, University of Fribourg, Fribourg, Switzerland

[5]Division of Thoracic Surgery, University Hospital Zürich, Zürich, Switzerland

Correspondence to: Emanuela Felley-Bosco, **e-mail:** emanuela.felley-bosco@usz.ch

Keywords: *malignant pleural mesothelioma, calretinin, promoter, NRF-1, cell-cycle regulated expression*

Received: *September 08, 2015* ***Accepted:*** *January 18, 2016* ***Published:*** *February 01, 2016*

ABSTRACT

Calretinin (*CALB2*) is a diagnostic marker for epithelioid mesothelioma. It is also a prognostic marker since patients with tumors expressing high calretinin levels have better overall survival. Silencing of calretinin decreases viability of epithelioid mesothelioma cells. Our aim was to elucidate mechanisms regulating calretinin expression in mesothelioma. Analysis of calretinin transcript and protein suggested a control at the mRNA level. Treatment with 5-aza-2′-deoxycytidine and analysis of TCGA data indicated that promoter methylation is not likely to be involved. Therefore, we investigated *CALB2* promoter by analyzing ~1kb of genomic sequence surrounding the transcription start site (TSS) + 1 using promoter reporter assay. Deletion analysis of *CALB2* proximal promoter showed that sequence spanning the −161/+80bp region sustained transcriptional activity. Site-directed analysis identified important *cis*-regulatory elements within this −161/+80bp *CALB2* promoter. EMSA and ChIP assays confirmed binding of NRF-1 and E2F2 to the *CALB2* promoter and siRNA knockdown of NRF-1 led to decreased expression of calretinin. Cell synchronization experiment showed that calretinin expression was cell cycle regulated with a peak of expression at G1/S phase. This study provides the first insight in the regulation of *CALB2* expression in mesothelioma cells.

INTRODUCTION

Malignant pleural mesothelioma (MPM) are tumors originating from the surface serosal cells of the pleura [1]. With the established standard of care, i.e. pemetrexed with platinum-based chemotherapy, MPM patients have a median survival of one year [2], therefore it is important to better understand the biology of mesothelioma development that would allow for designing and developing novel and more effective therapy strategies.

Calretinin (CR, gene *CALB2*) is a ~30kDa calcium-binding protein belonging to the EF-hand family [3]. In 1996, Doglioni et al demonstrated specificity of calretinin immunoreactivity in mesothelioma compared to other tumor types [4]. Currently, calretinin is the most commonly used diagnostic mesothelioma marker [5]. Reactive mesothelial cells and malignant mesothelioma cells show nuclear and cytosolic calretinin staining allowing differentiation of mesothelioma from adenocarcinoma [6]. MPM can be categorized into three groups based on the histological characteristics: epithelial, biphasic and sarcomatoid characterized by strong, intermediate and weak (absent) calretinin immunoreactivity, respectively [7]. Three independent studies suggested that calretinin can be also utilized as a prognostic marker since strong calretinin immunostaining correlated with improved survival [7–9].

In two epithelioid mesothelioma cell lines, down-regulation of calretinin by a lentiviral short hairpin

approach impaired cell proliferation and triggered apoptosis via the intrinsic caspase-9-dependent pathway [10] suggesting that calretinin is important for epithelioid mesothelioma cell survival.

Calretinin is physiologically expressed in different neuronal cell populations, e.g. in the retina and the cerebellum [11] as well as in Leydig cells, Sertoli cells and adipocytes [5]. Little is known about the mechanisms regulating calretinin expression in various tissues or in cancer. It has been reported that the mouse *Calb2* and human *CALB2* promoter region contain TATA and CAAT boxes [12]. A mouse *Calb2* promoter fragment (–115/+54bp) was shown to be active in neuronal and cancer cells [13, 14]. In human colon cancer cells, calretinin expression is downregulated by butyrate, a substance that induces cell differentiation [15]. Butyrate–induced calretinin downregulation is mediated through butyrate dependent repressive elements which are not operational in mesothelioma cells [16].

In this study, our aim was to investigate and characterize transcriptional control of calretinin expression in mesothelioma cells.

RESULTS

Calretinin protein levels correlate with *CALB2* transcript levels across a panel of different mesothelioma cell lines

To characterize calretinin expression, we assessed mRNA and protein levels across a panel consisting of 11 mesothelioma cell lines, one SV-40 immortalized human pleural mesothelial cell line (MeT5A) and HEK293 cells (Figure 1A and 1B). Five cell lines were of epithelioid type (NCI-H226, ACC-MESO-4, ZL55, MERO-84, and ZL5), four were biphasic (MSTO-211H, MERO-82, MERO-83, SPC111) and two were sarcomatoid (ZL34 and ONE58). Levels of *CALB2* transcript were significantly higher ($p = 0.0285$) in epithelioid histotype. Calretinin was also expressed in HEK293 cells, which might be expected since HEK293 cells are of kidney embryonic origin [17] and both kidney and mesothelium originate from the mesoderm. Importantly, *CALB2* mRNA expression was strongly positively ($p = 0.0002$) correlated with calretinin protein levels (Figure 1C), suggesting that calretinin expression could be regulated either through copy number variation or through control of mRNA levels.

Calretinin promoter is not inhibited by DNA methylation in mesothelioma cell lines and tumor samples

Analysis of genomic copy number abnormalities (CNA) in mesothelioma, using arrayMap [18] showed no indications of genetic alteration in *CALB2* gene (Supplementary Figure 1) while a study has described loss at 16q22 in two out of 18 mesothelioma cases [19], indicating that upregulation of calretinin expression in mesothelioma is not linked to increased gene copy number.

We then took advantage of the known differential expression of calretinin between epithelioid and sarcomatoid mesothelioma to explore whether this might represent a hint that calretinin expression is controlled by methylation of the promoter, since this mechanism controls the expression of several genes in MPM [20]. A putative *CALB2* proximal promoter region was defined based on two criteria: the observation that most human promoters are found between –800 upstream and +200 bp downstream of putative transcription start site (TSS; +1) [21] and according to publicly available data on high throughput ChIP data reported in the UCSC browser (Supplementary Figure 2). *In silico* analysis (http://www.bioinformatics.org/sms2/cpg_islands.html) of the –838/+80bp region of *CALB2* promoter using the method defined by Gardiner-Garden [22], documented the presence of CpG islands and a high GC content starting from 338bp upstream of the TSS. Inactivation of gene expression by methylation of CpG islands present in promoters is a common epigenetic mechanism in health and diseases [23]. Therefore, to test the hypothesis that calretinin expression might be partly driven by epigenetic mechanisms, ZL55 (high-calretinin, epithelioid) and SPC111 (low-calretinin, biphasic) cells were treated for seven days with the hypomethylating agent 5-aza-2′-deoxycytidine (5-Aza-CdR) at 100 and 250 nM and the expression of calretinin was evaluated. The expression of two cancer-associated testis antigens *CTAG1B* and *MAGE-C1* genes was used as a positive control, since their promoters are known to be controlled by DNA methylation [24]. Although the expression of *CTAG1B* and *MAGE-C1* mRNA was strongly enhanced by 5-Aza-CdR treatment in SPC111 and ZL55 cells (Figure 2A), the expression of calretinin mRNA and protein (Figure 2A and 2B) did not increase. On the contrary, treatment with 5-Aza-CdR resulted in a decrease in calretinin protein levels, especially in SPC111 cells. Moreover, the methylation status of nine CpG sites in the *CALB2* promoter of epithelioid ($n = 57$) and biphasic ($n = 23$) mesothelioma samples from The Cancer Genome Atlas (TCGA) database generally showed low methylation levels, particularly at CpG sites nearest to the TSS (Figure 2C). *CALB2* promoter CpG methylation was not significantly negatively correlated with *CALB2* gene expression in epithelioid or biphasic tumors (Table 1). As control, the methylation status of *MAGEC1* promoter was also investigated. The region of the *MAGEC1* promoter exhibits high levels of methylation (Supplementary Figure 3) and the gene is lowly expressed in TCGA mesothelioma tumors. Importantly, several of the CpGs located at or near the transcriptional start site are significantly negatively correlated with gene expression (Supplementary Table 2) and the gene is lowly expressed

in both biphasic and epithelioid tumors. The high levels of DNA methylation and low levels of expression coupled with our experimental evidence of reactivation of gene expression with treatment with hypomethylating agents suggest that *MAGEC1* serves as an appropriate control gene in our study. Taken together, our data suggest that promoter methylation is not driving differential expression of calretinin between mesothelioma histotypes.

The –161/+80bp *CALB2* promoter region drives expression of luciferase reporter in mesothelioma cells

We then investigated the activity of the *CALB2* promoter to define *cis*-regulatory sequences important for calretinin expression. Four 5′-deletion promoter fragments (–838, –419, –264, –161bp upstream and +80bp downstream of TSS +1) were cloned into the firefly

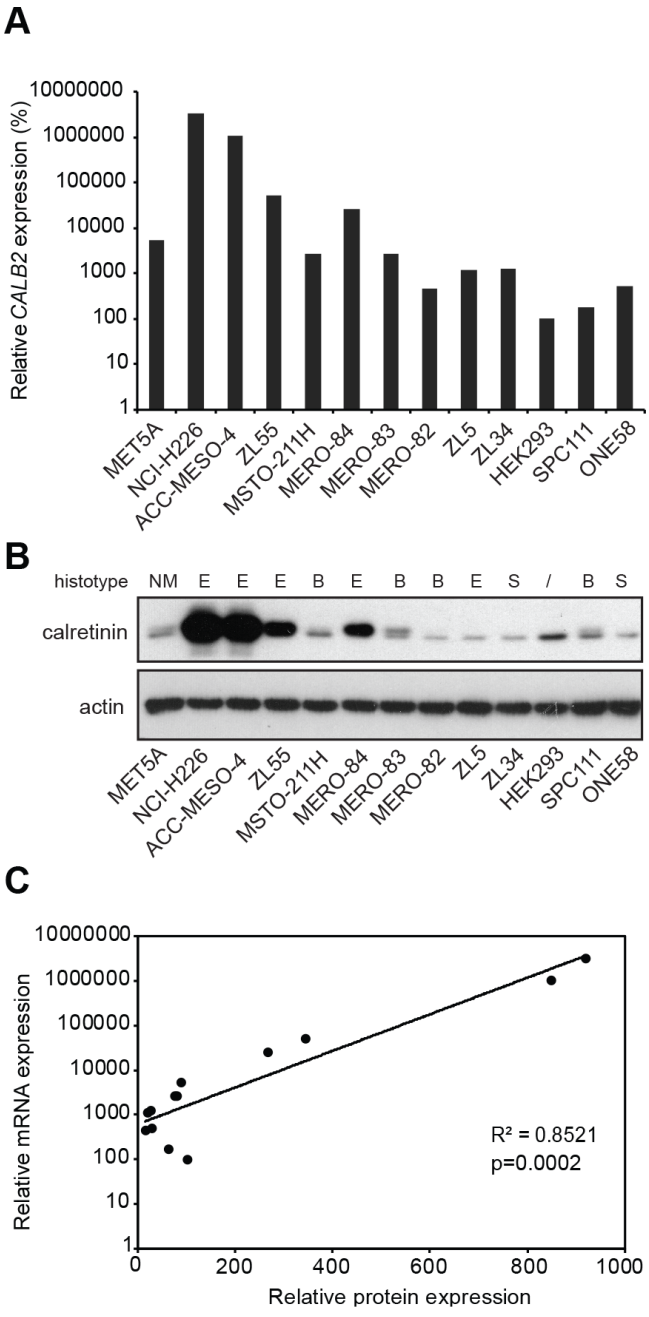

Figure 1: Differential expression of calretinin in a panel of 13 cell lines. (**A**) Quantitative RT-PCR analysis of *CALB2* expression in 11 mesothelioma cell lines, one immortalized mesothelial cell line (MET5A) and HEK293 cells using histones as an internal control. Levels are shown relative to the HEK293 cells according to the –ΔΔCt method. (**B**) Western blot analysis of calretinin protein levels in the same panel of cell lines. Actin was used as loading control. (**C**) Relative mRNA levels are plotted against the relative protein levels; each dot represents a cell lines as in A and B.

luciferase basic reporter pGL3-B (Figure 3A). To test transcriptional activity of the promoter constructs, NCI-H226, Zl55, SPC111 and ONE58 cells were transiently transfected with the promoter constructs along with the pRL-TK plasmid as an internal control. The shortest –161/+80bp *CALB2* promoter construct appeared to be as active as the other longer sequences in all tested cell lines (Figure 3B) defining this fragment as the minimal *CALB2* promoter. The 240bp minimal promoter has more activity than any of the longer versions (Supplementary Figure 4) indicating the presence of negative regulators. In addition, –161/+80bp *CALB2* promoter activity was correlated ($p = 0.017$) with *CALB2* expression (Figure 3C) with the lowest transcriptional activity observed in ONE58 cells which express extremely low levels of calretinin, and the highest transcriptional activity in NCI-H226 cells, expressing the highest levels of calretinin. Since the –161/+80bp fragment was sufficient to drive reporter expression in the tested mesothelioma cells, the next step was to further characterize its *cis*-regulatory elements.

Mutation of E2F2/NRF-1-like site strongly reduced promoter activity

To search for putative protein binding sites, *in silico* analysis was performed on the sequence from –161bp to +80bp of the *CALB2* promoter using MatInspector software [25]. Most frequently identified binding sites were the ones for NRF-1 (nuclear respiratory factor 1), as well as for E2F family members and CREB (cAMP

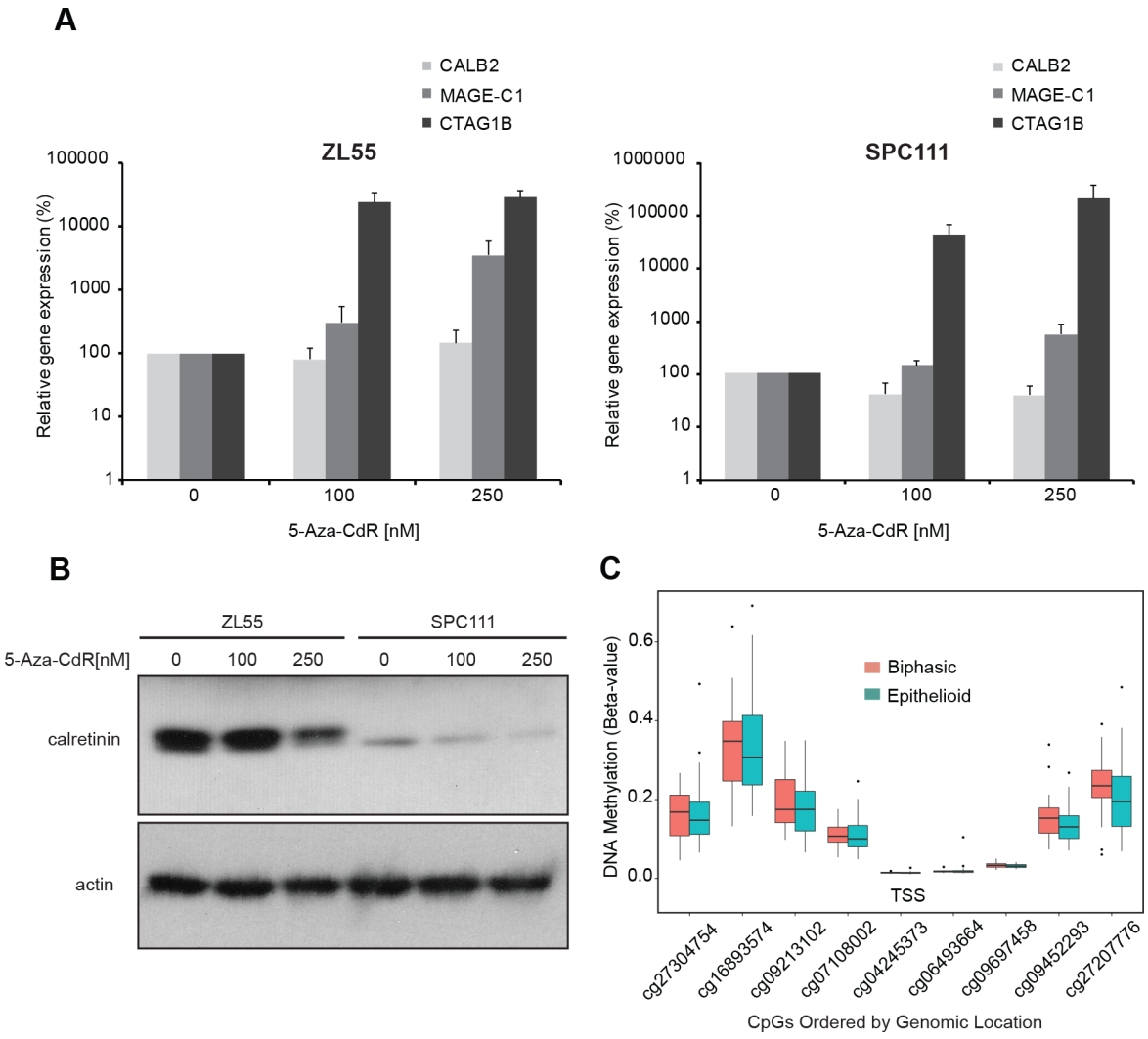

Figure 2: Promoter methylation does not regulate calretinin expression in cell lines and tumor samples. (**A**) ZL55 and SPC111 cells were treated for 7 days with the hypomethylating agent 5-Aza-CdR (100 nM and 250 nM). Analysis of mRNA showed no change in *CALB2* expression but strong upregulation of *MAGE-C1* and *CTAG1B* expression. Mean ± SD, $n = 3$. (**B**) Calretinin protein levels decreased upon 5-Aza-CdR treatment in both ZL55 and SPC111 cells. Representative of three independent experiments. (**C**) CpG sites in the promoter region of *CALB2* from the Illumina HumanMethylation450 array are shown in 5′ to 3′ order versus methylation beta-value which represents the percent methylation of the sample. Mesotheliomas are stratified by tumor histology, epithelioid ($n = 57$), and biphasic ($n = 23$).

Table 1: Correlation between *CALB2* gene promoter CpG methylation and *CALB2* expression (*Spearman's test)

cgID	Chromosome	Position	Epithelioid Correlation	Epithelioid *P*-value*	Biphasic Correlation	Biphasic *P*-value*
cg27304754	16	71392088	0.12	0.385	0.45	0.034
cg16893574	16	71392095	–0.14	0.296	0.42	0.047
cg09213102	16	71392373	–0.14	0.312	0.35	0.122
cg07108002	16	71392377	–0.24	0.068	0.23	0.285
cg04245373	16	71392615	0.02	0.893	–0.26	0.223
cg06493664	16	71392628	0.04	0.749	–0.41	0.053
cg09697458	16	71392748	–0.09	0.502	0.05	0.823
cg09452293	16	71392838	–0.16	0.230	0.05	0.823
cg27207776	16	71393801	–0.25	0.063	–0.07	0.740

response element binding protein) (Figure 4A). The activation of the latter has been observed *in vitro* after exposure of mesothelial cells to asbestos [26]. Promoter constructs containing selective mutations were created using a site-directed mutagenesis approach (Figure 4B) and their transcriptional activity was measured in ZL55 and SPC111 cells. All mutated promoter constructs showed significantly decreased transcriptional activity compared to the control construct in both cell lines (Figure 4C). The transcriptional activity of the E2F2/NRF-1 (–64)-like mutant resulted in a 80% decrease compared to the wild-type promoter sequence suggesting that E2F2 or NRF-1 might be important for the transcriptional control of calretinin expression. A strongly reduced activity of the E2F2/NRF-1 mutant construct was also observed in HEK293 cells (Supplementary Figure 5), indicating that this transcriptional control is not restricted to mesothelioma cells, but possibly to other cells of mesodermal origin.

In vitro and *in situ* binding of NRF-1 and E2F2 to E2F2/NRF-1-like binding motif in the *CALB2* promoter

Alignment of the *CALB2* promoter ortholog nucleotide sequences (Supplementary Figure 6) revealed that the stretch containing the putative binding sites for E2F2 or NRF-1 (–75 to –51bp) shows the highest degree of identity across various species (Figure 5A). Therefore, to experimentally demonstrate potential functionally relevant binding of E2F2 or NRF-1, an EMSA assay was performed using biotin labeled 25-bp oligonucleotide containing the putative E2F2/NRF-1 binding site (Figure 5B). Upon incubation of ZL55 nuclear extract with the specific labeled probe, DNA-protein complexes C1, C2 and C3 were formed (Figure 5B, lane 2). All three DNA-protein complexes were diminished with increasing amounts of unlabeled competitor (Figure 5B, lane 3 and 4) but were not outcompeted using an unrelated oligo competitor (data not shown). However, in the reaction with mutated competitor, the C3 complex was detected again but not the complexes C1 and C2 (Figure 5B, lane 5). Addition of a specific antibody against NRF-1 resulted in the appearance of a heavier complex (Figure 5B, lane 6) and a decrease of the C2 complex, while no change was observed with an anti-E2F2 antibody (Figure 5B, lane 7).

To confirm *in situ* in cultured cells the presence of NRF-1 or E2F2 on the *CALB2* promoter, chromatin immunoprecipitation assay (ChIP) was performed in ZL55 cells with antibodies against NRF-1 and E2F2. The promoter of *CDC25A* gene, a known E2F target [27] lacking a binding site for NRF-1, was used as a negative control for NRF-1 and as a positive control for E2F2. Chromatin immunoprecipitation assay showed that compared to *CDC25A*, NRF-1 was significantly enriched in *CALB2* promoter whereas E2F2 bound to both, *CDC25A* and *CALB2* promoters (Figure 5C). These data demonstrate that NRF-1 and E2F2 are able to bind to *CALB2* promoter.

NRF-1 expression levels are likely not responsible for differences in calretinin expression levels observed in the various MPM lines since NRF-1 levels were rather homogenous in the tested cell lines (Figure 5D). However, silencing of NRF-1 resulted in calretinin downregulation in SPC111 cells (Figure 5E and Supplementary Figure 7). Taken together, these data provide evidence that NRF-1 is an important positive regulator for calretinin expression.

Calretinin expression is cell cycle-dependent

Besides NRF-1, members of the E2F family were among the most frequently identified putative transcription factors binding to the –161/+80bp *CALB2* promoter

region and E2F2 binding was detected by ChIP analysis. Since E2F family members regulate cell cycle-dependent expression of many genes [28], we hypothesized that calretinin expression might be regulated in a cell cycle-dependent manner. To investigate the kinetics of calretinin expression, ZL55 and SPC111 cell were exposed to double thymidine treatment followed by nocodazole treatment, after which calretinin expression was assessed at different time points (Figure 6A and 6B). The progression through the cell cycle was monitored by flow cytometry analysis (data not shown), while the expression pattern of cyclin A and cyclin E (Figure 6A) served to document the transition of cells from G1/S to M phase [29, 30]. Double thymidine treatment synchronized the majority of cells at the G1/S transition, where high levels of calretinin expression were observed (Figure 6A). Calretinin expression then significantly decreased 5 h after thymidine removal when the majority of cells were in the G2/M phase. The same

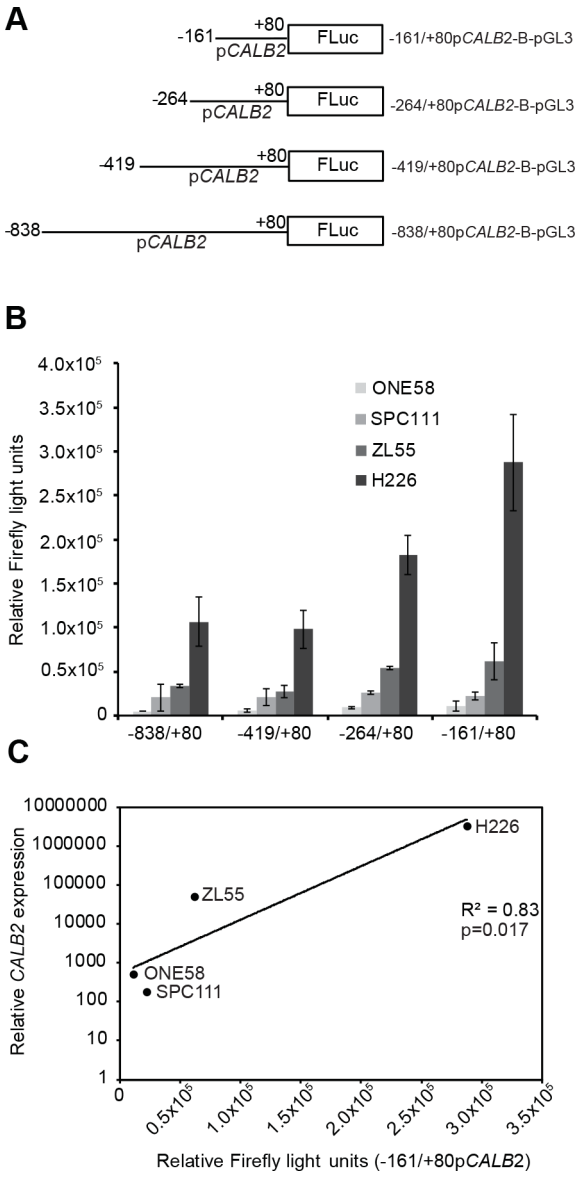

Figure 3: Transcriptional activity of the minimal *CALB2* promoter is proportional to calretinin expression. Transcriptional activity of different promoter constructs was assessed by transient transfection and dual luciferase assay using pTK-RL as an internal control. (**A**) 5′-deletion constructs of the *CALB2* promoter engineered in the pGL3-basic (pGL3-B) luciferase reporter plasmid. Lines represent *CALB2* promoter fragment; the name and the size are indicated by nucleotide position upstream (–) or downstream (+) relative to the transcription start site (+1). (**B**) *CALB2* promoter activity in ONE58, SPC111, ZL55 and NCI-H226 cells, which express different levels of calretinin. To allow for comparison of the absolute promoter activity between the cell lines, Firefly light units were multiplied by a correction factor that compensates for differences in the transfection efficac . The correction factor was based upon the Renilla Light Units (ReLU) of the internal control, pTK-RL, and was calculated by dividing the mean ONE58 ReLU by the mean of ZL55, SPC111 and H226 ReLU for each construct. Mea*n* ± SD, *n* = 3. (**C**) Relative mRNA abundance is plotted versus the relative Firefly light units reflecting absolute –161/+80bp *CALB2* activity for the indicated cell lines.

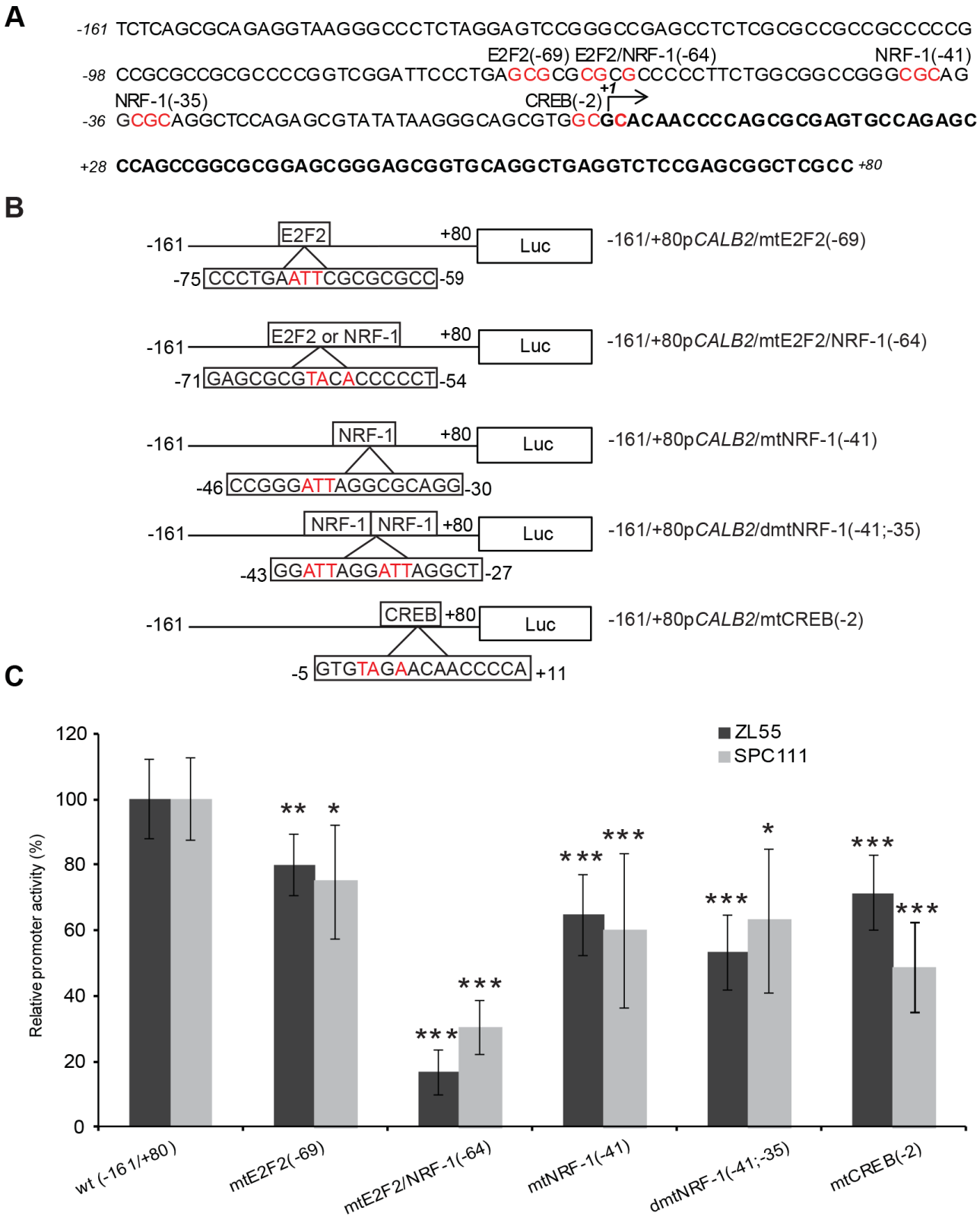

Figure 4: Effect of site-directed mutagenesis of transcription factor binding sites on the –161/+80bp *CALB2* promoter activity. (**A**) Predicted potential TF binding sites (highly conserved nucleotides selected for site-directed mutagenesis are colored in red). (**B**) A series of mutant constructs harboring mutated nucleotides (in red) of predicted E2F2, NRF-1 and CREB binding sites. Numbers indicate the position of the first (from the left to the right) mutated nucleotide. (**C**) The wild-type reporter plasmid expression was arbitrarily set to 100% and the reporter activity of the mutants was expressed as a percentage of the wild-type construct. Mean ± SD $n = 3$; *$p < 0.05$; **$p < 0.01$; ***$p < 0.005$.

kinetics of transient and cell cycle-dependent calretinin expression was observed by immunofluorescence (Figure 6B), suggesting that calretinin expression is cell cycle- dependent, being upregulated in G1/S phase of the cell cycle.

DISCUSSION

In the present study we found *cis*-regulatory sequence elements that are essential for calretinin expression in mesothelioma cells, and identified NRF-1/E2F2 as transcription factors binding to this regulatory sequence.

Mechanisms regulating calretinin expression have been investigated in neuronal cells and colon adenocarcinoma cells, whereas in mesothelioma cells they have not been thoroughly explored yet. A 1.5 kb stretch of the mouse *Calb2* promoter (–1485/+60bp) was demonstrated to drive reporter expression in cultured neuronal cell derived from primary embryonic mouse brain tissue [12]. Additionally, a bipartite butyrate-responsive element in the human *CALB2* promoter was found to act as a repressor element upon butyrate treatment in colon carcinoma but not in mesothelioma cells [16]. However, specific *cis*-regulatory elements positively regulating calretinin expression had not yet been identified

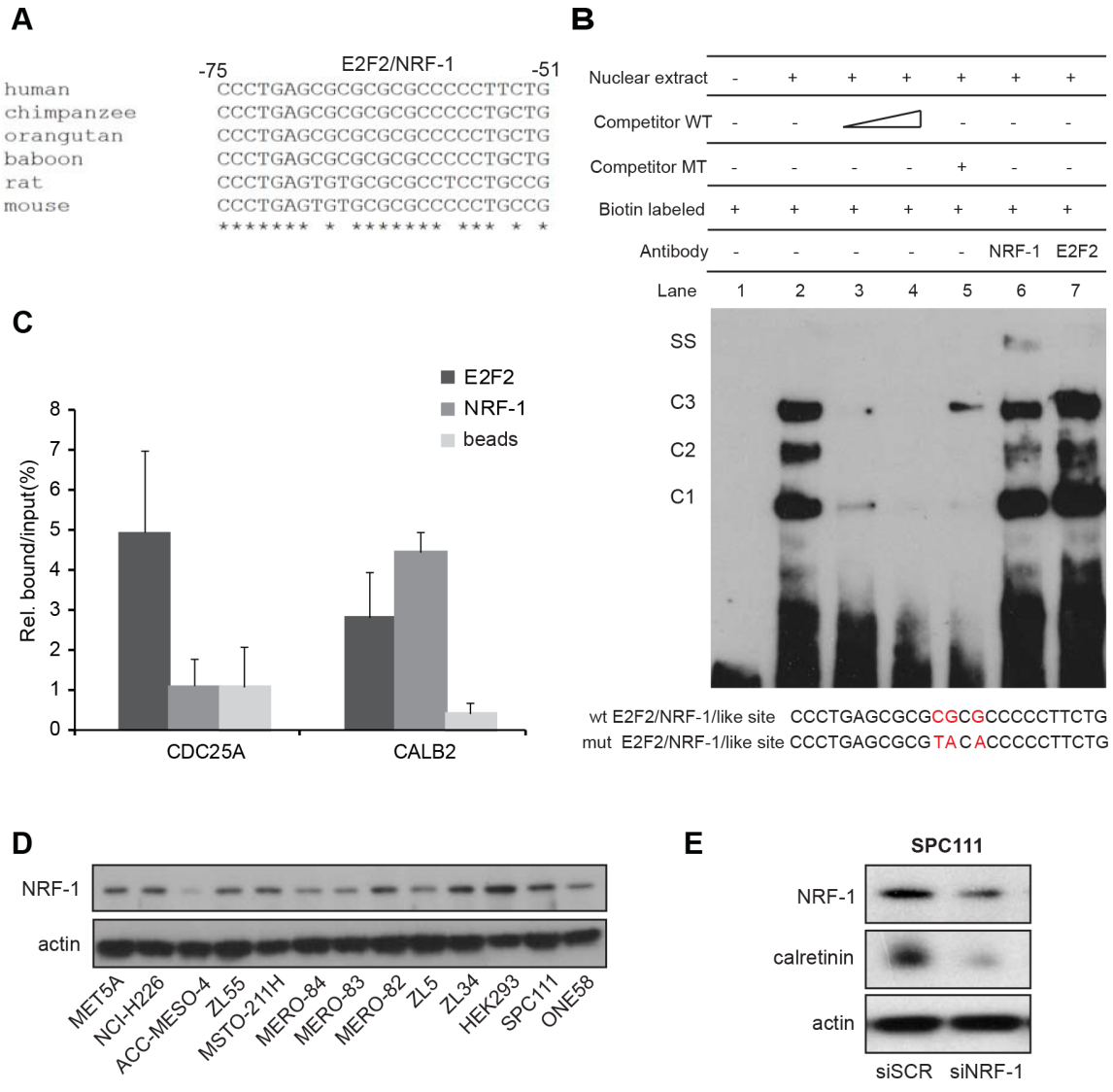

Figure 5: NRF-1 and E2F2 bind to the *CALB2* promoter. (**A**) Nucleotide sequence comparison reveals high homology in the *CALB2* promoter regions of different species in the stretch containing E2F2/NRF-1 predicted binding sites. The analysis was performed using the ClustalW2 software. Asterisks indicate conserved nucleotides. (**B**) EMSA assay showing that a 25bp-oligo containing E2F2/NRF-1-like sites forms three DNA-protein complexes (C1, C2, C3) when incubated in with the ZL55 cells-derived nuclear extracts. Addition of a NRF-1 antibody but not of one against E2F2 resulted in a supershift (SS). (**C**) qPCR analysis on *CDC25A* and *CALB2* promoter regions after ChIP-experiments. Data of two independent experiments were normalized to input. (**D**) NRF-1 protein expression in different cell lines. Actin is used as loading control. (**E**) NRF-1 silencing resulted in downregulation of calretinin expression.

Genomic sequence surrounding transcription start site of *CALB2* gene contains a GC-rich region indicating a possible role for DNA methylation in regulating calretinin expression. However, 5-Aza-CdR, a DNA hypomethylating agent, did not increase calretinin expression in low-calretinin expressing SPC111 cells. It even resulted in a decrease in calretinin expression levels indicating that a certain degree of methylation is required for optimal/maximal *CALB2* transcription. Additionally, we did not observe differential methylation status of *CALB2* promoter between epithelioid and biphasic mesothelioma in tumors from TCGA database or a strong negative correlation of promoter methylation with gene expression. Thus altered DNA methylation of the *CALB2* promoter is very likely not responsible for the differences in calretinin expression levels between low-expressing biphasic/sarcomatoid and high-expressing epithelioid mesothelioma cells.

We further characterized a stretch of ~1 kb (–835/+80bp) of the human *CALB2* promoter by creating four different 5′-deletion promoter reporter constructs and testing their activity in four different mesothelioma cell lines. The –161/+80bp fragment of the *CALB2* promoter was identified as the minimal element resulting in sustained transcriptional activity in all tested mesothelioma cell lines. This is consistent with the previously defined minimal mouse *Calb2* promoter (–115/+54bp) shown to be active in rat cortical neuronal cells, rat cerebellar granule cells, colon adenocarcinoma (WiDr) and mesothelioma cells (SPC111) [13, 14]. Moreover, we found that the transcriptional activity of the –161/+80bp *CALB2* promoter reporter was highly correlated with *CALB2* expression levels. We are aware that using as normalizer pRL-TK plasmid, which carries the Renilla luciferase gene under the HSV-1 TK promoter might theoretically be affected by different levels of

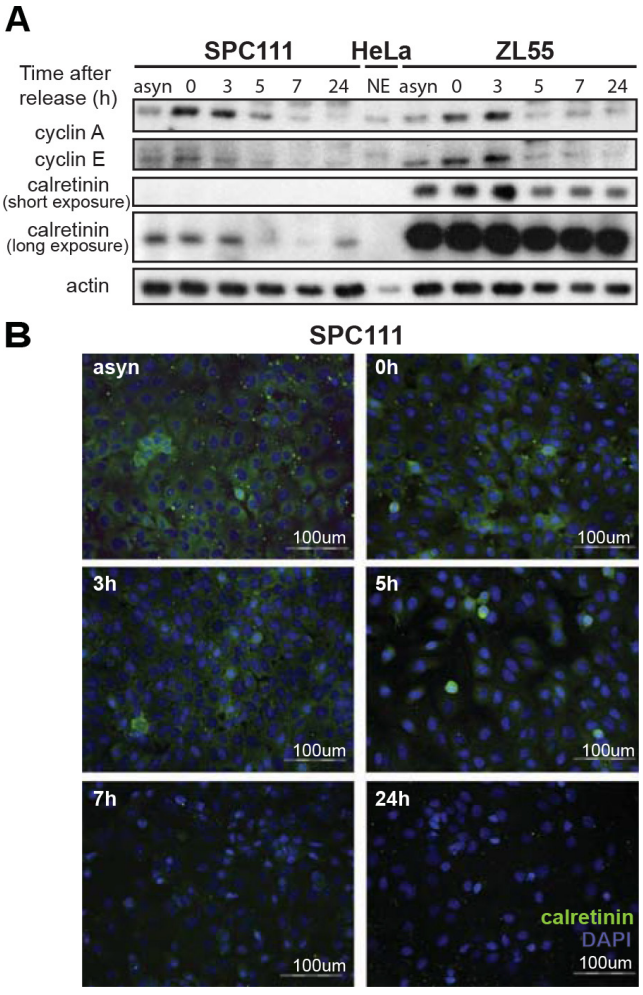

Figure 6: Cell cycle-dependent regulation of calretinin expression. (**A**) Calretinin levels in protein lysates from ZL55 and SPC111 synchronized cells collected at different time points (0 h, 3 h, 5 h, 7 h, 24 h) after removal of thymidine block. Analysis of cyclin A and cyclin E expression was used as a reference for cell cycle progression. A nuclear extract of HeLa cells is used to identify the position of the bands of cyclin A and cyclin E Due to the considerably different calretinin expression levels of ZL55 and SPC111 cells, two different exposure times are presented. (**B**) Immunofluorescence analysis of SPC111 cells using calretinin antibody (green) at the same time points as in (A) Cells nuclei are stained with DAPI (blue), and calretinin immunofluorescence is shown in green

Specificity protein 1 (Sp1) [31]. Rao et al reported recently overexpression of Sp1 in mesothelioma compared to normal mesothelium [32]. However, the variation of Sp1 levels between the lowest and the highest expressing mesothelioma cell line investigated was 4-fold. Since we observed an about 30-fold difference in *CALB2* promoter activity between the different mesothelioma cell lines, we can reasonably assume that the difference is not due to differential expression of the normalizer.

In silico analysis of the human –161/+80bp *CALB2* minimal promoter region revealed a series of potential functional transcription factors (TF) among which NRF-1, E2F2 and CREB were of greatest interest for the following reasons. NRF-1 is a transcription factor implicated in mitochondrial biogenesis and function [33] and was predicted as TF binding to the *CALB2* promoter [34]. Computer-assisted identification predicted *CALB2* to be an E2F target gene as well [35]. Finally, CREB had been demonstrated as an asbestos activated TF in human mesothelial cells [26]. Mutation of E2F2 (–69), NRF-1 (–41), two NRF-1 (–41;–35) and CREB (–2) predicted binding sites significantly reduced *CALB2* promoter activity in ZL55 and SPC111 cells. Mutations in the E2F2/NRF-1 (-64;-63;-61) putative binding sites (GA**GCGCG*CG*C*G***CCCCCT; bold indicates NRF-1 consensus, underlined are the nucleotides mutated in the functional assay) led to a 70–80% decrease in the promoter activity revealing this sequence as the most important *cis*-acting site. In the studies of Billing-Marczak et al [13, 14], an essential element for the promoter activity in the mouse *Calb2* promoter (–115/+54bp) was located at the –91/–80bp position and identified as an "AP-2 like" sequence (**CGCC**CCCTTCCG, in bold are nucleotides overlapping with NRF-1 consensus, underlined are the nucleotides that had been mutated in the functional assay). Although *trans*-acting factors were not identified, functional inactivation in neuronal cells was obtained by mutating one nucleotide also present in the E2F2/NRF-1 putative binding site. The same mutation did not abolish promoter activity in cancer cells [14]. This could be interpreted in two ways: either mutating a single base in the E2F2/NRF-1 binding site is not enough to abolish activity in cancer cells or different transcription factors are operational in neuronal and cancer cells.

A nucleotide sequence analysis revealed that the E2F2/NRF-1-site in the *CALB2* promoter region displays a high degree of identity across different species. An EMSA assay revealed three different DNA-protein complexes and chromatin immunoprecipitation assay showed the presence of both NRF-1 and E2F2 bound to *CALB2* promoter. This is consistent with a previous study demonstrating that NRF-1 is a co-regulator of E2F family members target genes [27]. For all these reasons and since we observed similar expression of NRF-1 in a panel of mesothelioma cell lines with different calretinin expression levels, it is most likely that NRF-1 is a part of a protein complex that altogether activates calretinin expression. Identified proteins interacting with NRF-1 include SP4 (specificity protein 4) [36]. Interestingly, the *in silico* analysis on –160/+80bp *CALB2* promoter region predicted a SP4 binding site located next to the E2F2/NRF-1 site. SP4 expression is tissue specific, primarily expressed in the brain, some epithelial tissues, testis and developing teeth [37] and its coordinate activity with NRF-1 has been described to couple energy generation and neuronal activity [38]. Further studies should investigate whether SP4 is involved in the regulation of calretinin expression.

E2F factors are known to regulate S-phase entry [39]. Consistent with E2F regulating *CALB2* promoter activity, calretinin expression was found to be cell cycle-dependent with a maximum level of expression at G1, and progressively decreased during cell cycle progression. Since calretinin expression is associated with better clinical outcome [7–9], it would be interesting to investigate whether tumor cells positive for calretinin are growth arrested cells.

Knowledge about mechanisms regulating NRF-1 and E2F would help for a better understanding of the complex biology of mesothelioma, where loss of calretinin expression during epithelioid tumor progression is associated with worst outcome (Vrugt et al, ms in preparation).

Investigation of the promoter of another MPM marker, mesothelin, has led to the discovery of a cancer-specific element driving mesothelin overexpression in cancers [40]. In the transgenic MexTAg mouse model, where the mesothelin promoter is placed upstream of the large T antigen, the promoter becomes active in mesothelial cells after asbestos exposure, leading to asbestos induced mesothelioma [41]. This suggests that different transcription factors act on the mesothelin promoter in normal cells and cancer cells. In several studies aiming at driving suicide gene expression in cancer cells, a 2.2kb human *CALB2* promoter fragment was reported not to be specific for cancer cells [42, 43]. In our study, we describe a *CALB2* promoter fragment (–161/+80bp) with activity proportional to calretinin expression and identified NRF-1/E2F2 as specific *trans*-activating factors. Future studies will assess whether this promoter activity is differently regulated in cancer and neuronal cells.

Although this work cannot directly exclude a role of post-transcriptional mechanisms such as RNA stability in regulating calretinin expression in mesothelioma cells, this is the first study defining *trans*-activating factors in a gene that is not only a diagnostic and prognostic marker, but also has a functional role in MPM. Our experiments demonstrate that calretinin expression is activated at the transcriptional level by NRF-1 and E2F2 transcription factors and that expression levels are cell cycle-dependent. Given recent findings about E2Fs involvement in processes such as regulation of cell fate, occasionally linked to

metabolic adaptation [44], our results on the regulation of calretinin expression are expected to have a persistent impact for the understanding of MPM development.

MATERIALS AND METHODS

Cell culture

The following mesothelioma cell lines have been used: ZL55, ZL5, ZL34 and SPC111 from our laboratory [45]; NCI-H226, MSTO-211H, MeT5A [46] were obtained from ATCC; ACC-MESO-4 [47] were obtained from Riken BRC; and MERO-82, MERO-83, MERO-84 [48] and ONE58 [49] were obtained from the European Collection of Cell Cultures. MPM cells established in our laboratory were maintained as described by Thurneysen et al [50] and were authenticated by DNA fingerprinting of short tandem repeat loci (Microsynth, Switzerland). The other cell lines were cultured in D-MEM-F12 supplemented with 15% FCS and 1% Penicillin/Streptomycin solution. HEK293 cells were cultured in DMEM high glucose medium supplemented with 10% FCS and 1% penicillin/streptomycin. All cells were cultured at 37°C in a humidified 5% C_2 atmosphere.

Gene expression analysis

RNA extraction using Qiagen RNAeasy® and cDNAs was prepared from 400–500 ng of total RNA (Qiagen QuantiTect® Reverse Transcription protocol) [51]. Selected gene expression analysis using MIQE [52] compliant protocols was conducted as previously described [51]. Briefl , cDNA was amplified by the SYBR-Green PCR assay and products were detected on a 7900HT Fast real-Time PCR system (SDS, ABI/Perkin Elmer). Relative mRNA levels were determined by comparing the PCR cycle thresholds between cDNA of a specific gene and histone (ΔCt method). The following primers were used: calretinin (5′-GCGAACCGGCCGTACGATGA-3′ and 5′-AGAGGCCCAATTTGCCATCCCCG-3), Mage-C1 (5′-GGGATGTGCTGAGTGGAATAG-3′ and 5′-CTCCC GGTACTCTAGGTAATGT-3′), CTAG1B (NY-ESO-1) (5′-GTCCGGCAACATACTGACTATC-3′ and 5′-GTGA TCCACATCAACAGGGAA-3′).

Western blot analysis

Total protein extracts were prepared by lysing the cells with hot Laemmli sample buffer (60 mM Tris-Cl pH 6.8, 100 mM DTT, 5% glycerol, 1, 7% SDS) and pressed few times through syringes (26 G). Protein concentration was determined using a Pierce™ 660nm Protein Assay (Thermo Scientific). A total of 5 µg protein per extract was separated on denaturing 10–20% gradient SDS-PAGE gels. Proteins were transferred on PVDF transfer membranes (0.45 µm, Perkin Elmer). For Western blotting, membranes were probed with the following primary antibodies: anti-calretinin (Sigma, HPA007306), anti-cyclin E (Santa Cruz Sc-247), anti-cyclin A (Millipore, 06–138), anti-NRF-1 (Santa Cruz SC33771, H300) and mouse anti-actin (#69100) from MP Biomedicals. Membranes were then incubated with the secondary antibody rabbit anti-mouse IgG-HRP (A-5420) from Antell, and goat anti-rabbit IgG-HRP (#7074) from Cell Signaling. The signals were detected by enhanced chemiluminescence (ECL™ Western Blotting Reagents, GE Healthcare) and detected on photosensitive film (Super RX Fuji x-Ray Film, Fujifilm). Relative quantification was assessed using ImageJ (NIH).

5-aza-2′deoxycytidine treatment of cells

On the first day, 2.5×10^4 cells were seeded in a 6-well plate and on the next day the medium was replaced with the medium containing 100 nM and 250 nM of 5-Aza-2-CdR. After 24 h, the drug containing medium was replaced with the fresh medium. On the fifth day, cells were treated again with 5-Aza-2CdR for 24 h and then the medium was replaced by fresh one. Cells were kept in culture for another 24 h after which samples were collected for RT-PCR and Western blot analysis.

In silico analysis

Analysis of the 241bp of the promoter sequence for potential functional transcription factors was carried out using MatInspector software (Genomatix Software GmbH, Munich, Germany) [25].

Level 3 normalized DNA methylation data and clinical information was downloaded from The Cancer Genome Atlas (TCGA) data portal on August 10th, 2015. Normalized *CALB2* gene expression values (RNAseq) from the same TCGA samples were downloaded from the UCSC cancer genome browser on August 10th, 2015. There were 87 mesotheliomas with available Illumina HumanMethylation450 methylation, gene expression, and clinical data. The majority of tumors were epithelioid histology ($n = 57$), with $n = 23$ biphasic, $n = 5$ diffuse not otherwise specified and $n = 2$ sarcomatoid tumors. Patient demographic and tumor characteristics are provided in Supplementary Table 1.

Plasmids constructs and side-directed mutagenesis

To investigate the control of *CALB2* transcription, 838bp, 419bp, 216bp and 161bp upstream and 80bp downstream of the *CALB2* transcription starting site were amplified from genomic DNA ZL55 cells using following primers: F: 5′-ACGT ^{NheI}GCTAGC $^{-838}$ACATTCCCACGATGTCCCTA-3′ (Addgene, 66750); F: 5′- ACGT^{NheI}GCTAGC^{-419}AGCTCTTCCTGCTGTGGA

AGGATCAGAA-3′ (Addgene, 66747); F: 5′-ACGT^{NheI}GC TAGC $^{-264}$AAGTGGTGGATGTACTCAAG-3′ (Addgene, 66746); F:5′- ACGT ^{HindIII}AAGCTT $^{-161}$TCTCAGCGCA GAGGTAAGGG-3′ (Addgene 66745)- along with the reverse primer: R: 5′-ACGT ^{HindIII}AAGCTT $^{+155}$CC ATATTTCCAGGAACTGGGACGCCGTC-3′. In order to avoid ORF shifts due to the start codon of *CALB2* gene but still to include the 5′-UTR, NcoI restriction sites in 3' site of the PCR product along with the restriction site within the forward primer (5′) were used to subclone amplicons into the pGL3-basic vector. To obtain constructs with specific mutations, the QuikChange II Site-Directed Mutagenesis kit (Stratagene) was used (mtE2F (–69)-, Addgene 66743; mtCREB (–2), Addgene 66751; mtNRF-1 (–41), Addgene 66744, dmtNRF-1 (–41;–35)-, Addgene 66741, E2F2/NRF-1 (–64), Addgene 66742).

Transient transfections and reporter assays

To investigate *CALB2* transcription, the dual luciferase assay was used. Briefl , the different constructs were transfected together with Renilla Luciferase (50:1) in cells seeded in 12 wells (100'000 cells/well) as previously described [53]. After 48 h, cells were lysed and analyzed using Dual-Luciferase reporter assay system according to manufacturer's instruction (Promega, Madison, Wi, USA).

Electrophoretic mobility shift assay (EMSA)

Nuclear extracts were prepared using the NE-PER Nuclear and Cytoplasmic Extraction Reagent (Pierce) following the manufacturer's protocol. The binding reaction was performed by incubating 5 µg of nuclear extract with 125fmol biotin labelled oligonucleotide (5′-CCCTGAGCGCGCGCCCCCTTCTG-3′) in the presence of 10mM Tis-HCl pH8.0, 25 mM NaCl, 10 mM DTT, 5% glycerol, 10 mM MgCl, 2 µM ZnCl, 1 µg salmon sperm dsDNA, 1%NP-40 and incubated on ice for 50 min. For competition reactions, the nuclear extracts were incubated with the specific unlabelled oligonucleotides for 10 min prior to addition of biotin-labelled oligonucleotides and incubated 40 min on ice. For the supershift experiments, specific antibodies (NRF-1 ab34682 and E2F2 sc699 ×) were added after 30min incubation of the nuclear extracts and biotin-labeled probes and incubated another 20 min on ice. The samples were separated on a 6% 0.5 × TBE gel, transferred on a nylon membrane and visualized using the Chemiluminescent Nucleic Acid Detection Module (89880) according to the manufacturer's protocol.

Chromatin immunoprecipitation (ChIP)

ChIP was carried out according to the protocol previously described [54]. In brief, cultured cells (4×10^6) were treated with 1% formaldehyde to crosslink proteins to DNA. Chromatin was sonicated using a Bioruptor ultrasonic cell disruptor (Diagenode) to shear genomic DNA to fragments between 100bp and 200bp. Chromatin (20 µg) was diluted tenfold with immunoprecipitation buffer (16.7 mM Tris-HCl (pH 8.1), 167 mM NaCl, 1.2 mM EDTA, 0.01% SDS and 1.1% Triton X-100) and then immunoprecipitated overnight with the corresponding antibodies (NRF-1 Abcam ab34682 and E2F2 Santa Cruz sc699X). After washing, elution and de-crosslinking, the precipitated DNA was purified with phenol-chloroform, ethanol precipitated and quantified by quantitative PCR. Following primers were used: *CDC25A* (5′-TTTCGCGGTAATAGCGGCTC-3′ and 5′-TAGCTGCCATTCGGTTGAGAG-3′) and *CALB2* (5′-AGGTAAGGGCCCTCTAGGAGT-3′ and 5′-CTGCCC TTATATACGCTCTGGA-3′).

RNA interference by siRNA

For the down-regulation of NRF-1 with small interfering RNAs (siRNA), SPC111 cells were transfected with 25 nM Qiagen smartpool or individual siRNAs targeting NRF-1 or control non targeting (NT) siRNA (Thermo Scientific Dharmacon), according to the manufacturer's reverse transfection protocol as previously described [53]. 3×10^4 cells were then plated in and whole cell lysate was prepared after 72 h.

Cell synchronization

Cells were synchronized at the G1/S and G2/M border using a thymidine double-block/nocodazole release protocol [55]. Briefl , cells were seeded in 6-well (5×10^4 cells/well) then 24 h later were treated with 2 mM thymidine for 12 h and released for 12 h in fresh medium before the second block was performed for another 12 h with 2 mM thymidine. Cells were then washed three times in phosphate buffer saline (PBS) and either collected (hours after treatment = 0) or released in fresh medium containing 40 ng/ml nocodazole to induce mitotic arrest (G2/M) for different time periods.

Immunofluorescence

SPC111 cells were grown on 12-mm glass coverslips in 24-well plates. Using the same synchronization protocol described above, asynchronized and synchronized cells were fixed for 10 min with 4% paraformaldehyde and permeabilized with 0.05% saponin for 5 min. The cells were then incubated over night at 4 C with an anti-calretinin antibody diluted in PBS containing 1% bovine serum albumin. Secondary antibodies, Alexa Fluor 488- conjugated goat anti-rabbit IgG (Life Technologies) antibody was added for 1 h at RT. Nuclear DNA was stained using DAPI. Coverslips were mounted using Prolong Gold antifade reagent (Life Technologies). Images

were acquired using an Olympus B × 61 microscope (Schwerzenbach, Switzerland) equipped with an F-view camera for conventional fluorescence imaging. The image capture was controlled with the AnalySISPro software (Soft Imaging System, Münster, Germany).

Statistics

Data are expressed as mean ± standard deviation of multiple experiments. Statistical analysis was performed using Mann-Whitney tests using StatView 5.0.1 (SAS institute). Spearman's correlation tests were used to compare TCGA promoter methylation versus gene expression levels. Differences were considered statistically significant at $p < 0.05$.

ACKNOWLEDGMENTS

The authors are grateful to the members of Laboratory of Molecular Oncology for helpful discussion.

GRANT SUPPORT

This work was supported by the Swiss National Science Foundation Sinergia grant CRSII3 147697/1 (to EFB and BS), P20GM104416 (to BC) and the Stiftung für Angewandte Krebsforchung (to EFB, RS and WW).

CONFLICTS OF INTEREST

The authors declare no conflicts of interest

REFERENCES

1. Tsao AS, Wistuba I, Roth JA, Kindler HL. Malignant pleural mesothelioma. J Clin Oncol. 2009; 27:2081–2090.
2. Roe OD, Stella GM. Malignant pleural mesothelioma: history, controversy and future of a manmade epidemic. European respiratory review : an official journal of the European Respiratory Society. 2015; 24:115–131.
3. Kawasaki H, Kretsinger RH. Calcium-binding proteins 1: EF-hands. Protein profile. 1995; 2:297–490
4. Doglioni C, Tos APD, Laurino L, Iuzzolino P, Chiarelli C, Celio MR, Viale G. Calretinin: A novel immunocytochemical marker for mesothelioma. Am J Surgical Pathol. 1996; 20:1037–1046.
5. Ordonez NG. Value of calretinin immunostaining in diagnostic pathology: a review and update. Appl Immunohistochem Mol Morphol. 2014; 22:401–415.
6. Kim JH, Kim GE, Choi YD, Lee JS, Lee JH, Nam JH, Choi C. Immunocytochemical panel for distinguishing between adenocarcinomas and reactive mesothelial cells in effusion cell blocks. Diagn Cytopathol. 2009; 37:258–261.
7. Otterstrom C, Soltermann A, Opitz I, Felley-Bosco E, Weder W, Stahel RA, Triponez F, Robert JH, Serre-Beinier V. CD74: a new prognostic factor for patients with malignant pleural mesothelioma. Br J Cancer. 2014; 110:2040–2046.
8. Kao SC, Klebe S, Henderson DW, Reid G, Chatfield M, Armstrong NJ, Yan TD, Vardy J, Clarke S, van Zandwijk N, McCaughan B. Low calretinin expression and high neutrophil-to-lymphocyte ratio are poor prognostic factors in patients with malignant mesothelioma undergoing extrapleural pneumonectomy. J Thorac Oncol. 2011; 6:1923–1929.
9. Linton A, Pavlakis N, O'Connell R, Soeberg M, Kao S, Clarke S, Vardy J, van Zandwijk N. Factors associated with survival in a large series of patients with malignant pleural mesothelioma in New South Wales. Br J Cancer. 2014; 111:1860–1869.
10. Blum W, Schwaller B. Calretinin is essential for mesothelioma cell growth/survival *in vitro*: a potential new target for malignant mesothelioma therapy? Int J Cancer. 2013; 133:2077–2088.
11. Camp AJ, Wijesinghe R. Calretinin: modulator of neuronal excitability. Int J Biochem Cell Biol. 2009; 41:2118–2121.
12. Strauss KI, Kuznicki J, Winsky L, Kawagoe JI, Hammer M, Jacobowitz DM. The mouse calretinin gene promoter region: structural and functional components. Brain research Molecular brain research. 1997; 49:175–187.
13. Billing-Marczak K, Buzanska L, Winsky L, Nowotny M, Rudka T, Isaacs K, Belin MF, Kuznicki J. AP2-like cis element is required for calretinin gene promoter activity in cells of neuronal phenotype differentiated from multipotent human cell line DEV. Biochimica et biophysica acta. 2002; 1577:412–420.
14. Billing-Marczak K, Zieminska E, Lesniak W, Lazarewicz JW, Kuznicki J. Calretinin gene promoter activity is differently regulated in neurons and cancer cells. Role of AP2-like cis element and zinc ions. Biochimica et biophysica acta. 2004; 1678:14–21.
15. Marilley D, Vonlanthen S, Gioria A, Schwaller B. Calretinin and calretinin-22k increase resistance towards sodium butyrate-induced differentiation in CaCo-2 colon adenocarcinoma cells. Exp Cell Res. 2001; 268:93–103.
16. Haner K, Henzi T, Pfefferli M, Kunzli E, Salicio V, Schwaller B. A bipartite butyrate-responsive element in the human calretinin (CALB2) promoter acts as a repressor in colon carcinoma cells but not in mesothelioma cells. J Cell Biochem. 2010; 109:519–531.
17. Graham FL, Smiley J, Russell WC, Nairn R. Characteristics of a human cell line transformed by DNA from human adenovirus type 5. J Gen Virol. 1977; 36:59–74.
18. Cai H, Kumar N, Baudis M. arrayMap: a reference resource for genomic copy number imbalances in human malignancies. PLoS One. 2012; 7:e36944.
19. Krismann M, Muller KM, Jaworska M, Johnen G. Severe chromosomal aberrations in pleural mesotheliomas with unusual mesodermal features. Comparative genomic hybridization evidence for a mesothelioma subgroup. J Mol Diagn. 2000; 2:209–216.

20. Destro A, Ceresoli GL, Baryshnikova E, Garassino I, Zucali PA, De Vincenzo F, Bianchi P, Morenghi E, Testori A, Alloisio M, Santoro A, Roncalli M. Gene methylation in pleural mesothelioma: Correlations with clinico-pathological features and patient's follow-up. Lung Cancer. 2007; 59:369–376.

21. Ren B, Cam H, Takahashi Y, Volkert T, Terragni J, Young RA, Dynlacht BD. E2F integrates cell cycle progression with DNA repair, replication, and G/M checkpoints. Genes Dev. 2002; 16:245–256.

22. Gardiner-Garden M, Frommer M. CpG islands in vertebrate genomes. J Mol Biol. 1987; 196:261–282.

23. Li E, Zhang Y. DNA methylation in mammals. Cold Spring Harb Perspect Biol. 2014; 6:a019133.

24. Sigalotti L, Coral S, Altomonte M, Natali L, Gaudino G, Cacciotti P, Libener R, Colizzi F, Vianale G, Martini F, Tognon M, Jungbluth A, Cebon J, et al. Cancer testis antigens expression in mesothelioma: role of DNA methylation and bioimmunotherapeutic implications. Br J Cancer. 2002; 86:979–982.

25. Quandt K, Frech K, Karas H, Wingender E, Werner T. MatInd and MatInspector: new fast and versatile tools for detection of consensus matches in nucleotide sequence data. Nucleic acids research. 1995; 23:4878–4884.

26. Shukla A, Bosenberg MW, Macpherson MB, Butnor KJ, Heintz NH, Pass HI, Carbone M, Testa JR, Mossman BT. Activated cAMP Response Element Binding Protein Is Overexpressed in Human Mesotheliomas and Inhibits Apoptosis. Am J Pathol. 2009; 175:2197–2206.

27. Cam H, Balciunaite E, Blais A, Spektor A, Scarpulla RC, Young R, Kluger Y, Dynlacht BD. A common set of gene regulatory networks links metabolism and growth inhibition. Molecular cell. 2004; 16:399–411.

28. Hateboer G, Wobst A, Petersen BO, Le Cam L, Vigo E, Sardet C, Helin K. Cell cycle-regulated expression of mammalian CDC6 is dependent on E2F. Mol Cell Biol. 1998; 18:6679–6697.

29. Dulic V, Lees E, Reed SI. Association of human cyclin E with a periodic G1-S phase protein kinase. Science. 1992; 257:1958–1961.

30. Pagano M, Pepperkok R, Verde F, Ansorge W, Draetta G. Cyclin A is required at two points in the human cell cycle. The EMBO journal. 1992; 11:961–971.

31. Shifera AS, Hardin JA. Factors modulating expression of Renilla luciferase from control plasmids used in luciferase reporter gene assays. Analytical biochemistry. 2010; 396:167–172.

32. Rao M, Atay S, Shukla V, Hong Y, Upham T, Ripley T, Hong JA, Zhang M, Reardon E, Fetsch P, Miettinen M, Li X, Peer CJ, et al. Mithramycin Depletes Specificity Protein 1 and Activates p53 to Mediate Senescence and Apoptosis of Malignant Pleural Mesothelioma Cells. Clin Cancer Res. 2015.

33. Kelly DP, Scarpulla RC. Transcriptional regulatory circuits controlling mitochondrial biogenesis and function. Genes Dev. 2004; 18:357–368.

34. Virbasius CA, Virbasius JV, Scarpulla RC. NRF-1, an activator involved in nuclear-mitochondrial interactions, utilizes a new DNA-binding domain conserved in a family of developmental regulators. Genes Dev. 1993; 7:2431–2445.

35. Kel AE, Kel-Margoulis OV, Farnham PJ, Bartley SM, Wingender E, Zhang MQ. Computer-assisted identification of cell cycle-related genes: new targets for E2F transcription factors. J Mol Biol. 2001; 309:99–120.

36. Rual JF, Venkatesan K, Hao T, Hirozane-Kishikawa T, Dricot A, Li N, Berriz GF, Gibbons FD, Dreze M, Ayivi-Guedehoussou N, Klitgord N, Simon C, Boxem M, et al. Towards a proteome-scale map of the human protein-protein interaction network. Nature. 2005; 437:1173–1178.

37. Suske G. The Sp-family of transcription factors. Gene. 1999; 238:291–300.

38. Johar K, Priya A, Wong-Riley MT. Regulation of Na(+)/K(+)-ATPase by neuron-specific transcription factor Sp4: implication in the tight coupling of energy production, neuronal activity and energy consumption in neurons. Eur J Neurosci. 2014; 39:566–578.

39. Dimova DK, Dyson NJ. The E2F transcriptional network: old acquaintances with new faces. Oncogene. 2005; 24:2810–2826.

40. Hucl T, Brody JR, Gallmeier E, Iacobuzio-Donahue CA, Farrance IK, Kern SE. High cancer-specific expression of mesothelin (MSLN) is attributable to an upstream enhancer containing a transcription enhancer factor dependent MCAT motif. Cancer Res. 2007; 67:9055–9065.

41. Robinson C, van Bruggen I, Segal A, Dunham M, Sherwood A, Koentgen F, Robinson BW, Lake RA. A novel SV40 TAg transgenic model of asbestos-induced mesothelioma: malignant transformation is dose dependent. Cancer Res. 2006; 66:10786–10794.

42. Fukazawa T, Matsuoka J, Naomoto Y, Maeda Y, Durbin ML, Tanaka N. Malignant pleural mesothelioma-targeted CREBBP/EP300 inhibitory protein 1 promoter system for gene therapy and virotherapy. Cancer Res. 2008; 68: 7120–7129.

43. Inase N, Miyake S, Yoshizawa Y. Calretinin promoter for suicide gene expression in malignant mesothelioma. Anticancer Res. 2001; 21:1111–1114.

44. Julian LM, Blais A. Transcriptional control of stem cell fate by E2Fs and pocket proteins. Front Genet. 2015; 6:161.

45. Schmitter D, Lauber B, Fagg B, Stahel RA. Hematopoietic growth factors secreted by seven human pleural mesothelioma cell lines: interleukin-6 production as a common feature. Int J Cancer. 1992; 51:296–301.

46. Phelps RM, Johnson BE, Ihde DC, Gazdar AF, Carbone DP, McClintock PR, Linnoila RI, Matthews MJ, Bunn PA, Jr., Carney D, Minna JD, Mulshine JL. NCI-Navy Medical

Oncology Branch cell line data base. J Cell Biochem Suppl. 1996; 24:32–91.

47. Usami N, Fukui T, Kondo M, Taniguchi T, Yokoyama T, Mori S, Yokoi K, Horio Y, Shimokata K, Sekido Y, Hida T. Establishment and characterization of four malignant pleural mesothelioma cell lines from Japanese patients. Cancer Sci. 2006; 97:387–394.

48. Versnel MA. . Mesothelioma. In: Masters JR, Palson, B., ed. Human cell culture. (The Netherlands: Springer), pp. 87–106.

49. Manning LS, Whitaker D, Murch AR, Garlepp MJ, Davis MR, Musk AW, Robinson BW. Establishment and characterization of five human malignant mesothelioma cell lines derived from pleural effusions. Int J Cancer. 1991; 47:285–290.

50. Thurneysen C, Opitz I, Kurtz S, Weder W, Stahel RA, Felley-Bosco E. Functional inactivation of NF2/merlin in human mesothelioma. Lung Cancer. 2009; 64:140–147.

51. Sidi R, Pasello G, Opitz I, Soltermann A, Tutic M, Rehrauer H, Weder W, Stahel RA, Felley-Bosco E. Induction of senescence markers after neo-adjuvant chemotherapy of malignant pleural mesothelioma and association with clinical outcome: an exploratory analysis. Eur J Cancer. 2011; 47:326–332.

52. Bustin SA, Benes V, Garson JA, Hellemans J, Huggett J, Kubista M, Mueller R, Nolan T, Pfaffl MW, Shipley GL, Vandesompele J, Wittwer CT. The MIQE guidelines: minimum information for publication of quantitative real-time PCR experiments. Clin Chem. 2009; 55:611–622.

53. Shi Y, Moura U, Opitz I, Soltermann A, Rehrauer H, Thies S, Weder W, Stahel RA, Felley-Bosco E. Role of hedgehog signaling in malignant pleural mesothelioma. Clin Cancer Res. 2012; 18:4646–4656.

54. Santoro R. Analysis of chromatin composition of repetitive sequences: the ChIP-Chop assay. Methods Mol Biol. 2014; 1094:319–328.

55. Harper JV. Synchronization of cell populations in G1/S, G2/M phases of the cell cycle. Methods Mol Biol. 2005; 296:157–166.

4.2. Post-transcriptional regulation of calretinin expression in mesothelioma cells

Submitted

Contribution: JKR performed Q-PCR, *in silico* analysis, RNA folding prediction, dual luciferase assay, mutational constructs, mimics and anti-Mir treatments, Western blot - (1A, B / 2 A, B, C, D / 3A / 4 B, C / 5A, C). MS carried out cloning of calretinin 3'UTR, dual luciferase assay, EMSA assay (3B). MR carried out Western blot and Q-PCR (4 A, C / 5B). EFB and JKR designed experiments and interpreted data. MBK, SK and GR provided data on the relationship between CR and miR-30e in clinical samples (4 D).

JKR and EFB wrote the manuscript. All authors read and approved the final manuscript.

Post-transcriptional regulation controls calretinin expression in malignant pleural mesothelioma

Jelena Kresoja-Rakic[1], Merve Sulemani[1], Michaela B. Kirschner[2], Manuel Ronner[1], Glen Reid[3,4], Steven Kao[3,4,5], Beat Schwaller[6], Walter Weder[2], Rolf A. Stahel[7], Emanuela Felley-Bosco[1*]

[1] Laboratory of Molecular Oncology, Division of Thoracic Surgery, University Hospital Zurich, Switzerland

[2] Division of Thoracic Surgery, University Hospital Zurich, Switzerland

[3] Asbestos Diseases Research Institute, Sydney, Australia

[4] School of Medicine, The University of Sydney, Sydney Australia

[5] Department of Medical Oncology, Chris O'Brien Lifehouse, Sydney, Australia

[6] Department of Medicine, Anatomy, University of Fribourg, Fribourg, Switzerland

[7] Clinic for Oncology, University Hospital Zurich, Zurich

*** Correspondence:**

Emanuela Felley-Bosco,
Laboratory of Molecular Oncology, Division of Thoracic Surgery,
University Hospital Zürich, Sternwartstrasse 14, Zurich, Switzerland,
P: +41 44 255 27 71,
email: emanuela.felley-bosco@usz.ch

Keywords: cancer, 3' untranslated region, microRNA, non-coding RNA, mesothelioma, calretinin

Number of words: 4443

Number of figures: 5

Abstract

Calretinin (CALB2) is a diagnostic and prognostic marker in malignant pleural mesothelioma (MPM). We previously reported that calretinin expression is regulated at the mRNA level. The presence of a medium sized (573 nucleotide) 3'-untranslated region (3'-UTR) predicted to contain binding sites for miR-30a/b/c/d/e and miR-9 as well as an A/U-rich element (ARE) in all three transcripts arising from the CALB2 gene, suggests that calretinin expression is regulated via post-transcriptional mechanisms. Our aim was to investigate the role of the CALB2-3'UTR in the post-transcriptional regulation of calretinin expression in MPM. CALB2-3'UTR was inserted downstream of the luciferase reporter gene using pmirGLO vector and reporter expression was determined after transfection into MPM cells. Targeted mutagenesis was used to generate variants harboring mutated miR-30 family and ARE binding sites. Electrophoretic mobility shift assay was used to test for the presence of ARE binding proteins. Data mining allowed to correlate calretinin and miR-30e expression in tumor samples.

CALB2-3'UTR significantly decreased luciferase activity in MPM cells. Analysis of mutation in the ARE site revealed a further destabilization of the reporter and a cytosolic protein binding to the ARE sequence was detected. The mutation of two mir-30 binding sites abolished CALB2 3'UTR destabilization effect; a transient delivery of miR-30e-5p mimics or anti-miR into MPM cells resulted in a significant decrease/increase of the luciferase reporter expression and calretinin protein, respectively. Moreover, overexpression of CALB2-3'UTR quenched the effect of miR-30e-5p mimics on calretinin protein levels, possibly by sequestering the mimics, thereby suggesting a competitive endogenous RNA network. Finally, expression of miR-30e-5p was found to negatively correlate with the calretinin expression in a cohort of MPM patient samples. Our data show the role of I) AU-binding proteins in calretinin stabilization and II) miR-30e-5p in the post-transcriptional negative regulation of calretinin expression via interaction with its 3'-UTR. Furthermore, our study demonstrates a possible physiological role of calretinin's alternatively spliced transcripts.

1 Introduction

Malignant pleural mesothelioma (MPM) is an aggressive form of cancer arising from mesothelial cells lining the pleural cavity and is mainly resulting from the inhalation of asbestos fibers (Porpodis et al., 2013). Calretinin, a Ca^{2+} binding protein, is a diagnostic and prognostic marker for mesothelioma (Kao et al., 2011;Linton et al., 2014;Ordóñez, 2014;Otterstrom et al., 2014). So far, molecular mechanisms driving calretinin expression in mesothelioma remain largely unknown. We have recently described that the expression of calretinin is regulated at the level of transcription by NRF-1 and E2F2 transcription factors (Kresoja-Rakic et al., 2016). As the *CALB2* mRNA includes a so-called medium size (Fanourgakis et al., 2016) 3'UTR (573bp) containing an Adenine/Uridine-rich element (ARE) motif as well as a microRNA binding sequences, this suggests that post-transcriptional mechanisms of regulation are also involved.

The ARE motif is the most frequently studied *cis*-acting element that plays a role in the post-transcriptional control of gene expression by affecting mRNA stability. Its dysregulation has also been described in cancer (Khabar, 2010). The ARE-containing mRNAs are directly or indirectly bound by *trans*-acting RNA-binding proteins known as AU-binding proteins (AUBPs), which can in turn promote degradation, deadenylation (ARE-mediated decay - AMD) or even stabilization of mRNA. There are 21 AUBP implicated either stabilization or destabilization of targeted ARE-mRNA (von Roretz et al., 2011). The most extensively studied AUBPs are HuR/ELAVL1 (Human antigen R, Embryonic Lethal Abnormal Vision, Drosophila - stabilization (Brennan and Steitz, 2001)), TTP (tristetraprolin) and AUF (ARE/poly(U)-binding/degradation factor 1 - destabilization) (Barreau et al., 2005).

MicroRNAs (miRNAs) are small (18-22nt) non-coding RNAs that affect gene expression on the post-transcriptional level. miRNAs bind to partially complementary microRNA recognition elements (MREs) within targeted mRNA, leading to inhibition of translation or mRNA destabilization (Krol et al., 2010). In general, there is a global decrease of miRNA expression in MPM in concordance with other cancer types (Lu et al., 2005;Volinia et al., 2006;Reid, 2015). The TargetScan (Agarwal et al., 2015), miRanda (Betel et al., 2008) and PicTar (Krek et al., 2005) databases predict potential binding sites for miR-30a/b/c/d/e and miR-9 within the calretinin 3'UTR. Based on the analysis of 1319 differentially expressed genes, Cheng et al (Cheng et al., 2016) identified the miR-30 family amongst the top 20 enriched microRNA families in mesothelioma. Furthermore, miR-30e-5p is a part of the 6-microRNA signature shown to predict long survival in mesothelioma patients (Kirschner et al., 2015). So far there was no study on the biological function of the miR-30 family or AUBP in mesothelioma.

An additional level of complexity is achieved through the interaction (antagonistic or cooperative) between miRNA and RBPs (von Roretz and Gallouzi, 2008;van Kouwenhove et al., 2011). For example, it has been observed that fine-tuning of p53 expression at post-transcriptional level occurs through the antagonistic effect between HuR and miR-125b. Namely, the binding of HuR to p53 mRNA causes removal of p53 mRNA from RISC complex and thus prevents miR-125b-mediated translation repression of p53 upon genotoxic stress (Ahuja et al., 2016). Therefore, 3'UTR can mediate post-transcriptional gene expression regulation, acting as a platform for the individual effect or the crosstalk between miRNA or AUBP.

An indirect evidence for a functional role of the CALB2-3'UTR has been suggested in a study using *Calb*2-IRES-Cre transgene, in which Cre recombinase was inserted into the 3' UTR of the mouse *Calb2* gene (Tasic et al., 2016), apparently disrupting regulatory elements and leading to discrepancy between Cre expression and endogenous calretinin expression in adult mice. Here, using a reporter system and mutational analysis of the predicted putative *cis*-regulatory sites in the CALB2-3'UTR followed by overexpression or inhibition, we demonstrated that miR-30e-5p is able of modulating calretinin expression. Additionally, we show that the ARE element in the 3'UTR stabilizes *CALB2* mRNA. Furthermore, we suggest a role for alternative transcripts of the calretinin gene, where their 3'UTRs compete for the pool of *trans*-acting factors, thus affecting calretinin expression.

2 Materials and Methods

2.1 Cell lines

Four mesothelioma cell lines were used were used in experiments. ACC-MESO-4 cell line was obtained from RIKEN BioResource Centre (Usami et al., 2006) and maintained in RPMI-1640 medium (Sigma-Aldrich) supplemented with 15% Fetal Calf Serum (FCS), 1% penicilin/streptomycin (P/S) and 2mM L-glutamine. Both ZL55 and SPC111 cell lines were established in our lab (Schmitter et al., 1992) whereas ONE58 was obtained from the European Collection of Cell Cultures (Salisbury, UK) (Manning et al., 1991). ZL55 cells were cultured as described by Thurneysen (Thurneysen et al., 2009). SPC111 and ONE58 cells were maintained in DMEM/F12 supplemented with 15% FCS, 1% P/S and 2 mM L-glutamine.

2.2 Generation of the CALB2 3'UTR and mutant luciferase reporters

To generate the luciferase reporter construct pmiRGLO-CALB2-3'UTR (72800 Addgene), CALB2 3'UTR was amplified from genomic DNA (ZL55) using the following tailed primers: forward ^{NheI} 5'-ATTTGCTAGC AGTGGGGACGGGGGCTGCTT-3', and reverse ^{SalI}5'-ACGTGTCGACGGGTAAGTTTCCACAGCAGG-3'. The PCR reaction was performed in a total volume of 50 µl containing 1X Colorless Go Taq® Flexi Buffer (Promega), 2 mM MgCl2 solution, 0.2 mM PCR Nucleotide Mix, 0.2 µM of each primer, 1.25 U of Go Taq® G2 Hot Start Polymerase (Promega) and 25 ng of genomic DNA. The sequence of interest was amplified by means of touchdown PCR system: Denaturation at 95°C, annealing at 60°C/63°C/65°C/68°C, extension at 74°C (10 cycles for each different annealing temperature condition). Amplified CALB2 3'UTR was cloned downstream of the Firefly luciferase coding sequence in the pmiRGLO vector (Cat. No. 1330, Promega). The QuickChange Site-Directed mutagenesis kit (200518, Agilent technologies) was employed to introduce mutations in the ARE or miR-30 sites with the following primers: pmir-GLO-CALB2-3'UTRmtARE, (74425 Addgene) 5'-ctctgttggacatagaagcccagaccatacagcgagggagctcat-3', 5'-atgagctccctcgctgtatggtctgggcttctatgtccaacagag–3'; pmir-GLO-CALB2-3'UTRmir30mt, (74428 Addgene) 5'-cgtgctccttttctctttgggtttcttttatcccaaagaagagtttacagacaat-3', 5'-attgtctgtaaactcttctttgggataaaagaaacccaaagagaaaaggagcacg-3'; pmir-GLO-CALB2-3'UTRmir30dmt,

(74429 Addgene) 5'-ttgggtttcttttatcccaaagaagattatccagacaataaaatggaaaggtcctgc-3', 5'-gcaggacctttccattttattgtctggataatcttctttgggataaaagaaacccaa-3' and, a combination of primers above to construct pmirGLO-CALB2-3'UTR-mir30dmt-mtARE (74430 Addgene).

2.3 Stable and transient transfection, and luciferase reporter assay

To generate stable cell lines carrying pmirGLO-*CALB2*-3'UTR or empty pmiRGLO, 1 x 10^5 ACC-Meso-4 or ONE58 cells were transfected with 200 ng of the corresponding plasmid and 1 µl of Lipofectamine 2000 in 6-well plate. On the following day, geneticin-containing medium was added and replaced every 3-4 days until cells reached confluence for a further expansion.

For transient plasmid transfection, 0.8-1 x 10^5 cells were seeded in 12-well plate. On the following day, 200 ng plasmid along with 1 µl of DMRIE-C transfection reagent mixed in 800 µl of OPTIMEM, was added to the corresponding wells and incubated for 9 h. After 48 h, transfected cells were lysed and reporter activity was measured afterwards using the Dual-Luciferase reporter assay according to manufactures instructions (Promega, Madison, Wi, USA).

2.4 miRNA mimic and inhibitor treatment

For mimics and anti-miR treatment, following mimics were used: 1 or 5 nM of has-miR-30b-5p (MSY0000420, QiaGen), has-miR-30c-5p (MSY0000244, Qiagen), hsa-miR-9-5p (MSY0000441, QiaGen), hsa-miR-30e-5p (Shanghai GenePharma Co., Ltd); or 10 nM or 30 nM anti-hsa-miR-30e-5p (MIN0000692, QiaGen), respectively, was transiently delivered using Lipofectamine RNAiMAX according to the manufacturer's reverse transfection protocol as previously described (Shi et al., 2012). 5×10^4cells were then plated in 12-wells plate and whole cell lysates were prepared after 72 h for the luciferase or protein measurement.

2.5 Relative gene expression

To extract RNA, Qiagen RNeasy® kit was used. cDNA was reverse transcribed from 400–500 ng of total RNA (Qiagen QuantiTect® Reverse Transcription protocol) (Sidi et al., 2011). To quantify expression, cDNA was amplified by the SYBR-Green PCR assay and products were detected on a 7900HT Fast real-Time PCR system (SDS, ABI/Perkin Elmer). Relative mRNA levels were determined by comparing the PCR cycle thresholds between cDNA of a specific gene and histone (ΔCt method) (Andre and Felley-Bosco, 2003). Selected gene expression analysis using MIQE compliant protocols was conducted as previously described (Bustin et al., 2009). Following genes were quantified: HuR (5'- GGGCTATGGCTTTGTGAACTA -3; 5'-GCGAGCATACGACACCTTAAT-3'); TTP (5'-GGATCCGACCCTGATGAATATG-3'; 5'-GAAACAGAGATGCGATTGAAGATG-3; Firefly luciferase (5'-GTGGTGTGCAGCGAGAATAG-3'; 5'-CGCTCGTTGTAGATGTCGTTAG-3'); Renilla luciferase (5'-CGTTGGCTACCCGTGATATT-3'; 5'-CTCGTCAAGAAGGCGATAGAAG-3'), primers detecting *CALB2* alternative transcripts are listed in Additional file 1 Figure S1.

miRNA expression was determined according manufacturer's protocols using the miRNeasy Mini Kit (Qiagen), miScript II RT (Qiagen), miScript primer assays (Qiagen), and miScript SYBR Green PCR Kit (Qiagen) in the 7900HT Fast real-Time PCR system (SDS, ABI/Perkin Elmer). Relative miRNA levels were determined by comparing the PCR cycle thresholds between cDNA of a specific gene and RNU-6B- 2 (ΔCt method).

2.6 Electrophoretic mobility shift assay for RNA-protein complexes

Cytosolic protein extracts were isolated using the NE-PER™ Nuclear and Cytoplasmic Extraction Kit (78833, Pierce Biotechnology) according to manufacturer's instructions. To demonstrate possible interactions of RNA binding protein and single stranded RNA containing AUUUA pentamer, RNA-EMSA was performed using LightShift® Chemiluminescent RNA EMSA Kit (Pierce Biotechnology). The binding reaction (20□l total) contained 1X Binding Buffer (10 mM HEPES pH 7.3), 20 mM KCL, 1 mM MgCl2, 1 mM DTT), 2.5 % Glycerol, 100 mM KCl, 2.5 µg heparin (Sigma-Aldrich), 5□g of cytosolic protein extract. After 5 min incubation on ice, 2 nmoles specific biotinylated RNA oligonucleotides (5'-UCGCUGUAUGAUUUAGGCUUCUAUG-3') was added. For competition reactions, 200-fold excess of either specific or unrelated unlabeled RNA oligo probes (5'-UCCUGCUUCAACAGUGCUUGGACGGAAC-3') were incubated with binding reactions for 5 min prior to addition of specific biotinylated RNA oligo probe. The reactions were incubated for 25 min at room temperature and then separated on a 6 % polyacrylamide 0.5 x TBE native gel. After the transfer on a nylon membrane, RNA probe-protein complex was visualized using Chemiluminescent Nucleic Acid Detection Module Kit Module (89880) according to manufacturer's protocol.

2.7 Western blotting

Whole cellular protein extracts were prepared by lysing the cells with hot (95° C) Laemmli sample buffer (60 mM Tris-Cl pH 6.8, 100 mM DTT, 5% glycerol, 1.7% SDS) and mechanically sheared by pressing few times through syringes (26 G). Protein concentration was determined using a Pierce™ 660nm Protein Assay (Thermo Scientific). A total of 5 µg protein per extract was separated on denaturing 10–20% gradient SDS-PAGE gels. Proteins were transferred on PVDF transfer membranes (0.45 µm, Perkin Elmer). Membranes were probed with the following primary antibodies: anti-calretinin (Sigma, HPA007306), and mouse anti-actin (#69100) from MP Biomedicals. Membranes were then incubated with the secondary antibody rabbit anti-mouse IgG-HRP (A-5420) from Antell, and goat anti-rabbit IgG-HRP (#7074) from Cell Signaling. The signals were detected by enhanced chemiluminescence (ECL™ Western Blotting Reagents, GE Healthcare) and detected on photosensitive film (Super RX Fuji x-Ray Film, Fujifilm).

2.8 Relationship between miR-30e-5p and calretinin in tumor samples

We data-mined previous studies where both, calretinin IHC evaluation (Kao et al., 2011) and miR-30e-5p (Kirschner et al., 2015) had been determined in tumor samples from mesothelioma patients who underwent extrapleural pneumonectomy between 1994 and 2009 at Royal Prince Alfred and Strathfield Private Hospital, Sydney, Australia. Correlation between calretinin and miR-30e-5p expression was analyzed in a subset of 60 tumor samples, for which both measurements were available (Additional file 2, Table S1).

2.9 Statistics

Data are expressed as mean ± standard deviation of multiple experiments. Statistical analysis was performed using Mann-Whitney U tests using StatView 5.0.1 (SAS institute) and t-test using GraphPad. Spearman's correlation test was used to calretinin vs miR-30e-5p gene expression levels. Differences were considered statistically significant at $p<0.05$.

3 Results

3.1 Calretinin 3'UTR harbors a functional ARE motif and miR-30 sites

The calretinin gene (*CALB2*), located on chromosome 16, has three different transcripts: 1) the full length isoform 1 encoding the 29kDa protein - CALB2; 2) a non-coding alternatively spliced variant - CALB2b (*Δ*8); and 3) an alternatively spliced variant giving rise to a 22kDa calretinin protein isoform - CALB2c (*Δ*8, 9) (Figure 1A) (Schwaller et al., 1995). The length of the 3'UTR is 573nt and 716nt in CALB2 and CALB2c, respectively. The alternative transcript CALB2b contains the same sequence of the 573nt 3'UTR but the whole transcript is considered as a non-coding since the use of the 5'-most supported translation start codon introduces a premature termination codon rendering the transcript a candidate for nonsense-mediated mRNA decay.

To detect the presence of calretinin variants CALB2, CALB2b, and CALB2c, RT-qPCR was performed with cDNA from ZL55, ACC-MESO-4 and ONE58 cells using boundary-spanning primers approach (Figure 1A, Additional file 1 Figure S1). The highest level of all three transcripts was detected in ACC-MESO-4 cells followed by lower, but still detectable, expression of all three transcripts in ZL55 cells, whereas only the full-length isoform CALB2 was detected in ONE58 cells (Figure 1B). At the protein level, only the full-length 29kDa calretinin was detected in all three cells lines, ACC-MESO-4 (high-calretinin), ZL55 (intermediate calretinin) and ONE58 (low-calretinin), as reported in a previous study (Kresoja-Rakic et al., 2016).

The complete 3'UTR sequence of the full–length calretinin isoform CALB2, was used in further experiments (CALB2-3'UTR). Multiple sequence alignment of CALB2 3'UTR across 100 vertebrates listed in the UCSC Genome Browser, indicated two conserved stretches within the CALB2 3'UTR (Figure 2A). The AREsite2 software (Fallmann et al., 2016) revealed a putative ARE motif (AUUUA) within the first stretch, and TargetScan software predicted two binding sites for the miR-30 family and one for miR-9, within the second conserved stretch (Figure 2A, 2B).

In order to test its functionality, CALB2-3'UTR was inserted downstream of the Firefly luciferase reporter gene (pmirGLO vector) and transiently transfected into ONE58 cells (Figure 2C). Insertion of the CALB2-3'UTR led to 40% ($p=0.0012$) decreased expression of Firefly luciferase when compared to the empty vector (pmirGLO), indicating that the calretinin 3'UTR conveys a downregulatory effect (Figure 2D). We then generated an additional four constructs harboring mutations of the consensus sequence for the predicted ARE motif and miR-30 binding sites and transiently transfected all variants into ONE58 cells to test for their effects on luciferase expression (Figure 2C, 2D). Mutation of the predicted ARE motif induced an even further significant decrease of 20% ($p=0.0055$), indicating that the ARE site binds to a stabilizing factor. In contrast, mutation of both miR-30 binding sites restored the expression of the luciferase reporter to the level of the empty vector. Taken together, our data indicate that the 3'-UTR of the *CALB2* mRNA contains multiple elements contributing to post-transcriptional regulation and control of calretinin protein levels.

3.2 Specific binding of a protein to the 25nt-sequence containing ARE-motif

Having observed that the ARE motif in the calretinin 3'UTR is functional, we investigated the possible interaction between this site and a potential stabilizing *trans*-acting factor. Indeed, investigation of the optimal secondary structure of the *CALB2* 3'UTR sequence (317nt; 1152nt-1469nt) using the RNAfold prediction tool (Gruber et al., 2008), revealed a secondary structure in which the ARE site forms a bulge and thus might be accessible to an interactor. The reason for using a stretch of 317 nt containing the predicted regulatory sequences was to increase accuracy and to provide a better overview (Hofacker, 2009). Replacing the AUUUA with GUCUG results in a mutated ARE motif paired in a newly formed secondary structure predicted to be less likely to be accessible for putative interacting protein (Figure 3A).

We then employed a biochemical approach using electrophoretic mobility shift assay to demonstrate the specific interaction between a 25nt RNA containing the ARE motif (UCGCUGUAUGAUUUAGGCUUCUAUG) and a cytosolic extract containing RNA-binding proteins (RBPs) (Figure 3B). Incubation of the biotin-labeled 25nt RNA with a cytosolic protein extract of ACC-MESO-4, ZL55, and SPC111 cells showed a protein-RNA complex formation (Figure 3B - lanes 2,3,4). To further confirm the specificity of the RNA-protein interaction, competing reactions were performed using a 200-fold excess of the identical 25nt unlabeled sequence RNA (specific competitor) or unlabeled-unrelated RNA-oligo (unspecific competitor). Addition of the specific competitor decreased the detectable RNA-protein complex (Figure 3B - lanes 5,6,7), whereas the excess of the non-specific competitor did not outcompete the biotin-RNA-protein complex (Figure 3B – lanes 8, 9, 10). The presence of the additional lower bands in the lanes 9 and 10 are assumed to be different secondary structures formed by the biotin-RNA oligo.

Since the mutational reporter analysis had identified the ARE motif as a stabilizing element, we quantified the expression of HuR (stabilizer) along with TTP (destabilizer) across 10 mesothelioma cell lines and observed that HuR is abundantly expressed in all tested cells lines and 5 to 50 fold enriched compared to TTP (Figure 3C). We confirmed overexpression of HuR in mesothelioma compared to normal pleura along with a low TTP/HuR ratio by investigating microarray data (Gordon et al., 2005). These results demonstrated that some of the mostly studied AUBP (e.g. HuR, TTP) are expressed in mesothelioma cells and that the 25nt-fragment of *CALB2* 3'UTR harboring the ARE element binds a protein from mesothelioma cytosolic extract.

3.3 miR-30e-5p downregulates calretinin protein expression

The observation that the double miR-30 mutant construct (pmrGLO-CALB2-3'UTR-mir30-dmt) abolished the downregulatory effect mediated by *CALB2* 3'UTR, led us to identify the critical miR-30e-5p member conveying this effect. Computational analysis predicted that only the miR-30a/b/c/d/e -5p arm is assumed to target *CALB2* mRNA. Quantitative expression analysis showed that miR-30b/c/d/e (5p-arm) are abundantly expressed in ZL55, ONE58, ACC-MESO-4 cells (Figure 4A). Interestingly, unlike the other miR-30 members where the 3p arm was almost absent, both the miR-30e-5p and -3p arms were expressed in ZL55, ONE58, ACC-MESO-4 cells. miRNA-5p and -3p arms originate from the same pre-miRNA but have a different sequence. Both could become functional miRNA either targeting different mRNA or accomplish a synergistic effect on the same mRNA, but at different sites (Mitra et al., 2015).

ONE58 cells stably expressing Firefly luciferase-CALB2-3'UTR, were transiently transfected with 1 and 5nM of miR-30b/c/e-5p mimetic treatment. Of all tested mimics, 5nM miR-30e-5p lead to ~60% downregulation of luciferase expression from the CALB2-3'UTR reporter ($p=0.0039$) when compared with the negative control mimics (Figure 4B). Calretinin protein levels were also decreased after addition of miR-30e-5p in a concentration-dependent manner, i.e. a larger effect with 5 nM mimics (Figure 4B). Furthermore, anti-miR-mediated miR-30e-5p inhibition caused a moderate but still significant upregulation of the reporter-CALB2-3'UTR as well as an increase of calretinin protein levels (Figure 4C). Similar results were also observed in ACC-MESO-4 cells where the treatment with 5nM of miR-30e-5p mimetic resulted in ~50% decrease ($p=0.0039$) of the reporter expression and in calretinin protein expression (Additional File 3, Figure S2)

As we demonstrated that the miR-30e-5p was capable to directly regulate calretinin expression, we investigated whether miR-30e-5p expression correlated with calretinin expression, determined by immunohistochemistry scoring of mesothelioma tissue samples. In a pool of 60 mesothelioma tumor

samples, calretinin expression versus miR-30e-5p expression showed a weak, but significant negative correlation (Figure 4D). Altogether, these findings demonstrated an involvement of miR-30e-5p in negatively regulating calretinin expression.

3.4 Calretinin 3'UTR acts as competitive endogenous RNA (ceRNA)

According to the so called ceRNA (competitive endogenous RNA) hypothesis, all types of RNA transcripts (coding and non-coding) carrying the same MRE potentially compete for the same miRNA pool therefore acting as natural microRNA sponges (Salmena et al., 2011). Beside miRNA, transcripts may also compete for binding to different RBPs adding yet another level of complexity (Tay et al., 2014). The ONE58 cell line stably overexpressing the *CALB2* 3'UTR was used, with exogenous *CALB2*-3'UTR levels being ~580-fold higher (estimated by *Firefly luciferase* vs. *CALB2* mRNA) compared to the endogenous *CALB2* mRNA level. When ONE58 cells stably transfected with empty vector (ONE58-EV-pmirGLO) or the CALB2-3'UTR construct (ONE58-CALB2-3'UTR) were transiently transfected with miR-30e-5p (~130-fold more abundant compared to the endogenous miR-30e-5p pool), downregulation of calretinin expression was observed only in ONE58 empty vector expressing cells, suggesting that the constant exogenous overexpression of *CALB2*-3'UTR could sequester miR-30e-5p mimics (Figure 5A). In contrast, when anti-miR-30e-5p was transiently delivered, increase of calretinin protein levels was observed only in ONE58-CALB2-3'UTR and not in ONE58-EV-pmirGLO cells (Figure 5B). Based on our data, we suggest a model in which the *CALB2* 3'UTR might act as a competitor via sequestration of miR-30e-5p thereby decreasing its interaction with the protein coding *CALB2* mRNA isoform (Figure 5C). Indeed, ONE58 cells only express low amounts of the full-length isoform 29kDa calretinin (CALB2) and not the splice variants. In the situation of stable and strong overexpression of CALB2-3'UTR in ONE58 cells, delivery of miR-30e-5p mimics does not repress the expression of calretinin most likely due to the exogenous CALB2-3'UTRs which compete to bind the delivered miR-30e-5p and thus act as a molecular sponge. In contrast, when the same ONE58-CALB2-3'UTR cells were transfected with anti-miR-30e-5p, calretinin expression was increased (but not in ONE58-empty vector expressing cells), most likely due to repression of miR-30e-5p, which was exerted by both, the presence of exogenous CALB2-3'UTR and anti-miR-30e-5p treatment. Altogether, these data suggest that CALB2- transcripts sharing the same MRE in their 3'UTRs, could compete to bind the common miRNAs and create a ceRNA network modulating miR effects on calretinin expression.

4 Discussion

In a previous study we demonstrated a strong positive correlation between calretinin mRNA and protein levels in mesothelioma cell lines (Kresoja-Rakic et al., 2016) and demonstrated NRF-1 and E2F2 to act as transcription factors regulating calretinin expression. In this study, we determined that calretinin expression is additionally regulated in mesothelioma cells through a post-transcriptional mechanism mediated by the 3'-UTR. We determined that the CALB2-3'UTR contains two functional elements - a stabilizing ARE motif, and two destabilizing miR-binding sites; the identified miR-30e-5p site was shown to negatively regulate calretinin expression. Moreover, we propose a physiological relevance for the *CALB2* alternative spliced transcripts by their function within a ceRNA network.

3'UTRs play a functional role in the post-transcriptional regulation of mRNA, as the 3'UTR can modulate stability, drive subcellular localization and control translational efficiency of mRNA (Mayr, 2016). Since the 3'UTRs of all three *CALB2* transcripts contain a common 573-nt stretch, we used this region for further functional analysis. Employing a reporter plasmid assay, where the 573-nt stretch of the CALB2-3'UTR was inserted downstream of the Firefly luciferase reporter, we observed that

CALB2-3'UTR affected the reporter mRNA stability, as it downregulated the reporter expression in mesothelioma cells.

mRNA stability and therefore mRNA abundance in a cell is controlled by the best studied ARE *cis*-acting elements and by miRNA-binding sites. The core of the ARE sequence is the pentameric motif AUUUA. The ARE motifs exert their function (stabilization or destabilization) by interaction with different ARE-binding proteins (AUBP). Electrophoretic mobility shift assay demonstrated that the 25-nt RNA fragment of the *CALB2* 3'UTR containing one pentameric ARE element, binds specifically a protein present in cytosolic protein lysates of mesothelioma cells. Although we did not investigate the identity of the protein binding to the ARE sequence, given that the mutational approach revealed a stabilization element in the ARE site, one of the potential candidates is HuR, an mRNA stabilizing protein (Brennan and Steitz, 2001), which is ubiquitously expressed (Ma et al., 1996). There are several mechanisms through which HuR exerts its stabilization effect. For example, it has been proposed that HuR confers stabilization to mRNA by its ability to outcompete with either destabilizing AUBP (Tiedje et al., 2012) or miRNAs (Bhattacharyya et al., 2006;Srikantan et al., 2012). HuR has been reported to be overexpressed in mesothelioma and HuR cytoplasmic expression significantly correlated with a poor outcome in mesothelioma patients (Stoppoloni et al., 2008). Since a decrease, and not an increase, in calretinin expression is associated with the poorest overall survival, this may suggest that, if it is indeed HuR that stabilizes calretinin mRNA, it competes to bind other tumor progression-associated targets. In fact, in mesothelioma, HuR cytoplasmic expression is correlated with COX-2 (Stoppoloni et al., 2008) , a gene that bears 14 ARE (Sheng et al., 2000). In our panel of 6 mesothelioma cell lines and by data mining, we observed that HuR was highly expressed and more abundant compared to TTP (destabilizer), indicating that HuR might potentially outcompete the binding of TTP resulting in stabilization of *CALB2* mRNA, since both are able to bind to the same ARE sequence.

The second cis-acting element that we found to be functional within CALB2-3'UTR are destabilizing miRNA-binding sites. *CALB2* mRNA was found to interact with AGO1, a protein that is the part of the RISC complex, which executes the function of miRNA (Li et al., 2014) (Jha et al., 2015) indicating that calretinin transcripts are indeed regulated by microRNA. Utilizing several prediction algorithms, miR-30 family members were identified as potential candidates targeting calretinin mRNA; overexpression or inhibition experiments revealed that only miR-30e-5p is able to modulate calretinin protein levels through the calretinin 3'UTR. The miR-30 family includes 5 members, miR-30a through miR30e and is evolutionary well conserved. In mesothelioma, high expression of miR-30e-5p has been associated with the epithelioid histopathological subtype, which is generally associated with better prognosis (Busacca et al., 2010). However, upregulation of miR-30e-5p along with other miRNA forms the 6-micro RNA signature that predicts poorest survival of MPM patients (Kirschner et al., 2015) and this fits with low calretinin levels in epithelioid histotype patients associated with worse outcome (Kao et al., 2011;Otterstrom et al., 2014).

The identification of both positive and negative regulatory elements within CALB2-3'UTR suggests a possible interplay between AUBP and miRNA, adding another level of complexity in regulating calretinin expression, which would help understanding why even in epithelioid MPM not all cells are calretinin-positive (Kao et al., 2011). Different RNA-binding factors can target the same mRNA at different sites or competing for the same site, in a cooperative or antagonistic fashion that depends on their expression levels, localization in the cells or binding affinity (Vislovukh et al., 2014). Various miRNAs may act together with AUBP on the same 3'UTR and may cause reduced RNA stability and/or translation (Jing et al., 2005). For instance, it has been described that the RNA-binding protein PUM1 alters the secondary structure of target mRNA and thus allowing miR-221 and mir-22 to access the

target sites (Kedde et al., 2010). In another example, Dicer and Argonaut (recruited by miR-16) along with TTP are required for ARE-mediated mRNA decoy of TNFα (Jing et al., 2005).

The presence of the non-coding alternative spliced calretinin transcripts suggests a potential physiological role of these transcripts, exerted through their 3'UTR. Alternative mRNA calretinin transcripts (CALB2b and CALB2c) had been previously reported in different colon carcinoma cell lines (Schwaller et al., 1995) and in mesenchymal tissue of rat embryos (Schwaller et al., 1995). Almost all multi-exon genes can undergo alternative splicing (Pan et al., 2008). Alternative splicing is a tightly regulated process that contributes to transcriptome and proteome diversity, and has been suggested to be important in developmental stages (Revil et al., 2010). Relatively high abundance of all three transcripts was detected in ACC-MESO-4 cells (high calretinin protein levels), whereas only low abundance of the normally spliced 29-kDa isoform was detected in ONE58 cells (low calretinin protein levels). This may suggest that the expression of the alternative transcripts is proportional and may be useful to protect the full-length transcript from 3'UTR mediated degradation. Indeed, when using exogenous expression of CALB2-3'UTR, we increased ~580-fold the 3'UTR sequence compared to the endogenous *CALB2* transcripts, therefore likely contributing to the modulation of miR-30e-5p or anti-miR-30e-5p treatment effect in ONE58 cells. This observation led to the hypothesis that in physiological conditions, *CALB2* alternative transcripts might have their role exerted through their 3'UTR by creating a ceRNA network in which they compete to bind miR-30e-5p protecting the protein-coding *CALB2* transcript. Altogether, our study is providing evidence for the importance and the functionality of the *CALB2* 3'UTR in regulating calretinin expression. Indeed, our data show the role of I) AU-binding proteins in calretinin stabilization and II) miR-30e-5p in the post-transcriptional negative regulation of calretinin expression via interaction with its 3'-UTR. Furthermore, our study demonstrates a possible physiological role of calretinin's alternatively spliced transcripts.

5 Conflict of Interest

The authors declare that they have no competing interests.

6 Author Contributions

JK, MS, MR, carried out experiments and interpreted data. EF and JK designed experiments and interpreted data. MK, SK and GR provided data on the relationship between CALB2 and miR-30e in clinical samples. JK and MK generated figures and tables. JK and EF wrote the manuscript. All authors read and approved the final manuscript.

7 Funding

This work was supported by the Swiss National Science Foundation Sinergia grant CRSII3 147697/1 and the Stiftung für Angewandte Krebsforchung. Funding bodies had no role in the design of the study and collection, analysis, and interpretation of data and in writing the manuscript.

8 Acknowledgments

Prof. Brian Gregory at University of Pennsylvania is acknowledged for helping in secondary structure prediction using RNAfold.

9 References

Agarwal, V., Bell, G.W., Nam, J.W., and Bartel, D.P. (2015). Predicting effective microRNA target sites in mammalian mRNAs. *Elife* 4.

Ahuja, D., Goyal, A., and Ray, P.S. (2016). Interplay between RNA-binding protein HuR and microRNA-125b regulates p53 mRNA translation in response to genotoxic stress. *RNA Biol***,** 1-14.

Andre, M., and Felley-Bosco, E. (2003). Heme oxygenase-1 induction by endogenous nitric oxide: influence of intracellular glutathione. *FEBS Lett* 546**,** 223-227.

Barreau, C., Paillard, L., and Osborne, H.B. (2005). AU-rich elements and associated factors: are there unifying principles? *Nucleic Acids Res* 33**,** 7138-7150.

Betel, D., Wilson, M., Gabow, A., Marks, D.S., and Sander, C. (2008). The microRNA.org resource: targets and expression. *Nucleic Acids Res* 36**,** D149-153.

Bhattacharyya, S.N., Habermacher, R., Martine, U., Closs, E.I., and Filipowicz, W. (2006). Relief of microRNA-mediated translational repression in human cells subjected to stress. *Cell* 125**,** 1111-1124.

Brennan, C.M., and Steitz, J.A. (2001). HuR and mRNA stability. *Cell Mol Life Sci* 58**,** 266-277.

Busacca, S., Germano, S., De Cecco, L., Rinaldi, M., Comoglio, F., Favero, F., Murer, B., Mutti, L., Pierotti, M., and Gaudino, G. (2010). MicroRNA signature of malignant mesothelioma with potential diagnostic and prognostic implications. *Am J Respir Cell Mol Biol* 42**,** 312-319.

Bustin, S.A., Benes, V., Garson, J.A., Hellemans, J., Huggett, J., Kubista, M., Mueller, R., Nolan, T., Pfaffl, M.W., Shipley, G.L., Vandesompele, J., and Wittwer, C.T. (2009). The MIQE guidelines: minimum information for publication of quantitative real-time PCR experiments. *Clin Chem* 55**,** 611-622.

Cheng, Y.Y., Wright, C.M., Kirschner, M.B., Williams, M., Sarun, K.H., Sytnyk, V., Leshchynska, I., Edelman, J.J., Vallely, M.P., Mccaughan, B.C., Klebe, S., Van Zandwijk, N., Lin, R.C., and Reid, G. (2016). KCa1.1, a calcium-activated potassium channel subunit alpha 1, is targeted by miR-17-5p and modulates cell migration in malignant pleural mesothelioma. *Mol Cancer* 15**,** 44.

Fallmann, J., Sedlyarov, V., Tanzer, A., Kovarik, P., and Hofacker, I.L. (2016). AREsite2: an enhanced database for the comprehensive investigation of AU/GU/U-rich elements. *Nucleic Acids Res* 44**,** D90-95.

Fanourgakis, G., Lesche, M., Akpinar, M., Dahl, A., and Jessberger, R. (2016). Chromatoid Body Protein TDRD6 Supports Long 3' UTR Triggered Nonsense Mediated mRNA Decay. *PLoS Genet* 12**,** e1005857.

Gordon, G.J., Rockwell, G.N., Jensen, R.V., Rheinwald, J.G., Glickman, J.N., Aronson, J.P., Pottorf, B.J., Nitz, M.D., Richards, W.G., Sugarbaker, D.J., and Bueno, R. (2005). Identification of novel candidate oncogenes and tumor suppressors in malignant pleural mesothelioma using large-scale transcriptional profiling. *Am J Pathol* 166**,** 1827-1840.

Gruber, A.R., Lorenz, R., Bernhart, S.H., Neubock, R., and Hofacker, I.L. (2008). The Vienna RNA websuite. *Nucleic Acids Res* 36**,** W70-74.

Hofacker, I.L. (2009). RNA secondary structure analysis using the Vienna RNA package. *Curr Protoc Bioinformatics* Chapter 12**,** Unit12 12.

Jha, A., Panzade, G., Pandey, R., and Shankar, R. (2015). A legion of potential regulatory sRNAs exists beyond the typical microRNAs microcosm. *Nucleic Acids Res* 43**,** 8713-8724.

Jing, Q., Huang, S., Guth, S., Zarubin, T., Motoyama, A., Chen, J., Di Padova, F., Lin, S.C., Gram, H., and Han, J. (2005). Involvement of microRNA in AU-rich element-mediated mRNA instability. *Cell* 120**,** 623-634.

Kao, S.C., Klebe, S., Henderson, D.W., Reid, G., Chatfield, M., Armstrong, N.J., Yan, T.D., Vardy, J., Clarke, S., Van Zandwijk, N., and Mccaughan, B. (2011). Low calretinin expression and high neutrophil-to-lymphocyte ratio are poor prognostic factors in patients with malignant mesothelioma undergoing extrapleural pneumonectomy. *J Thorac Oncol* 6**,** 1923-1929.

Kedde, M., Van Kouwenhove, M., Zwart, W., Oude Vrielink, J.A., Elkon, R., and Agami, R. (2010). A Pumilio-induced RNA structure switch in p27-3' UTR controls miR-221 and miR-222 accessibility. *Nat Cell Biol* 12**,** 1014-1020.

Khabar, K.S. (2010). Post-transcriptional control during chronic inflammation and cancer: a focus on AU-rich elements. *Cell Mol Life Sci* 67**,** 2937-2955.

Kirschner, M.B., Cheng, Y.Y., Armstrong, N.J., Lin, R.C., Kao, S.C., Linton, A., Klebe, S., Mccaughan, B.C., Van Zandwijk, N., and Reid, G. (2015). MiR-score: a novel 6-microRNA signature that predicts survival outcomes in patients with malignant pleural mesothelioma. *Mol Oncol* 9**,** 715-726.

Krek, A., Grun, D., Poy, M.N., Wolf, R., Rosenberg, L., Epstein, E.J., Macmenamin, P., Da Piedade, I., Gunsalus, K.C., Stoffel, M., and Rajewsky, N. (2005). Combinatorial microRNA target predictions. *Nat Genet* 37**,** 495-500.

Kresoja-Rakic, J., Kapaklikaya, E., Ziltener, G., Dalcher, D., Santoro, R., Christensen, B.C., Johnson, K.C., Schwaller, B., Weder, W., Stahel, R.A., and Felley-Bosco, E. (2016). Identification of cis- and trans-acting elements regulating calretinin expression in mesothelioma cells. *Oncotarget*.

Krol, J., Loedige, I., and Filipowicz, W. (2010). The widespread regulation of microRNA biogenesis, function and decay. *Nat Rev Genet* 11**,** 597-610.

Li, J.H., Liu, S., Zhou, H., Qu, L.H., and Yang, J.H. (2014). starBase v2.0: decoding miRNA-ceRNA, miRNA-ncRNA and protein-RNA interaction networks from large-scale CLIP-Seq data. *Nucleic Acids Res* 42**,** D92-97.

Linton, A., Pavlakis, N., O'connell, R., Soeberg, M., Kao, S., Clarke, S., Vardy, J., and Van Zandwijk, N. (2014). Factors associated with survival in a large series of patients with malignant pleural mesothelioma in New South Wales. *Br J Cancer* 111**,** 1860-1869.

Lu, J., Getz, G., Miska, E.A., Alvarez-Saavedra, E., Lamb, J., Peck, D., Sweet-Cordero, A., Ebet, B.L., Mak, R.H., Ferrando, A.A., Downing, J.R., Jacks, T., Horvitz, H.R., and Golub, T.R. (2005). MicroRNA expression profiles classify human cancers. *Nature* 435**,** 834-838.

Ma, W.J., Cheng, S., Campbell, C., Wright, A., and Furneaux, H. (1996). Cloning and characterization of HuR, a ubiquitously expressed Elav-like protein. *J Biol Chem* 271**,** 8144-8151.

Manning, L.S., Whitaker, D., Murch, A.R., Garlepp, M.J., Davis, M.R., Musk, A.W., and Robinson, B.W. (1991). Establishment and characterization of five human malignant mesothelioma cell lines derived from pleural effusions. *Int J Cancer* 47**,** 285-290.

Mayr, C. (2016). Evolution and Biological Roles of Alternative 3'UTRs. *Trends Cell Biol* 26**,** 227-237.

Mitra, R., Sun, J., and Zhao, Z. (2015). microRNA regulation in cancer: One arm or two arms? *Int J Cancer* 137**,** 1516-1518.

Ordóñez, N.G. (2014). Value of calretinin immunostaining in diagnostic pathology: a review and update. *Appl Immunohistochem Mol Morphol* 22**,** 401-415.

Otterstrom, C., Soltermann, A., Opitz, I., Felley-Bosco, E., Weder, W., Stahel, R.A., Triponez, F., Robert, J.H., and Serre-Beinier, V. (2014). CD74: a new prognostic factor for patients with malignant pleural mesothelioma. *Br J Cancer* 110**,** 2040-2046.

Pan, Q., Shai, O., Lee, L.J., Frey, B.J., and Blencowe, B.J. (2008). Deep surveying of alternative splicing complexity in the human transcriptome by high-throughput sequencing. *Nat Genet* 40**,** 1413-1415.

Porpodis, K., Zarogoulidis, P., Boutsikou, E., Papaioannou, A., Machairiotis, N., Tsakiridis, K., Katsikogiannis, N., Zaric, B., Perin, B., Huang, H., Kougioumtzi, I., Spyratos, D., and Zarogoulidis, K. (2013). Malignant pleural mesothelioma: current and future perspectives. *J Thorac Dis* 5**,** S397-S406.

Reid, G. (2015). MicroRNAs in mesothelioma: from tumour suppressors and biomarkers to therapeutic targets. *J Thorac Dis* 7**,** 1031-1040.

Revil, T., Gaffney, D., Dias, C., Majewski, J., and Jerome-Majewska, L.A. (2010). Alternative splicing is frequent during early embryonic development in mouse. *BMC Genomics* 11**,** 399.

Salmena, L., Poliseno, L., Tay, Y., Kats, L., and Pandolfi, P.P. (2011). A ceRNA hypothesis: the Rosetta Stone of a hidden RNA language? *Cell* 146**,** 353-358.

Schmitter, D., Lauber, B., Fagg, B., and Stahel, R.A. (1992). Hematopoietic growth factors secreted by seven human pleural mesothelioma cell lines: interleukin-6 production as a common feature. *Int J Cancer.* 51**,** 296-301.

Schwaller, B., Celio, M.R., and Hunziker, W. (1995). Alternative splicing of calretinin mRNA leads to different forms of calretinin. *Eur J Biochem* 230**,** 424-430.

Sheng, H., Shao, J., Dixon, D.A., Williams, C.S., Prescott, S.M., Dubois, R.N., and Beauchamp, R.D. (2000). Transforming growth factor-beta1 enhances Ha-ras-induced expression of cyclooxygenase-2 in intestinal epithelial cells via stabilization of mRNA. *J Biol Chem* 275**,** 6628-6635.

Shi, Y., Moura, U., Opitz, I., Soltermann, A., Rehrauer, H., Thies, S., Weder, W., Stahel, R.A., and Felley-Bosco, E. (2012). Role of hedgehog signaling in malignant pleural mesothelioma. *Clin Cancer Res* 18**,** 4646-4656.

Sidi, R., Pasello, G., Opitz, I., Soltermann, A., Tutic, M., Rehrauer, H., Weder, W., Stahel, R.A., and Felley-Bosco, E. (2011). Induction of senescence markers after neo-adjuvant chemotherapy of malignant pleural mesothelioma and association with clinical outcome: an exploratory analysis. *Eur J Cancer* 47**,** 326-332.

Srikantan, S., Tominaga, K., and Gorospe, M. (2012). Functional interplay between RNA-binding protein HuR and microRNAs. *Curr Protein Pept Sci* 13**,** 372-379.

Stoppoloni, D., Cardillo, I., Verdina, A., Vincenzi, B., Menegozzo, S., Santini, M., Sacchi, A., Baldi, A., and Galati, R. (2008). Expression of the embryonic lethal abnormal vision-like protein

HuR in human mesothelioma: association with cyclooxygenase-2 and prognosis. *Cancer* 113**,** 2761-2769.

Tasic, B., Menon, V., Nguyen, T.N., Kim, T.K., Jarsky, T., Yao, Z., Levi, B., Gray, L.T., Sorensen, S.A., Dolbeare, T., Bertagnolli, D., Goldy, J., Shapovalova, N., Parry, S., Lee, C., Smith, K., Bernard, A., Madisen, L., Sunkin, S.M., Hawrylycz, M., Koch, C., and Zeng, H. (2016). Adult mouse cortical cell taxonomy revealed by single cell transcriptomics. *Nat Neurosci* 19**,** 335-346.

Tay, Y., Rinn, J., and Pandolfi, P.P. (2014). The multilayered complexity of ceRNA crosstalk and competition. *Nature* 505**,** 344-352.

Thurneysen, C., Opitz, I., Kurtz, S., Weder, W., Stahel, R.A., and Felley-Bosco, E. (2009). Functional inactivation of NF2/merlin in human mesothelioma. *Lung Cancer* 64**,** 140-147.

Tiedje, C., Ronkina, N., Tehrani, M., Dhamija, S., Laass, K., Holtmann, H., Kotlyarov, A., and Gaestel, M. (2012). The p38/MK2-driven exchange between tristetraprolin and HuR regulates AU-rich element-dependent translation. *PLoS Genet* 8**,** e1002977.

Usami, N., Fukui, T., Kondo, M., Taniguchi, T., Yokoyama, T., Mori, S., Yokoi, K., Horio, Y., Shimokata, K., Sekido, Y., and Hida, T. (2006). Establishment and characterization of four malignant pleural mesothelioma cell lines from Japanese patients. *Cancer Sci* 97**,** 387-394.

Van Kouwenhove, M., Kedde, M., and Agami, R. (2011). MicroRNA regulation by RNA-binding proteins and its implications for cancer. *Nat Rev Cancer* 11**,** 644-656.

Vislovukh, A., Vargas, T.R., Polesskaya, A., and Groisman, I. (2014). Role of 3'-untranslated region translational control in cancer development, diagnostics and treatment. *World J Biol Chem* 5**,** 40-57.

Volinia, S., Calin, G.A., Liu, C.G., Ambs, S., Cimmino, A., Petrocca, F., Visone, R., Iorio, M., Roldo, C., Ferracin, M., Prueitt, R.L., Yanaihara, N., Lanza, G., Scarpa, A., Vecchione, A., Negrini, M., Harris, C.C., and Croce, C.M. (2006). A microRNA expression signature of human solid tumors defines cancer gene targets. *Proceedings of the National Academy of Sciences of the United States of America* 103**,** 2257-2261.

Von Roretz, C., Di Marco, S., Mazroui, R., and Gallouzi, I.E. (2011). Turnover of AU-rich-containing mRNAs during stress: a matter of survival. *Wiley Interdiscip Rev RNA* 2**,** 336-347.

Von Roretz, C., and Gallouzi, I.E. (2008). Decoding ARE-mediated decay: is microRNA part of the equation? *J Cell Biol* 181**,** 189-194.

10 Legends to the Figures

Figure 1 Three different calretinin transcripts are present in mesothelioma cells. (A) The calretinin gene (*CALB2*) has been reported to have a normally spliced transcript (full isoform CALB2-29 kDa) with 11 exons, and two alternative splice variants CALB2b (non-coding RNA) and CALB2c (short isoform 22 kDa) with skipped exon 8 and exons 8-9, respectively. Labeled in grey box is the 3'UTR (untranslated region) of *CALB2* mRNA variants. Arrows in blue, green, and orange, depict the positions of boundary spanning primers used to detect the presence of calretinin transcripts. **(B)** RT-qPCR revealed the presence of all three transcripts in ZL55 and ACC-MESO-4 cells whereas only full isoform CALB2 (normal spliced transcript) and at low abundance is detected in ONE58 cells. Histones were used as internal control.

Figure 2 Calretinin 3'UTR contains a stabilizing and 2 destabilizing elements. (A) Multiple species alignment of calretinin 3'UTR using USCS genome browser revealed two conserved stretches. **(B)** Complete calretinin 3'UTR sequence 573 nt (CALB2-3'UTR) with the predicted putative *cis*-regulatory elements: an A/U-rich motif (ARE) (red), mir-30a/b/c/d/e (red), mir-9 (blue) binding sites and a poly-A site (PAS) (green). **(C)** 573-nt CALB2-3'UTR was inserted downstream of the luciferase reporter in the pmirGLO reporter plasmid. Four additional luciferase reporter constructs carrying mutations in either ARE and/or miR-30 binding sites were generated and their activity was tested in ONE58 cells. **(D)** Insertion of CALB2-3'UTR significantly downregulated luciferase expression when compared to the vector pmirGLO alone. Mutation of the ARE-motif further downregulated reporter expression, whereas the double mutation of miR-30 binding sites abolished the downregulatory effect of the calretinin 3'UTR. FLU- Firefly Luciferase Units. The empty vector pmirGLO plasmid expression was arbitrarily set to 100% and the reporter activity of the mutants was expressed as a percentage of the wild-type construct. Mean, ±SD n=8; * $p<0.05$; ** $p<0.01$; *** $p<0.005$ using Mann-Whitney U test.

Figure 3 25nt RNA oligo containing ARE-motif binds a protein from cytosolic extract of mesothelioma cell lines. **(A)** Predicted optimal secondary structures of the wt and mtARE calretinin 3'UTR fragment (317 nt; position 1152-1469) using RNAfold software. The ARE-motif (AUUUA) is forming a bulge, which upon mutation of the consensus sequence is abolished. The colors represent base pair probabilities (0 to 1) for paired- or unpaired bases. **(B)** EMSA assay demonstrating that the 25-nt RNA oligo containing the ARE element binds a protein present in cytosolic protein extracts of ACC-MESO-4, SPC111 and ZL55 cells (lanes 2,3,4). The complex is diminished in the presence of a 200-folds excess of the same unlabeled probe (lanes 5,6,7), but not outcompeted in a 200-folds excess of the unrelated unlabeled probe (lanes 8, 9, 10). **(C)** Quantification of two AU-binding proteins, HuR and TTP, across different mesothelioma cell lines, using histones as an internal control. Levels are shown relative to the TTP in MSTO-211H cells according to the $-\Delta\Delta$Ct method.

Figure 4 Members of miR-30 family are abundantly expressed in mesothelioma cell lines and miR-30e-5p regulates calretinin expression. (A) miR-30e-5p mimic treatment significantly repressed reporter expression in ONE58 cells stable expressing reporter-calretinin 3'UTR along with downregulation of calretinin protein levels. Mean±SD n=6; * $p<0.05$; ** $p<0.01$; *** $p<0.005$ using Mann-Whitney U test. **(B)** Depletion of miR-30e-5p by anti-miR-30e-5p increased the reporter expression as well as calretinin protein levels. Mean±SD n=3; * $p<0.05$; ** $p<0.01$; *** $p<0.005$ using t-test. **(C)** Quantitative RT-PCR analysis of miR-30 family members and miR-9 in 3 mesothelioma cell lines using as RNU-6B-2 as a reference gene. Levels are shown relative to the miR-30d-5p in ZL55 cells according to the $-\Delta\Delta$Ct method. **(D)** Weak negative correlation between calretinin expression (IHC) and miR-30e-5p in a cohort of 60 human mesothelioma samples. Spearman's correlation.

Figure 5 Overexpression of calretinin 3'UTR competes with trans-regulatory factors and reveals a ceRNA network in regulation of calretinin expression. (A) Exogenous overexpression of CALB2-3'UTR abolishes the effect of miR-30e-5p on calretinin expression in ONE58 cells. **(B)** Inhibition of miR-30e-5p using anti-miR-30e-5p increased calretinin expression in ONE58 cells stably overexpressing CALB2-3'UTR. **(C)** Model of ceRNA network created by introducing exogenous CALB2-3'UTR in ONE58cell. ONE58 cell overexpress 580-times more of calretinin 3'UTR (blue) compared to endogenous calretinin mRNA and 2-fold more of HuR than TTP (orange). Upon miR-30-5p mimetic treatment (red) no change is observed on calretinin protein levels due to exogenous CALB2-3'UTR that sponges miR-30e-5p. The effect of anti-miR-30e-5p (green) is observed in ONE58 cells with exogenous CALB2-3'UTR.

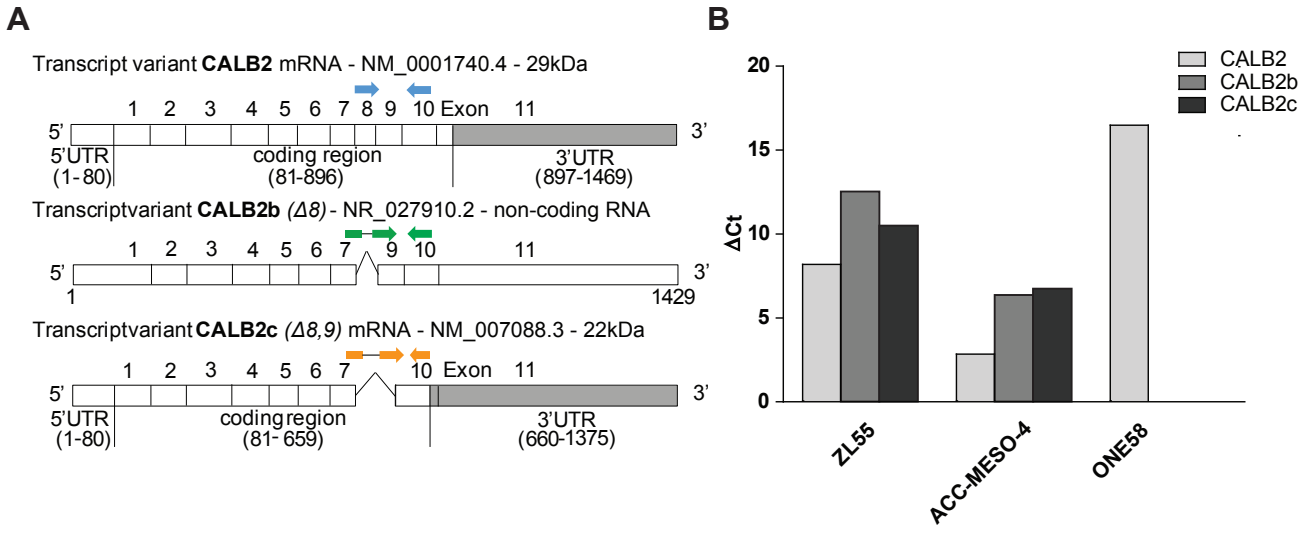
A
Transcript variant CALB2 mRNA - NM_0001740.4 - 29kDa
1 2 3 4 5 6 7 8 9 10 Exon 11
5'
3'
5'UTR (1-80)
coding region (81-896)
3'UTR (897-1469)
Transcriptvariant CALB2b (Δ8) - NR_027910.2 - non-coding RNA
1 2 3 4 5 6 7 9 10 11
5'
3'
1
1429
Transcriptvariant CALB2c (Δ8,9) mRNA - NM_007088.3 - 22kDa
1 2 3 4 5 6 7 10 Exon 11
5'
3'
5'UTR (1-80)
coding region (81-659)
3'UTR (660-1375)
B
CALB2
CALB2b
CALB2c
ΔCt
20
15
10
5
0
ZL55
ACC-MESO-4
ONE58

FIGURE 1

A

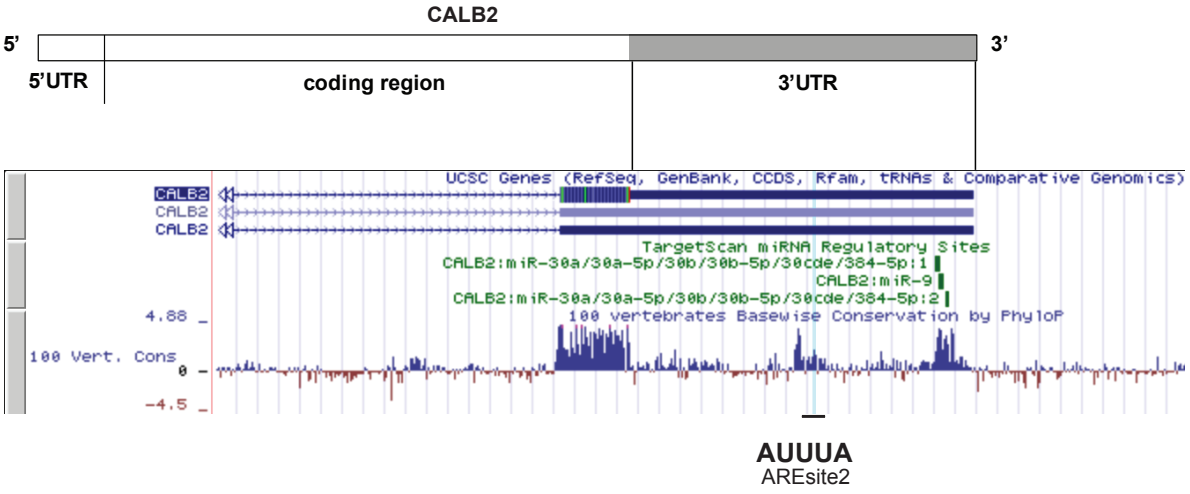

B

CALB2-3'UTR (29 kDa)

agtggggacgggggctgcttctccacctcccccaaaccctgcttctgctgccctgatgcgtctacccagactcagagaccgtgagcgccccg
ccccccaccctacagcctgcacacacctgcctgcagagcaggaaatgagagatagaggatgggcagctgggggctgtcctgagccccc
tgcacccacccctgcccaggcagtctttgctcagtggatcacacacatggaaggtgatgggggcatgggtggagggtccctaattctcttcgct
gtgatgcatgagctccctcgctgtatgatttaggcttctatgtccaacagagtggactcttccctctcgctcccctctgccggtcccccatgccacc
acccaccccaaacttccaggttccatccaccaccttgccaatggtgtagctgtcctctcagaactcctgtgtgtggaaggcacccgccctttcctt
gccttctttactcggcgtgctccttttctctttgggtttcttgtttaccaaagaagagtttacagacaataaaatggaaaggtcctgctgtggaaactt
acccaa

ARE
miR-30a/b/c/d/e-5p
miR-9-5p
miR-30a/b/c/d/e-5p
poly-A site

C

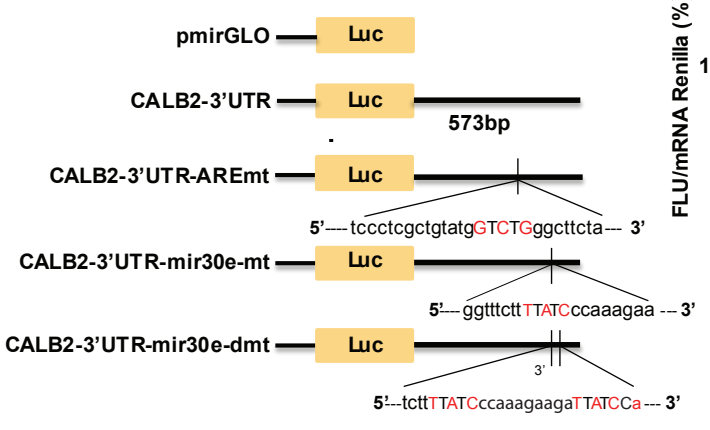

D

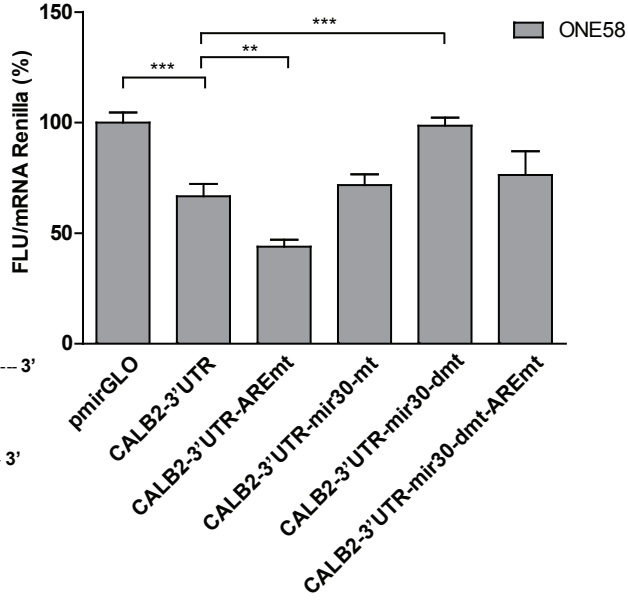

FIGURE 2

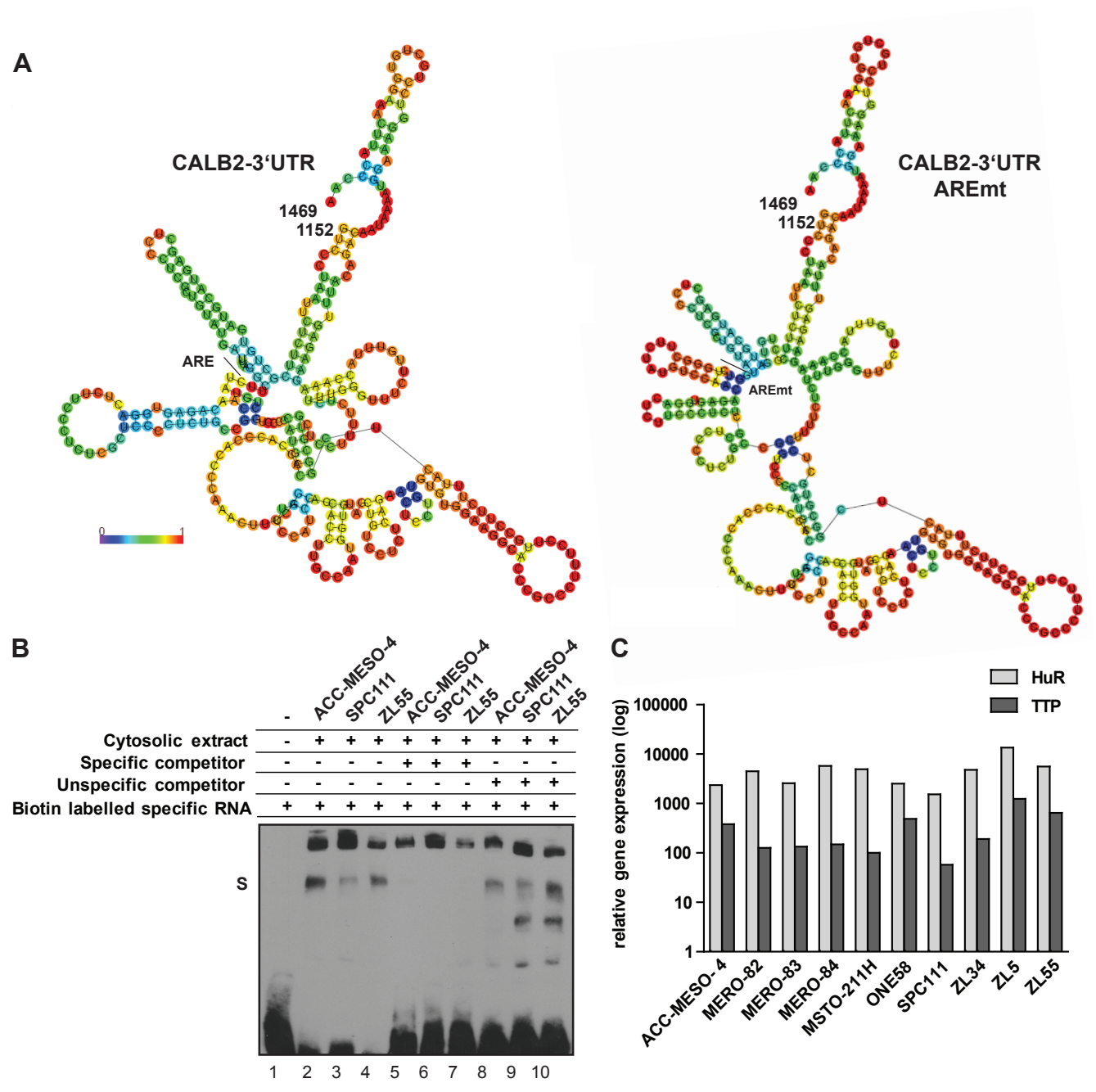
A
CALB2-3'UTR
1469
1152
ARE
0
1
CALB2-3'UTR
AREmt
1469
1152
AREmt
B
-
ACC-MESO-4
SPC111
ZL55
ACC-MESO-4
SPC111
ZL55
ACC-MESO-4
SPC111
ZL55
Cytosolic extract
Specific competitor
Unspecific competitor
Biotin labelled specific RNA
S
1 2 3 4 5 6 7 8 9 10
C
HuR
TTP
relative gene expression (log)
100000
10000
1000
100
10
1
ACC-MESO-4
MERO-82
MERO-83
MERO-84
MSTO-211H
ONE58
SPC111
ZL34
ZL5
ZL55

FIGURE 3

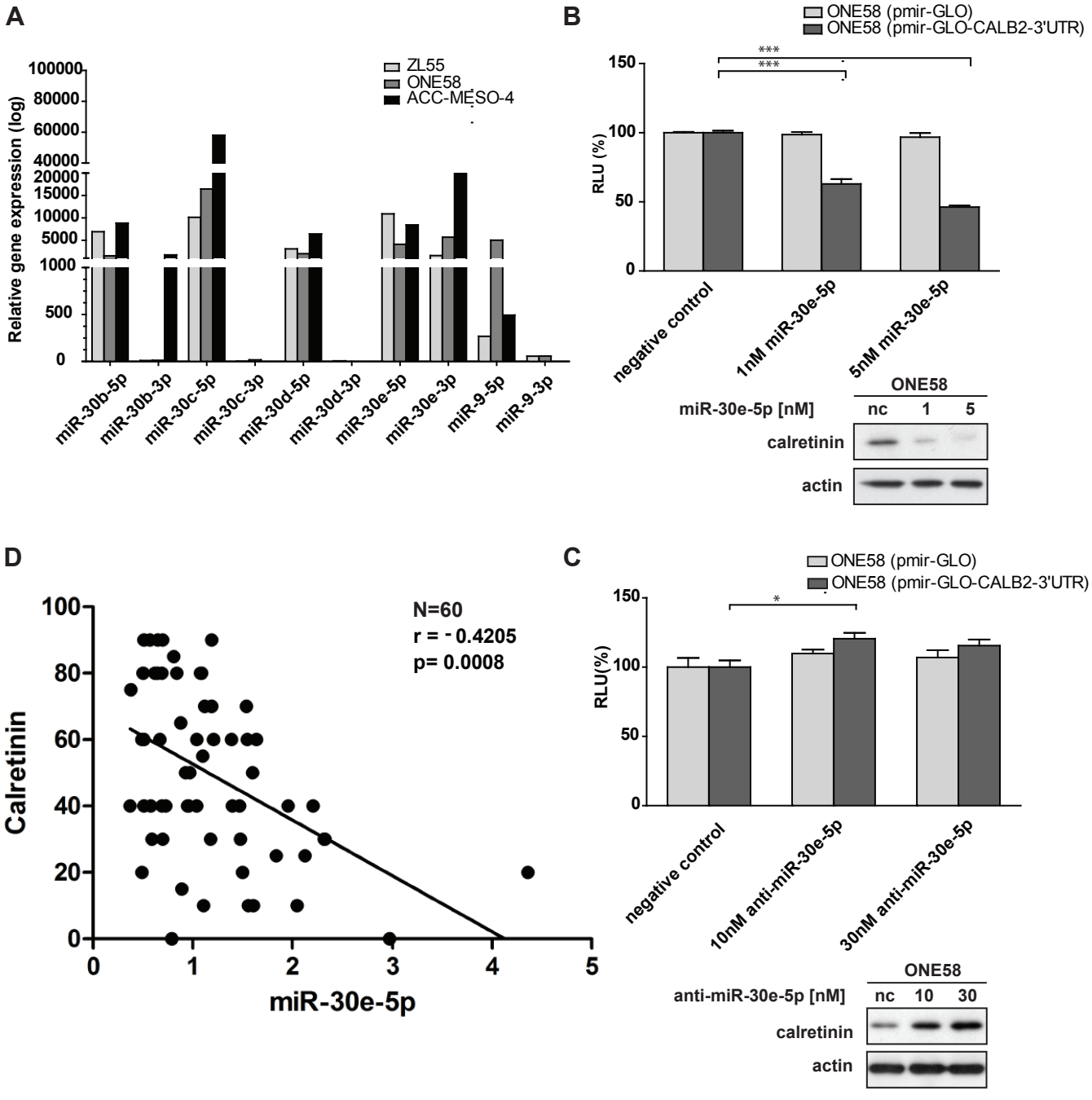
A
Relative gene expression (log)
100000
80000
60000
40000
20000
15000
10000
5000
1000
500
0
ZL55
ONE58
ACC-MESO-4
miR-30b-5p
miR-30b-3p
miR-30c-5p
miR-30c-3p
miR-30d-5p
miR-30d-3p
miR-30e-5p
miR-30e-3p
miR-9-5p
miR-9-3p
B
ONE58 (pmir-GLO)
ONE58 (pmir-GLO-CALB2-3'UTR)
***
***
RLU (%)
150
100
50
0
negative control
1nM miR-30e-5p
5nM miR-30e-5p
ONE58
miR-30e-5p [nM]
nc
1
5
calretinin
actin
D
Calretinin
100
80
60
40
20
0
0
1
2
3
4
5
miR-30e-5p
N=60
r = - 0.4205
p= 0.0008
C
ONE58 (pmir-GLO)
ONE58 (pmir-GLO-CALB2-3'UTR)
*
RLU(%)
150
100
50
0
negative control
10nM anti-miR-30e-5p
30nM anti-miR-30e-5p
ONE58
anti-miR-30e-5p [nM]
nc
10
30
calretinin
actin

FIGURE 4

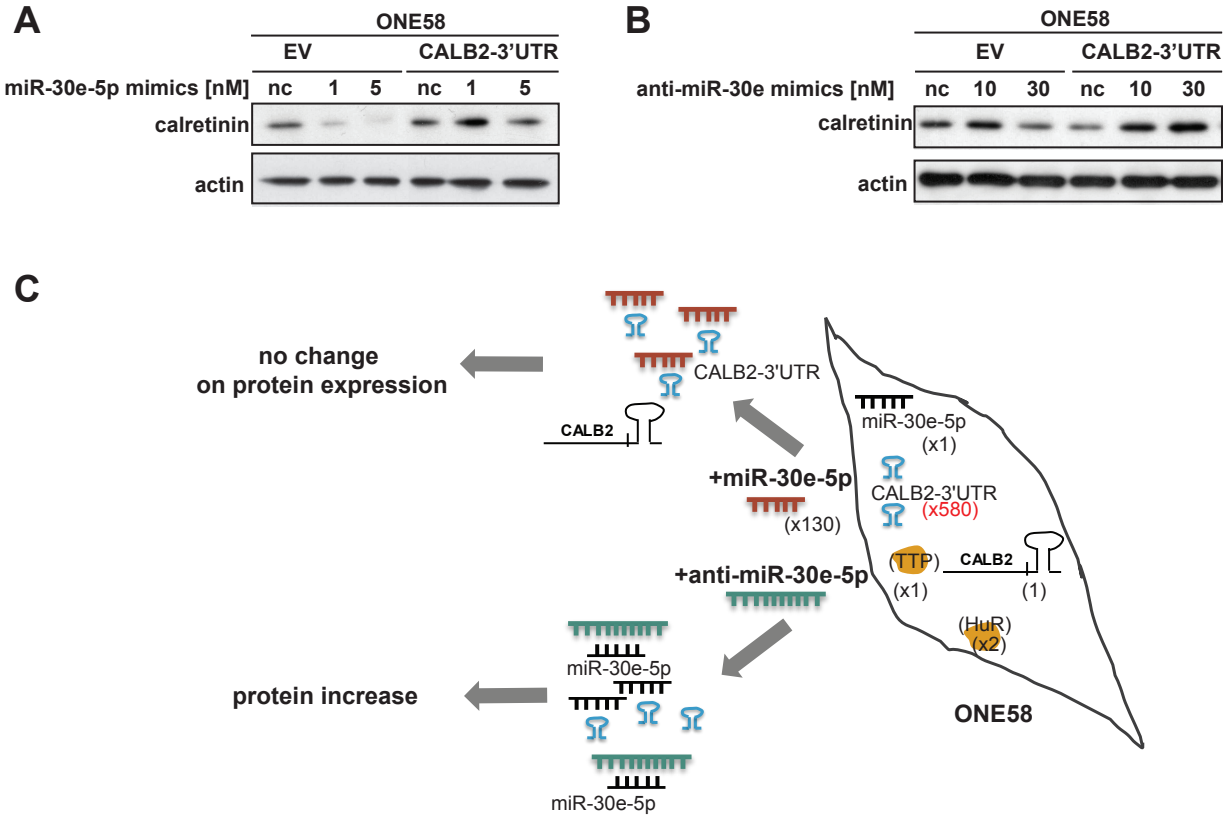
A
ONE58
EV
CALB2-3'UTR
miR-30e-5p mimics [nM]
nc 1 5 nc 1 5
calretinin
actin
B
ONE58
EV
CALB2-3'UTR
anti-miR-30e mimics [nM]
nc 10 30 nc 10 30
calretinin
actin
C
no change
on protein expression
CALB2-3'UTR
CALB2
+miR-30e-5p
(x130)
+anti-miR-30e-5p
miR-30e-5p
protein increase
miR-30e-5p
miR-30e-5p
(x1)
CALB2-3'UTR
(x580)
(TTP)
(x1)
CALB2
(1)
(HuR)
(x2)
ONE58

FIGURE 5

PRIMERS FOR RT-qPCR		
CALB2 Full-length isoforms- 29kDa NM_0001740.4	**CALB2b** Non-coding RNA NR_027910.2	**CALB2c** Calretinin isoform 22k NM_007088.3
5'-ACTCCTGCCTGTCCAGGA-3'	5'-AGATGTCCCGGGCATGAA-3'	5'-GATGTCCCGGATAGAAGC-3'
5'-CCTCTGCCAAGGACATGA-3'	5'-CGTCAATGTAGCCGCTTC-3'	5'-CCTCTGCCAAGGACATGA-3'

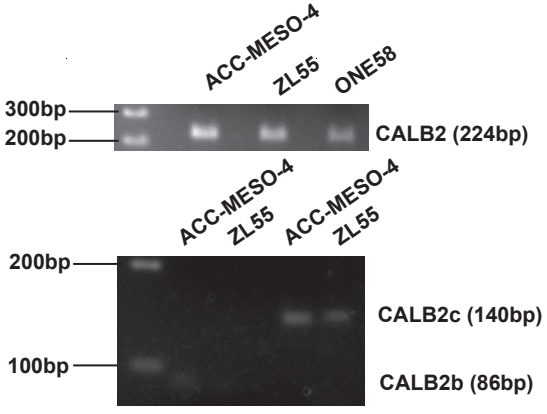

Supplementary figure 1

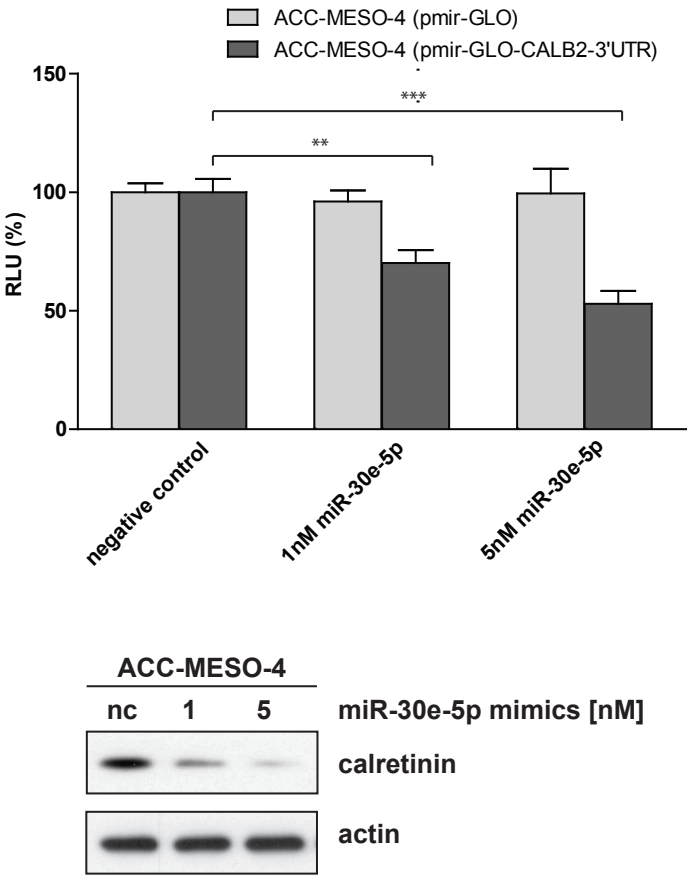

Supplementary figure 2

Supplementary Table 1

Baseline Patient Characteristics (N=60)

Median Age (Range)	58 (22 – 74)
Gender	
Male	46 (76.7 %)
Female	14 (23.3 %)
Histological Subtype	
Epithelioid	43 (71.7 %)
Biphasic	17 (28.3 %)
Sarcomatoid	0 (0 %)
Pathological Stage	
I	2 (3.3 %)
II	8 (13.3 %)
III	44 (73.3 %)
IV	6 (10.0 %)
Induction Chemotherapy	
Yes	13 (21.7 %)
No	47 (78.3 %)
Overall survival from surgery (months, range)	15.3 (0.1 – 90.5)

4.3. GAS5 long non-coding RNA in malignant pleural mesothelioma

Manuscript published in Molecular Cancer on May 23, 2014

Contribution: AR, JKR and EFB carried out most of the experiments and participated in the interpretation of the data. JKR cloned *Gas5* promoter and carried out 1D figure. GZ carried out the PCR analysis and RNA extraction from the tumors. IO provided clinical samples. BV was involved in the interpretation of the analysis of clinical samples. AR and EFB drafted the manuscript. RS, JKR and NE were involved in critically revising the manuscript. All authors read and approved the final manuscript.

MOLECULAR CANCER

RESEARCH Open Access

GAS5 long non-coding RNA in malignant pleural mesothelioma

Arun Renganathan[1], Jelena Kresoja-Rakic[1], Nohemy Echeverry[1], Gabriela Ziltener[1], Bart Vrugt[3], Isabelle Opitz[2], Rolf A Stahel[1] and Emanuela Felley-Bosco[1*]

Abstract

Background: Malignant pleural mesothelioma (MPM) is an aggressive cancer with short overall survival. Long non-coding RNAs (lncRNA) are a class of RNAs more than 200 nucleotides long that do not code for protein and are part of the 90% of the human genome that is transcribed. Earlier experimental studies in mice showed GAS5 (growth arrest specific transcript 5) gene deletion in asbestos driven mesothelioma. GAS5 encodes for a lncRNA whose function is not well known, but it has been shown to act as glucocorticoid receptor decoy and microRNA "sponge". Our aim was to investigate the possible role of the GAS5 in the growth of MPM.

Methods: Primary MPM cultures grown in serum-free condition in 3% oxygen or MPM cell lines grown in serum-containing medium were used to investigate the modulation of GAS5 by growth arrest after inhibition of Hedgehog or PI3K/mTOR signalling. Cell cycle length was determined by EdU incorporation assay in doxycycline inducible short hairpinGAS5 clones generated from ZL55SPT cells. Gene expression was quantified by quantitative PCR. To investigate the *GAS5* promoter, a 0.77 kb sequence was inserted into a pGL3 reporter vector and luciferase activity was determined after transfection into MPM cells. Localization of GAS5 lncRNA was identified by *in situ* hybridization. To characterize cells expressing GAS5, expression of podoplanin and Ki-67 was assessed by immunohistochemistry.

Results: GAS5 expression was lower in MPM cell lines compared to normal mesothelial cells. GAS5 was upregulated upon growth arrest induced by inhibition of Hedgehog and PI3K/mTOR signalling in *in vitro* MPM models. The increase in GAS5 lncRNA was accompanied by increased promoter activity. Silencing of GAS5 increased the expression of glucocorticoid responsive genes glucocorticoid inducible leucine-zipper and serum/glucocorticoid-regulated kinase-1 and shortened the length of the cell cycle. Drug induced growth arrest was associated with GAS5 accumulation in the nuclei. GAS5 was abundant in tumoral quiescent cells and it was correlated to podoplanin expression.

Conclusions: The observations that GAS5 levels modify cell proliferation *in vitro,* and that GAS5 expression in MPM tissue is associated with cell quiescence and podoplanin expression support a role of GAS5 in MPM biology.

Keywords: Malignant pleural mesothelioma, Long non-coding RNA, RNA FISH, Quiescence, Cell cycle length

Background

Malignant pleural mesothelioma (MPM) are tumors originating from the surface serosal cells of the pleura [1]. MPM are rare tumors mainly caused by exposure to asbestos and patients have a median survival around 12 months even after combined chemotherapy [2,3]. Molecular studies identified altered expression of critical genes in oncogenesis, especially tumor suppressor genes at the INK4 and NF2 loci (reviewed in [4]). A recent study has shown dysregulation of long non-coding RNA (lncRNA) expression in MPM compared to normal mesothelium [5]. LncRNA are part of the transcriptome that does not encode for proteins, which includes tens of thousands of lncRNA [6]. LncRNAs are defined as being longer than 200 nucleotides [7] and have poor sequence conservation across species [8] which led to the hypothesis that the function is most likely linked to the RNA structure itself. The functions of some lncRNAs have been

* Correspondence: emanuela.felley-bosco@usz.ch
[1]Laboratory of Molecular Oncology, Clinic of Oncology, University Hospital Zürich, Zürich, Switzerland
Full list of author information is available at the end of the article

described and include chromatin modifier, transcriptional and post-transcriptional regulator of gene expression [9-11]. In this context, lncRNAs are now emerging as mammalian transcription key regulators in response to developmental or environmental signals [12-14] and are associated to many cancer related pathways through gene regulation [15]. Although much has still to be investigated about the major part of lncRNAs, the involvement of some of them in tumor progression has already been shown, e.g. lncRNA HOTAIR which interacts with the chromatin-remodelling complex PRC2 [16].

Interestingly, a minimal region of deletion was identified in asbestos induced murine malignant mesothelioma which includes *gas5* locus [17]. The *GAS5* gene is a so-called host gene for small nucleolar RNA (snoRNA) and it is encoded at locus 1q25. It has up to 12 exons and 10 box C/D snoRNAs within its alternative introns together with conserved 5′-terminal oligopyrimidine tract (5′ TOP) [18]. GAS5 is named based on the finding that its expression levels increased upon cell growth arrest induced after serum starvation [19] or as the result of rapamycin-induced cell cycle arrest [18]. Recent studies have shown that GAS5 silencing in T cells increased the proportion of cells in S phase, reduced the rate of spontaneous apoptosis [20] and protected cells from rapalogue (temsirolimus, everolimus) induced proliferation arrest [21]. In epithelial cells GAS5 regulates glucocorticoid-dependent transcription by acting as a decoy outcompeting the DNA-binding site of the glucocorticoid receptor, thereby reducing cell metabolism [22]. More recently GAS5 has been described to act as sponge which sequesters miR-21 [23]. GAS5 is also part of lncRNA abundantly expressed in cancer cells [24]. In this study, we investigate whether GAS5 has a role in MPM biology.

Results

GAS5 lncRNA expression level is lower in MPM cell lines compared to normal mesothelial cells and it is increased by drugs inducing growth arrest

GAS5 expression in MPM cell lines (n = 22) is significantly lower (Figure 1A; $p < 0.005$; individual MPM cell line profile is shown Additional file 1: Figure S1) when compared to normal mesothelial cells (n = 7). The *GAS5* gene produces 29 different splice variants (Additional file 2: Table S1) including 10 processed lncRNAs containing or not one or more snoRNA sequences, and 19 unprocessed sequences. The only information available on splice variants expressed in experimental models is provided by one study, where the expression of both mature and unprocessed GAS5 was observed in phytohaemagglutinin stimulated primary lymphocytes [20]. In order to investigate which splice variant is expressed in MPM, we used two sets of primers, theoretically allowing the detection of 20 different cDNAs of GAS5 splice variants (Additional file 3: Table S2) to amplify GAS5 cDNA from four mesothelioma cell lines (ZL55SPT, SDM103T2, ZL55 and ACC-Meso4) that had been selected for functional studies. According to the size of PCR fragments observed for each primer set (Additional file 4: Figure S2) and taking into account the detection by the two primer sets, the list of cDNA expressed was narrowed down to three splice variants including two lncRNA and one intron retaining transcript (Table 1). The expression of the intron retaining transcript was further confirmed using specific primers (Additional file 4: Figure S2D). Quantitative abundance of the different transcripts varied depending on the cell line (Additional file 4: Figure S2B, C and D). To investigate whether GAS5 expression in MPM cells could be modulated by drugs inducing growth arrest, we treated MPM cells with either HhAntag or with NVP-BEZ235 as previously described [25,26]. ZL55SPT and SDM103T2 cells, grown in serum-free medium and at 3% of oxygen conditions, which allow maintenance of dedifferentiation properties [25], where treated during 48 h with HhAntag. A significant ($p < 0.05$) increase of GAS5 lncRNA levels (Figure 1B) and of the number of quiescent, ki67 negative (G_0) cells (Additional file 5: Figure S3) was observed compared to control. Similar results were observed by treating ZL55 and ACC-Meso4 cells, which are grown in serum-containing medium, during 6 h with GI50 (Echeverry, ms in preparation) concentration of NVP-BEZ235 (Figure 1C). While it is not possible to investigate the effect of HhAntag in cell grown in serum containing medium [25], a significant increase of GAS5 levels was observed after treatment of ZL55SPT and SDM103T2 to NVP-BEZ235 (Additional file 6: Figure S4), indicating that cells grown in dedifferentiating conditions remain sensitive to this drug.

To investigate whether increased GAS5 RNA levels observed after treatment with HhAntag and NVP-BEZ235 were associated with increased GAS5 promoter activity, we transfected ZL55SPT and ZL55 cells with a luciferase reporter gene under the control of GAS5 promoter sequences (pGL3-B-pGAS5). Luciferase activity was measured 24 hours after growth arrest-inducing treatment. Although basal pGL3-B-pGAS5 was very high (approximately a thousand fold higher than empty vector, data not shown), a dose dependent significant ($p < 0.05$) increase in promoter activity was identified in ZL55SPT and ZL55 cells after HhAntag and NVP-BEZ-235 treatment (Figure 1D), respectively. Altogether, these results suggest that GAS5 may participate to the growth inhibitory action of HhAntag and NVP-BEZ235 in MPM cells.

Silencing of GAS5 in MPM cells increases glucocorticoid receptor responsive genes and shortens the cell cycle length

To investigate whether GAS5 plays a role in MPM growth, stable doxycycline-inducible shRNA-GAS5 clones were generated using ZL55SPT cells. GAS5 expression levels

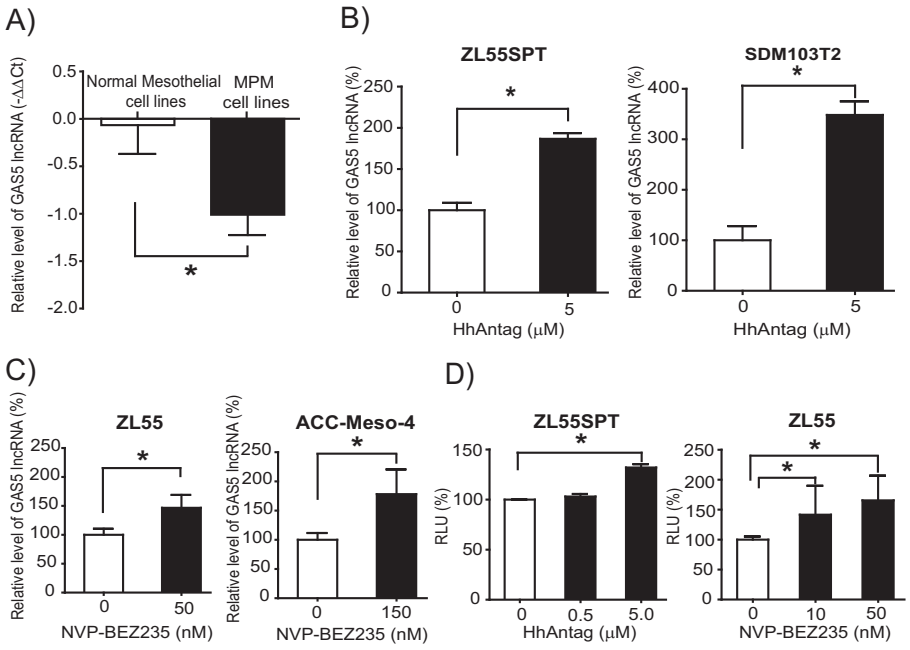

Figure 1 GAS5 expression is lower in MPM and it is increased upon drug induced growth arrest. A. GAS5 is lower in MPM cell lines compared to normal mesothelial cell lines. GAS5 lncRNA expression was analysed by qRT-PCR in 22 MPM cell lines and in 7 normal mesothelial cell lines. Expression of GAS5 was normalized to internal control histones relative to the mean expression of GAS5 in normal mesothelial cells in culture according to –ΔΔCt method. **B** and **C**. Drug induced growth arrest increases GAS5 expression in MPM primary cells (ZL55SPT and SDM103T2) and cell lines (ZL55 and ACC-Meso4). **D**. Expression of GAS5 promoter reporter gene was analysed in control versus HhAntag and NVP-BEZ235 treated samples. Promoter activity, expressed as relative light unit (RLU) normalized to control set at 100%, is significantly increased by treatment with HhAntag and NVP-BEZ235. Values are expressed as mean ± SD from three independent experiments *; $p < 0.05$.

decreased in a doxycycline dose-dependent manner in shGAS5-1 and shGAS5-2 while it was not affected in control cells (Figure 2A). The partial resistance to siRNA-mediated knockdown is consistent with what has been recently described [27] for nuclear lncRNA (see below). To determine whether the observed 35 and 25% (in shGAS-1 and shGAS5-2, respectively) decrease in GAS5 expression was functionally relevant, we determined the consequences on glucocorticoid regulated genes such as glucocorticoid inducible leucine-zipper (GILZ) and serum/glucocorticoid-regulated kinase-1 (SGK1). Indeed, GAS5 lncRNA functions as a decoy for glucocorticoid receptor [22]. As ZL55SPT cells are grown in a serum-free medium containing pharmacological concentrations of glucocorticoids, which are essential for optimal cell growth [25,28], we expected that modulation of GAS5 levels would modify the expression of glucocorticoid regulated genes. Accordingly, we observed that doxycycline-induced decrease of GAS5 expression in shGAS5 clones was accompanied by a significant increase of expression of GILZ in shGAS5-2 clone (Figure 2B) and of SGK1 in shGAS5-1 clone (Figure 2C) while no change was observed in sh control clone, indicating a negative role of GAS5 in the expression of these genes. These observations were confirmed using three independent GAS5 siRNA. Indeed, we observed a significant down-regulation of GAS5 accompanied by a significant increase of GILZ mRNA for the three siRNA tested compared to a control siRNA and a significant increase of SGK1 mRNA for two of the three tested siRNA (Additional file 7: Figure S5).

Next we determined whether GAS5 knockdown affects cell cycle. In order to measure cell cycle length, we performed a time course experiment after pulse labelling shGAS5-1 and shGAS-2 cells with 5-ethynyl-2′-deoxyuridine (EdU). EdU assay revealed an increase in EdU positive cells after doxycycline-induced silencing of GAS5 in shGAS5 clones (Figure 3A and B) while no effect was observed in control cells (data not shown). Using a linear regression method [29], we determined the time taken for 100% EdU incorporation, which corresponds to the time needed for single cell cycle length (Figure 3B). The cell cycle length of uninduced shGAS5 clones was 55–77 hours while the GAS5 silenced cells exhibited a shorter cell cycle of 40 to 47 hours (Figure 3C). Collectively these results confirm that silencing GAS5 has functional consequences in the growth of MPM cells grown in serum-free conditions.

HhAntag-induced growth arrest is accompanied by GAS5 accumulation into the nuclei

To further characterize the mechanism of GAS5 in controlling cell growth in serum-free conditions, we analysed

Table 1 List of GAS5 alternative splice variants corresponding to the size of RT-PCR products

	Vega Genome Browser 54 Transcript ID	Length (bp)	Type
GAS5-Ex-4-8	**207 bps**		
	OTTHUMT00000090577	632	LncRNA
	OTTHUMT00000090578	1698	Retained Intron
	OTTHUMT00000090585	632	Retained Intron
	OTTHUMT00000090586	712	Retained Intron
	OTTHUMT00000090590	688	LncRNA
	OTTHUMT00000090593	772	Retained Intron
	OTTHUMT00000090598	979	Retained Intron
	168 bps		
	OTTHUMT00000090579	565	LncRNA
	OTTHUMT00000090595	745	Retained Intron
	OTTHUMT00000090597	497	Retained Intron
	OTTHUMT00000090605	723	Retained Intron
GAS5-Ex-6-12	**281 bps**		
	OTTHUMT00000090577	632	LncRNA
	OTTHUMT00000090586	712	Retained Intron
	OTTHUMT00000090590	688	LncRNA
	242 bps		
	OTTHUMT00000090579	565	LncRNA
	OTTHUMT00000090584	542	LncRNA
	OTTHUMT00000090604	413	LncRNA

Transcripts that were detected by both primer sets are in bold.

the subcellular localization of GAS5 after treatment with HhAntag by *in situ* hybridization. We confirmed a dose-dependent significant ($p < 0.05$) increase in GAS5 accumulation in the cells and observed an enrichment into the nucleus (Figure 4A and B). Quantification revealed that GAS5 is twice as abundant in the nucleus as in the cytosol in the absence of HhAntag and prevalence in the nucleus was maintained after treatment with HhAntag (Figure 4C). Altogether, these data indicate that HhAntag-induced growth arrest involves accumulation of nuclear GAS5.

Podoplanin expression correlates with GAS5 in malignant pleural mesothelioma

In order to determine the relevance of our *in vitro* findings in clinical samples we determined GAS5 relative expression in MPM and normal tissue. Surprisingly, we found a significant six-fold ($p < 0.0001$) increase of GAS5 level in tumor tissue ($n = 116$) when compared to non-tumoral samples ($n = 10$) (Additional file 8: Figure S6A). This was unexpected considering the upregulation GAS5 during growth arrest and the shortening of cell-cycle observed upon GAS5 silencing. Because MPM tissue contains stromal cells [30] including immune system cells that are highly enriched for GAS5 expression [21], we performed *in situ* hybridization in a subset of samples to investigate and characterize the cells expressing GAS5. GAS5 expression was predominantly identified in quiescent tumor cells (Figure 5A). To further characterize GAS5 expression in relationship to MPM tumors we therefore investigated the relationship of GAS5 expression with mesothelial markers such as mesothelin, calretinin and podoplanin extending a previous analysis of these markers performed on a limited set of samples [30]. Hierarchical clustering of these mesothelial markers with GAS5 showed that the expression of GAS5 clustered with podoplanin in epithelioid, biphasic and sarcomatoid tissue samples (Figure 5B) and a positive correlation between GAS5 and podoplanin levels ($p < 0.05$) was observed (Figure 5C). Furthermore, GAS5 expression was higher in samples with high podoplanin (D2-40) expression (Figure 5A and Additional file 8: Figure S6B). No correlation was observed between GAS5 and mesothelin or calretinin.

Overall, these results indicate that *in vivo* GAS5 expression may play a role not only in growth control but may have additional functions such as the already described miRNA sponge activity [23].

Discussion

In this study we revealed the functional consequences of the expression of GAS5, a lncRNA abundantly expressed in MPM. When compared to normal mesothelial cells, MPM cell lines expressed lower levels of GAS5 and exposure to drugs inducing growth arrest increased GAS5 expression level, in line with what had been previously described with rapamycin-induced cell cycle arrest of NIH3T3 cells [18]. We identified that increased GAS5 levels were associated to increased promoter activity. This is important since it has been shown that GAS5, as other mRNAs carrying 5' TOP, can be stabilized by interaction with La motif-related protein 1 [31]. Interestingly, basal levels of GAS5 promoter were quite high. The promoter is likely to be bidirectional (Additional file 9: Figure S7) controlling both *GAS5* and *zinc finger and BTB domain containing 37* (*ZBTB37*). Not much is known about *ZBTB37* except that it is a transcription factor known to be expressed during embryonic development [32]. It might be interesting to verify whether *ZBTB37* is expressed in MPM after that the mechanisms of induction of *GAS5* promoter have been elucidated.

GAS5 plays an essential role in growth arrest state of both T-cell lines and non-transformed lymphocytes [21].

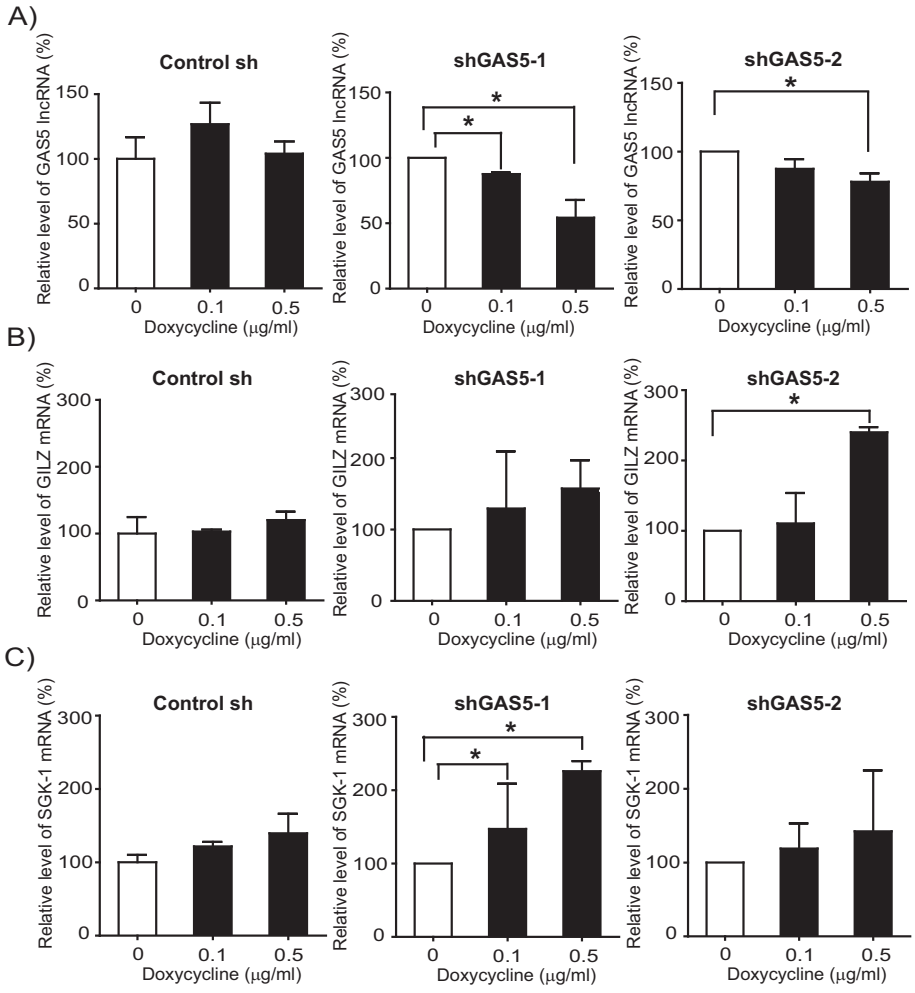

Figure 2 Silencing of GAS5 increases glucocorticoid responsive genes. A. GAS5 lncRNA silencing increases the expression of glucocorticoid responsive genes GILZ **(B)** and SGK1 **(C)**. Values are normalized with histones and shown as mean ± SD from three to four independent experiments. *; $p < 0.05$.

Silencing of GAS5 resulted in shortening cell cycle in MPM cells demonstrating that also in these cells GAS5 controls cell growth. The underlying mechanism can be linked to the fact that GAS5 is a glucocorticoid receptor-decoy and it inhibits transcription of glucocorticoid responsive genes [22]. Glucocorticoids are essential for optimal MPM cell growth [25,28] and are present at pharmacological concentrations in culture medium [33,34]. We estimated that GAS5 is present at the level of ten thousand copies/cell, which is in the range of the reported abundancy of glucocorticoid receptors [35-37]. Therefore it is not surprising that under our experimental conditions a change of glucocorticoid-regulated genes was observed upon GAS5 silencing. Quantitative *in situ* hybridization allowed determining that two thirds of GAS5 is present in the nucleus. Assuming that 10% of total cellular volume is occupied by nucleus this means that nuclear GAS5 concentration is approximately 18 fold higher in the nuclei compared to the cytosol. It had already been shown that GAS5 is located both in cytoplasm and the nucleus and translocates from the cytoplasm into the nucleus with glucocorticoid receptor in response to dexamethasone [22] but quantitative data were not available. Because there are cell to cell variations in the nuclear abundancy of GAS5 and 35% of cells are in quiescent state, it is tempting to speculate that cells with high nuclear levels of GAS5 are quiescent cells. Although we could not address this question in cultured cells, since *in situ* hybridization of nuclear RNA is not compatible with e.g. Ki-67 immunohistochemistry within the same specimen, we observed in MPM tumors that GAS5 expressing tumor cells were Ki-67 negative supporting the idea of nuclear GAS5 being associated with growth arrest. Besides interference with glucocorticoids signalling, other mechanisms may involve chromatin remodelling, since GAS5 expression is increased after growth arrest induced by silencing of Brahma ATPase subunit of mammalian SWI/SNF

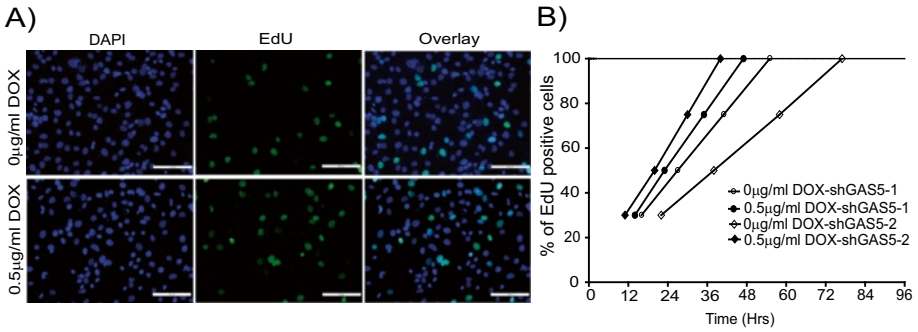

C) Time in hours needed to label 30, 50, 75 & 100% of cells with EdU

	shGAS5-1		shGAS5-2	
% of EdU +	0ug/ml DOX	0.5ug/ml DOX	0μg/ml DOX	0.5ug/ml DOX
30	16	14	22	11
50	27	23	38	20
75	41	35	58	30
100	55	47	77	40

Figure 3 Silencing of GAS5 shortens the cell cycle length as determined by EdU incorporation assay. A. Representative micrographs of shGAS5 cells pre-treated with or without doxycycline during 72 h then incubated with EdU for 12 hrs. Scale bar: 100 μm. **B**. Cell cycle length was measured from a time course of EdU incorporation. Five different fields were imaged for each group in each of three independent experiments under fluorescence microscope and number of EdU positive cells was counted in approximately 1200 cells (DAPI). The graph plots the percentage of EdU positive cells vs. time in axes. The time taken for 100% of EdU positive cells was determined from the linear regression and slopes in presence or absence of doxycycline were compared $p < 0.0001$. **C**. Time in hours needed for 30, 50, 75 and 100% of cells to become EdU positive calculated according to the linear regression method.

complexes [29]. The latter are a family of chromatin remodeling enzymes that regulate gene expression by disrupting histone-DNA contacts in an ATP-dependent manner.

After drug treatment inducing growth arrest GAS5 levels were higher. Interestingly, genome-wide data on RNA and protein quantities in proliferating vs. quiescent yeast cells has revealed that although the proteome size is similar in proliferating and quiescent cells, the transcriptome is decreased to 20% in quiescent compared to proliferating cells [38], indicating that the increase in GAS5 levels observed upon drug treatment inducing cell-cycle arrest are probably underestimated in the context of whole transcriptome.

GAS5 was mostly accumulating in the nucleus after growth arrest induced by HhAntag, suggesting that the control of cell cycle is dependent on nuclear GAS5. Control of cell cycle mediated by lncRNA has been demonstrated for MALAT1, whereby silencing MALAT1 resulted in decreased proliferation because MALAT1 is required for mitotic progression [39] during which MALAT1 migrated from the nucleus to the cytoplasm shuttling heterogeneous ribonucleoprotein C, which is necessary to increase IRES-dependent translation of *c-myc* [40]. Altogether, these data support that nuclear-cytoplasmic shuttling of lncRNA is tightly regulated by mechanism controlling cell cycle.

Surprisingly, GAS5 was expressed at higher level in tumor tissue compared to non-tumoral tissue. This in contradiction with other tumor tissues such as breast [41], bladder [42] and pancreatic [43] cancer where GAS5 expression was lower in tumor compared to non-tumoral tissue. One reason might be that primers recognizing all GAS5 ESTs were used in the breast cancer study [41], while in our case primers were recognizing only 20 out of 29 different splice variants, which nevertheless included the splice variants detected in cancer cells. In the other two studies primer sequence was not specified so the comparison is not possible. Another explanation for this discrepancy could have been that GAS5 expression seems tissue-dependent, accordingly to publicly available integrated database on transcriptome [44]. Therefore, a high expression in tumoral tissue could have resulted from e.g. lymphocytes infiltration. By *in situ* hybridization of MPM tissue we observed a high GAS5 expression in quiescent tumor cells. In order to find an explanation why GAS5 expression should be high in tumor cells, we compared GAS5 expression to known mesothelioma markers and found that GAS5 expression was positively correlated to podoplanin expression. The latter is a type I transmembrane sialomucin-like glycoprotein, which induces platelet aggregation and which is highly expressed in malignant pleural mesothelioma [45]. Due to the coincidence of GAS5 expression with podoplanin immunoreactivity and the fact that GAS5 has been recently demonstrated to have miRNA sponge activity [23] one possibility is that high GAS5 expression is not only controlling cell cycle, but it is acting as miRNA natural sponge [46] to scavenge podoplanin mRNA degradation by miRNA, which is known to occur at least in glioblastoma [47]. Further work

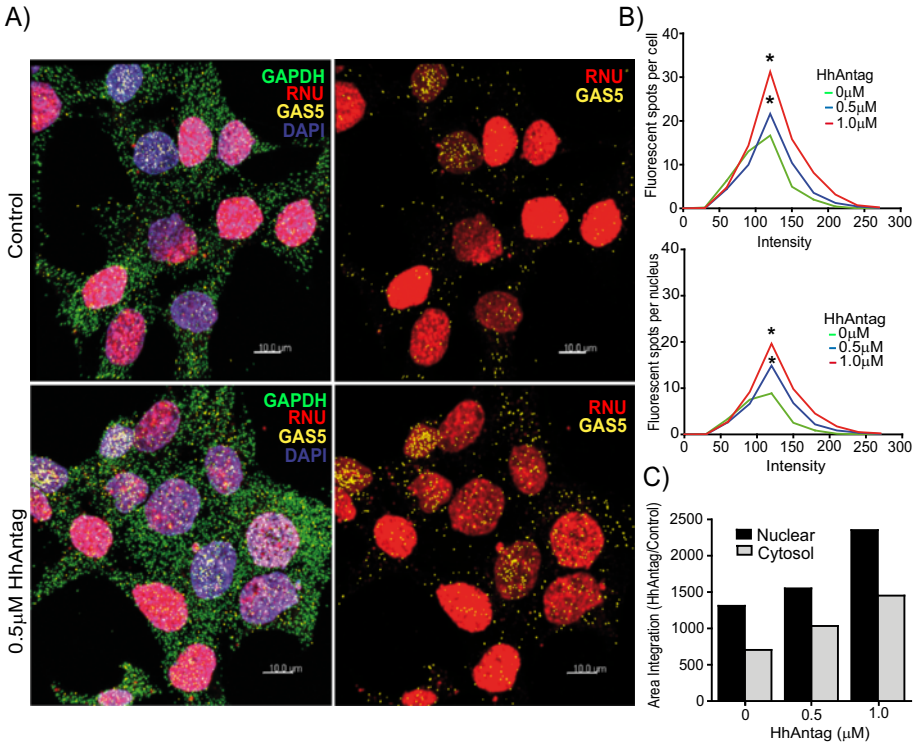

Figure 4 Nuclear enrichment of GAS5 lncRNA after induction of growth arrest by HhAntag. A. Left panel: Representative micrographs of fluorescence *in situ* hybridization showing GAS5 (yellow), GAPDH (green) for cytosolic control, RNU (red) for nuclear mRNA control, and nuclei stained with DAPI (blue). Right panel: same image as left panel showing only RNU and GAS5. Scale bar: 10 μm. **B**. Quantification of GAS5 in ZL55SPT cells and nuclei was determined by calculating intensity of fluorescent spots by Imaris image analysis using spot detection method. The graph plots the fluorescent spots per cell vs. intensity. *; $p < 0.05$ compared to the non-treated control. **C**. Integration of area under the curve to evaluate the proportion of nuclear GAS5 in control and HhAntag-induced growth arrest. Representative of three independent experiments.

is necessary to investigate this hypothesis, nevertheless sequence analysis revealed shared miRNA target sequence in GAS5 and podoplanin (http://www.mircode.org).

Conclusions

In conclusion, accumulating evidences shows that lnc RNAs have a definitive role in carcinogenesis, invasion and metastasis [15,48]. Our experiments demonstrate that GAS5 expression plays a role in MPM biology.

Methods

Tumor specimens

Tumor specimens were obtained for diagnostic purpose before chemotherapy or at the time of resection and were immediately processed as previously described for total RNA extraction using Qiagen RNAeasy® and cDNAs was prepared from 400–500 ng of RNA (Qiagen QuantiTect® Reverse Transcription protocol) [30]. In addition, parts of tumor specimens were fixed in paraformaldehyde for paraffin embedding. Normal pleural tissue was received from ten patients undergoing mesothelioma unrelated thoracic surgery. The study was approved by the Zurich University Hospital ethic committee and a written informed consent was obtained from all patients.

Cell culture and drug treatment

Primary MPM cultures were established from surgical specimens and maintained with serum and without serum as previously described [25,49]. MPM cells-SPC111, SPC212, ZL34 and ZL55, were established in our laboratory [50] and were maintained in DMEM:F12 (Ham) medium (Sigma-Aldrich, St. Louis, MO, USA) with 15% foetal calf serum (FCS, Invitrogen/GIBCO) and 1% penicillin/streptomycin (Sigma-Aldrich); Mero- 14, Mero-41, Mero-48, Mero-82, Mero-83, Mero-84 and Mero-95 were maintained in DMEM:F10 (Ham) medium (Sigma-Aldrich) with 15% FCS and 1% penicillin/streptomycin; ONE-58, ACC-Meso-1 and ACC-Meso-4 were maintained in RPMI-1640 (Sigma-Aldrich) with 15% FCS and 1% penicillin/streptomycin; MSTO-211H, H2052, H2452, H226, NO36 and H596 cells were maintained in RPMI-1640 with 10% FCS and 1% penicillin/streptomycin. ZL55SPT and SDM103T2 primary cells were grown in serum-free medium [25]. Normal mesothelial cells NP3, SDM77, SDM85, SDM104, SDM58 and SDM71 were

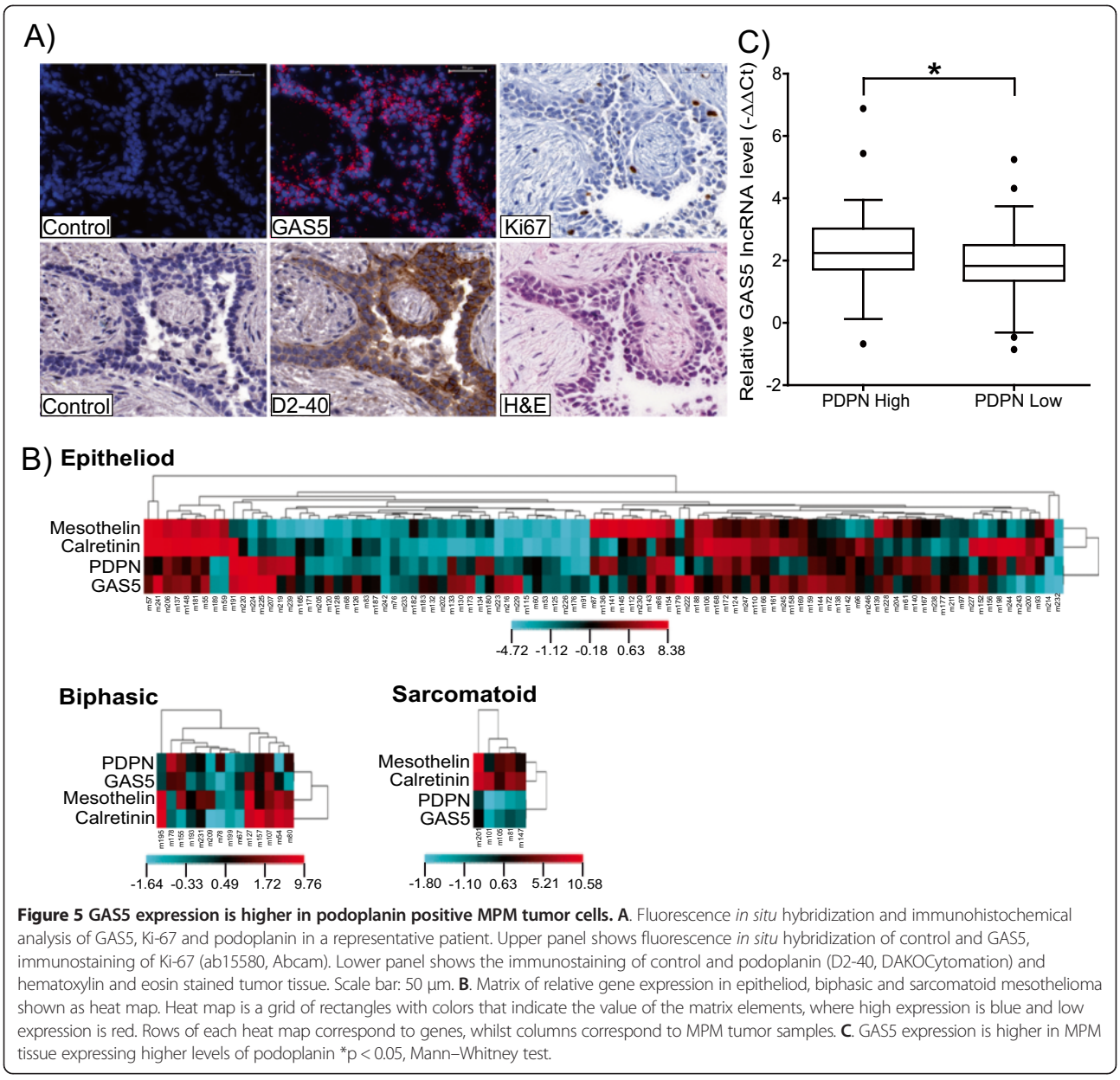

Figure 5 GAS5 expression is higher in podoplanin positive MPM tumor cells. A. Fluorescence *in situ* hybridization and immunohistochemical analysis of GAS5, Ki-67 and podoplanin in a representative patient. Upper panel shows fluorescence *in situ* hybridization of control and GAS5, immunostaining of Ki-67 (ab15580, Abcam). Lower panel shows the immunostaining of control and podoplanin (D2-40, DAKOCytomation) and hematoxylin and eosin stained tumor tissue. Scale bar: 50 μm. **B**. Matrix of relative gene expression in epitheliod, biphasic and sarcomatoid mesothelioma shown as heat map. Heat map is a grid of rectangles with colors that indicate the value of the matrix elements, where high expression is blue and low expression is red. Rows of each heat map correspond to genes, whilst columns correspond to MPM tumor samples. **C**. GAS5 expression is higher in MPM tissue expressing higher levels of podoplanin *$p < 0.05$, Mann–Whitney test.

cultured as previously described [51]. NP3 cells were also grown in serum-free medium. To induce growth arrest, cells were treated either with Hedgehog signaling inhibitor (HhAntag) [25] or with dual PI3K/mTOR inhibitor (NVP-BEZ235, Novartis, Switzerland) [26], as previously described.

Gene expression

Selected gene expression analysis using MIQE [52] compliant protocols was conducted as previously described [30]. Briefly, cDNA was amplified by the SYBR-Green PCR assay and products were detected on a 7900HT Fast real-Time PCR system (SDS, ABI/Perkin Elmer). Relative mRNA levels were determined by comparing the PCR cycle thresholds between cDNA of a specific gene and histone (ΔCt). The 5′ and 3′ primers for GAS5 - AAGCCATTGG CACACAGGCATTAG and AGAACCATTAAGCTGGTC CAGGCA, glucocorticoid-induced leucine zipper protein (GILZ) [22] – AACAGGCCATGGATCTGGTGAAGA and AGGGTCTTCAACAGGGTGTTCTCA, serum/glucocorticoid-regulated kinase 1 (SGK1) - CTATGCTGCTGAAATA GC and GTCCGAAGTCAGTAAGG, respectively. RNA extraction and cDNA preparation from cell cultures was achieved as detailed for tumor samples. The heatmap of expression level of GAS5, mesothelin, calretinin and podoplanin was produced as previously described [30,49].

Plasmid constructs

To investigate the role of GAS5 on cell growth we have generated a system, which allows inducing the silencing of GAS5 by the addition of doxycycline. The shRNA sequence against GAS5 is based on published results [22]. The template for shRNA expression has been obtained by annealing oligonucleotides (GATCCCC *CTTGCCTGGA CCAGCTTAA* TTCAAGAGA *TTAAGCTGGTCCAGG CAAG* TTTTTA and AGCTTAAAAA *CTTGCCTGGAC CAGCTTAA* TCTCTTGAA *TTAAGCTGGTCCAGGCA AG* GGG). The sense and antisense strands of the 19-nucleotide (nt) which targets nucleotides 199 to 217 of the human GAS5 sequence (GenBank accession number NR_002578) are indicated in italics and are separated by a 9-nt loop sequence (TTCAAGAGA). For the negative control a scrambled sequence was used [22,53]. These 60-base long oligonucleotides containing the coding and complementary sequence of these components, together with BglII and HindIII restriction site sequences at the 5′ and 3′ ends respectively, have been annealed and ligated into pSUPERIOR. PURO vector digested with BglII and HindIII restriction sites. The construct has been checked by DNA sequencing and was deposited in Addgene repository (46370, pSuperior-sh-GAS5).

Stable doxycycline-inducible shGAS5 and sh control clones have been generated by co-transfection of the inducible shGAS5 or control constructs with the plasmid pcDNA6/TR (Invitrogen), encoding high levels of the tetracycline repressor, in human MPM ZL55SPT cells grown in the absence of serum using Lipofectamine 2000 (Invitrogen). After selection with puromycin (0.4 μg/ml) and blasticidin (2.5 μg/ml), stable clones have been isolated. Optimal dose and time for doxycycline to induce silencing of GAS5 was obtained as 0.1 and 0.5 μg/ml for 72 hrs (refreshing doxycycline after 48 hrs). Under these conditions no cell growth alteration, assessed by MTT cell viability assay, was observed in parental ZL55SPT cells.

To investigate the control of GAS5 transcription, 771 bp upstream GAS5 transcription starting site was amplified using the following primers with NheI and HindIII restriction sites:

5′- ACGTGCTAGCTCAGGTGAGAACTAGGAAGG −3′
and
5′- ACGTAAGCTTAAGACAGTATGGTGCCTGGG −3′
and subcloned into pGL3 luciferase reporter (pGL3-B-pGAS5, Addgene 46371).

RNA interference by siRNA

For down-regulation of *GAS5* with small interfering RNAs (siRNA), ZL55SPT cells were transfected with 25 nM Qiagen siRNAs targeting GAS5: siGAS5_1 FlexiTube siRNA (targeting exon 11), siGAS5_2 FlexiTube siRNA (targeting exon 3), siGAS5_4 FlexiTube siRNA (targeting exons 10–11) or control non targeting (NT) siRNA (Thermo Scientific Dharmacon), according to the manufacturer's reverse transfection protocol as previously described [25]. Cells were then plated at 7000 cells/cm^2 and RNA was extracted after 72 h.

GAS5 promoter reporter assays

To confirm upregulation of GAS5 transcription upon treatment inducing growth arrest dual luciferase assay was used. Briefly, pGL3-B-pGAS5 was transfected together with Renilla Luciferase (50:1) in cells seeded in 12 wells (40'000-100'000 cells/well) as previously described [25]. After 24 h, transfected cells were either treated with HhAntag, NVP-BEZ235 or vehicle for 24 h then were lysed and analyzed using Dual-Luciferase reporter assay system according to manufacturer instruction (Promega, Madison, Wi, USA).

Analysis of GAS5 splice variants

To identify which GAS5 splice variant is expressed in cell lines that were used in functional assays, we designed three primers sets. PCR reaction was carried out with the following conditions: initial denaturation at 94°C 5 min, then 35 cycles at 95°C 1 min, annealing at 55°C 1 min; and extension at 72°C 2 min. Primer sequences were: GAS5-Ex-4-8-F,- 5′-GTCCTAAAGAGCAAGCCTAACT-3′ and GAS5-Ex-4-8-R,- 5′-TAGTCAAGCCGACTCTC CATA-3′, GAS5-Ex-6-12-F,- 5′-TAATGGTTCTGCTCC TGGTAAC-3′ and GAS5-Ex-4-8-R,- 5′-CAAAGGCCAC TGCACTCTA-3′, GAS5-SV-586-F, 5′- CCCAAGGAAG-GATGAGAATAGC –3′ and GAS5-SV-586-R, 5′- CTCT TTAGGACCTGGGAAGAAAC –3′. Amplified PCR products were analyzed on 3% agarose gel, then, they were excised from gels, purified (Qiagen Qiaquick® Gel Extraction Kit) and sequenced (Microsynth, Balgach, Switzerland). PCR bands were quantitated with densitometry using Image J software (Version 1.42q, USA).

Flow cytometric analysis

The analysis of quiescent (G_0) vs proliferative state (G_1 or $S/G_2/M$) of cells was performed using Attune flow cytometer (Applied Biosystems) and analyzed with the Attune cytometric software v1.2.5 (Applied Biosystems) accordingly to a previously described method [54]. Briefly, cells were fixed with 70% ethanol and stained with FITC-conjugated anti-Ki-67 (clone B56, BD Pharmingen) monoclonal antibody, accordingly to manufacturer instructions. DNA was stained with DAPI (1 μg/ml) after 15 min digestion with RNase A (10 μg/ml).

EdU incorporation assay

Cell cycle length was measured by Click iT™ EdU cell proliferation assay kit (Molecular Probes, Invitrogen). The EdU (5-ethynyl-2′-deoxyuridine) is a nucleoside

analog of thymidine that is incorporated into DNA only during DNA synthesis allowing the visualization of newly synthesized DNA [29]. To perform the assay shGAS5 cells were plated on 4 well chambered slides and incubated at 37°C for overnight to 24 h. The cells were treated with doxycycline for 72 hours with drug refreshment at 48 hrs. At time intervals of 0, 6, 12 and 24 h, cells were treated with 10 μM EdU and incubated at 37°C to ensure capture of the majority of proliferating cells. Following EdU addition, cells were fixed with ice cold 100% methanol for 20 min and permeabilised with ice cold acetone and methanol (50:50) for 20 min followed by 0.2% triton X 100 for 10 min at room temperature. Incorporation of EdU was observed by incubating fixed cells with 2% BSA in PBS for 30 minutes and Alexa fluor 488 for a further 30 minutes under Cu(I)-catalyzed click reaction conditions, as described by the manufacturer. Cells were washed with PBS, and mounted with prolong GOLD antifade agent with DAPI (Invitrogen) and visualized under fluorescence microscopy.

RNA *in-situ* hybridization in MPM cells

To localize GAS5 lncRNA in MPM cells we performed RNA ISH by using QuantiGene® ViewRNA cell assay kit (Panomics Srl, Vignate-Milano, Italy). The oligonucleotide probe was designed commercially using the human GAS5 sequence (accession number NM_002578). ShGAS5 cells in 4-well chamber slides was treated at different concentrations of HhAntag for 48 hours and permeabilized with working detergent solution, and digested with protease at 1:8000 in PBS. The cells were hybridized for 3 hours at 40° C with a cocktail of custom-designed QuantiGene ViewRNA probes against human GAS5 (type 6 probe), RNU2-1 (type 1 probe) and GAPDH (type 4 probe). Unhybridized probes were flushed out with wash buffer and the hybridized probes were amplified with pre-amp hybridization for 1 hour at 40°C, followed by amp hybridization for 1 hour at 40°C. Label Probes (LP) targeting the GAS5, RNU2-1 and GAPDH probe types were added for 30mins at 40°C. Cells were washed with wash buffer and slides were mounted with prolong GOLD anti-fade agent with DAPI and stored at 4°C. The cells were imaged under CLSM Leica SP5 Resonant APD with confocal point-scanning and real optical section (Centre for Microscopy and Image analysis, UZH, Irchel). Twenty five Z stack steps per 0.5 μm at 40 × magnification imaging have been performed for each group with zoom factor fixed as 2. The number of GAS5 lncRNA transcripts inside the nucleus as well in single cell was quantified from z-stacked images of at least 100 randomly selected cells on different fields for each condition using the Spot detection module of Imaris 7.6.1 image analysis software (Bitplane) with fixed spot size and adjusted threshold. Intensity of fluorescent spots of GAS5 lncRNA in both cell and nuclei was measured by filtering the spots with red channel (RNU2-1) and this quantifies the spots which are present in the nucleus of a cell. From the analysed images the total number of fluorescent spots per cell or nucleus was calculated with mean intensity of spots.

RNA *in-situ* hybridization in MPM tissue

Tissue sections of MPM patients were processed for RNA-ISH by using QuantiGene® ViewRNA ISH tissue assay kit (Panomics Srl, Vignate-Milano, Italy). Briefly, 3-micron sections were deparaffinized, boiled in pretreatment solution (Affymetrix, Santa Clara, CA) for 5 minutes and digested with proteinase K for 10 minutes. Sections were hybridized for 3 hours at 40°C with custom designed QuantiGene ViewRNA probes against human GAS5 (type 1 probe) and no probe as a control. After the probe hybridization the slides were stored overnight in supplied 1X storage buffer. Hybridized probes were then amplified the following day as per protocol from Affymetrix using PreAmp and Amp molecules. Multiple Label Probe oligonucleotides conjugated to alkaline phosphatase (LP-AP Type 1) were then added and Fast Red Substrate was used to produce signal (red dots). Slides were then counterstained with Hematoxylin. Slides were scanned in Zeiss Mirax Midi Slide Scanner equipped with fluorescence scanner (Centre for Microscopy and Image analysis, UZH, Irchel) and tissue sections were analysed by using Pannoromic viewer 1.15.2 (3DHISTECH, Budapest, Hungary).

Immunohistochemistry

Deparaffinized sections were subjected to antigen retrieval using Tris/EDTA (pH9.0) or sodium citrate (pH 6.0) buffer. Following quenching in 0.3% H_2O_2 (20 min) and permeabilization in 0.05% Saponin (5 min), blocking was performed in 2% bovine serum albumin in PBS with 1% horse serum (20 min; Vector Laboratories) at room temperature. Sections were incubated with primary antibodies (D2-40, 1:50; DAKO M3619, Baar, Switzerland and Ki-67, 1:50; Abcam ab15580, Abcam, Cambridge, UK) overnight at 4°C. Negative controls were incubated with secondary biotinylated antibody only (Vectastain® Elite® ABC Kit; Vector Laboratories, Servion, Switzerland). Sections were washed with PBS and incubated with secondary biotinylated antibody for 45 min at room temperature. Staining was visualized using 3,3′-diaminobenzidine tetrahydrochloride (Sigma–Aldrich), counterstained with Vector® hematoxilyn QS (Vector Laboratories) and analyzed using a Zeiss Mirax Midi Slide Scanner and image acquisition with a 3 CCD color camera and Pannoromic viewer (3DHISTECH, Budapest, Hungary).

Statistical analysis

Data are expressed as mean ± standard deviation of multiple experiments. Statistical analysis was performed using

student *t*-test and Mann–Whitney tests and cell cycle length was analyzed by linear regression and regression slopes were evaluated by StatView 5.0.1 (SAS institute). The comparison of GAS5 expression in PDPN low versus PDPN high samples was performed by dichotomizing the samples according to PDPN median relative expression value. All statistical analysis was performed in GraphPad Prism v5.03. Differences were considered statistically significant at $p < 0.05$.

Additional files

Additional file 1: Figure S1. Profile of GAS5 lncRNA in different MPM cell line. GAS5 lncRNA expression was analysed by qRT-PCR in 22 MPM cell lines and in 7 normal mesothelial cell lines. Expression of GAS5 was normalized to internal control histones relative to the mean expression of GAS5 in normal mesothelial cells in culture according to –ΔΔCt method.

Additional file 2: Table S1. List of GAS5 alternative splice variants.

Additional file 3: Table S2. List of GAS5 alternative splice variants detectable by RT-PCR primer sets.

Additional file 4: Figure S2. Different GAS5 alternative splice variants are identified in MPM. A. Schematic representation of 3 alternative splice variants of GAS5 expressed in MPM. Gray rectangles represent GAS5 exons, lines represent introns and white rectangle snoRNA. Arrows show the location of primer sets. B, C and D. Semi-quantitative RT-PCR of transcripts for GAS5 differentially expressed in the MPM primary cells and cell lines selected for functional assays. The arrows point to the RT-PCR amplicon corresponding to the different products that can be obtained (207 bp and 168 bp with exons 4 to 8 primer set; 281 bp and 242 bp with exon 6–12 primer set; 233 bp with exon 3 together with SNORD76 (OTTHUMT00000090586, SV-586) . E. GAPDH was amplified from the cDNA and was used for relative quantification.

Additional file 5: Figure S3. Cell cycle distribution of ZL55SPT cells upon HhAntag induced growth arrest. HhAntag induced growth arrest accumulates more cells at G_0 state. Values are shown as mean ± SD from three independent experiments. *; $p < 0.05$ compared to control.

Additional file 6: Figure S4. NVP-BEZ-235 increases GAS5 expression in MPM primary cells ZL55SPT and SDM103T2 grown without serum in 3% oxygen. Values are expressed as mean ± SD from three independent experiments.

Additional file 7: Figure S5. Silencing of GAS5 with siRNA increases glucocorticoid responsive genes. A. GAS5 lncRNA silencing increases the expression of glucocorticoid responsive genes GILZ (B) and SGK1 (C). Values are normalized with histones and shown as mean ± SD from four independent experiments. *; $p < 0.05$.

Additional file 8: Figure S6. GAS5 expression in MPM. A. GAS5 expression is higher in MPM tumor samples compared to non-tumoral tissue, *$p < 0.0001$ expression, Mann–Whitney test. B. Upper panel shows fluorescence *in situ* hybridization of control and GAS5 and immunostaining of Ki-67 (ab15580, Abcam) and lower panel shows the immunostaining of control and podoplanin (D2-40, DAKOCytomation) and hematoxylin and eosin stained tumor of another representative patient. Scale bar: 50 μm.

Additional file 9: Figure S7. *GAS5* promoter in Chromosome 1 region 1q25.1. A screenshot of the UCSC Genome Browser shows *GAS5* sharing its promoter with *ZBTB37*.

Competing interests
The authors declared that they have no competing interests.

Authors' contributions
AR, JKR and EFB carried out most of the experiments and participated in the interpretation of the data. GZ carried out the PCR analysis and RNA extraction from the tumors. IO provided clinical samples. BV was involved in the interpretation of the analysis of clinical samples. AR and EFB drafted the manuscript. RS, JKR and NE were involved in revising critically the ms. All authors read and approved the final manuscript.

Acknowledgements
Confocal imaging analysis was performed with equipment maintained by the Center for Microscopy and Image Analysis, University of Zurich. We thank Dr. Caroline Aemisegger, Center for Microscopy and Image Analysis, University of Zurich for skillfull assistance in confocal analysis. We also thank Dr. Raffaella Santoro for critical evaluation of the manuscript. This work was supported by Swiss national Science Foundation Sinergia grant CRSII3 147697/1. AR was supported by a Swiss Government Excellence Scholarships for Foreign Scholars.

Author details
[1]Laboratory of Molecular Oncology, Clinic of Oncology, University Hospital Zürich, Zürich, Switzerland. [2]Division of Thoracic Surgery, University Hospital Zürich, Zürich, Switzerland. [3]Institute of Surgical Pathology, University Hospital Zürich, Zürich, Switzerland.

Received: 28 January 2014 Accepted: 19 May 2014
Published: 23 May 2014

References
1. Tsao AS, Wistuba I, Roth JA, Kindler HL: **Malignant pleural mesothelioma.** *J Clin Oncol* 2009, **27:**2081–2090.
2. Stahel RA, Weder W, Felip E: **Malignant pleural mesothelioma: ESMO clinical recommendations for diagnosis, treatment and follow-up.** *Ann Oncol* 2009, **20**(Suppl 4):73–75.
3. Vogelzang NJ, Rusthoven JJ, Symanowski J, Denham C, Kaukel E, Ruffie P, Gatzemeier U, Boyer M, Emri S, Manegold C, Niyikiza C, Paoletti P: **Phase III study of pemetrexed in combination with cisplatin versus cisplatin alone in patients with malignant pleural mesothelioma.** *J Clin Oncol* 2003, **21:**2636–2644.
4. Jean D, Daubriac J, Le Pimpec-Barthes F, Galateau-Salle F, Jaurand MC: **Molecular changes in mesothelioma with an impact on prognosis and treatment.** *Arch Pathol Lab Med* 2012, **136:**277–293.
5. Wright CM, Kirschner MB, Cheng YY, O'Byrne KJ, Gray SG, Schelch K, Hoda MA, Klebe S, McCaughan B, van Zandwijk N, Reid G: **Long non coding RNAs (lncRNAs) are dysregulated in malignant pleural mesothelioma (MPM).** *PLoS One* 2013, **8:**e70940.
6. Kapranov P, Willingham AT, Gingeras TR: **Genome-wide transcription and the implications for genomic organization.** *Nat Rev Genet* 2007, **8:**413–423.
7. Saxena A, Carninci P: **Whole transcriptome analysis: what are we still missing?** *Wiley Interdiscip Rev Syst Biol Med* 2011, **3:**527–543.
8. Saxena A, Carninci P: **Long non-coding RNA modifies chromatin: epigenetic silencing by long non-coding RNAs.** *Bioessays* 2011, **33:**830–839.
9. Wapinski O, Chang HY: **Long noncoding RNAs and human disease.** *Trends Cell Biol* 2011, **21:**354–361.
10. Gibb EA, Brown CJ, Lam WL: **The functional role of long non-coding RNA in human carcinomas.** *Mol Cancer* 2011, **10:**38.
11. Mattick JS, Makunin IV: **Non-coding RNA.** *Hum Mol Genet* 2006, **15 Spec No 1:**R17–R29.
12. Derrien T, Johnson R, Bussotti G, Tanzer A, Djebali S, Tilgner H, Guernec G, Martin D, Merkel A, Knowles DG, Lagarde J, Veeravalli L, Ruan X, Ruan Y, Lassmann T, Carninci P, Brown JB, Lipovich L, Gonzalez JM, Thomas M, Davis CA, Shiekhattar R, Gingeras TR, Hubbard TJ, Notredame C, Harrow J, Guigo R: **The GENCODE v7 catalog of human long noncoding RNAs: analysis of their gene structure, evolution, and expression.** *Genome Res* 2012, **22:**1775–1789.
13. Bernstein BE, Birney E, Dunham I, Green ED, Gunter C, Snyder M: **An integrated encyclopedia of DNA elements in the human genome.** *Nature* 2012, **489:**57–74.
14. Kugel JF, Goodrich JA: **Non-coding RNAs: key regulators of mammalian transcription.** *Trends Biochem Sci* 2012, **37:**144–151.
15. Huarte M, Rinn JL: **Large non-coding RNAs: missing links in cancer?** *Hum Mol Genet* 2010, **19:**R152–R161.
16. Gupta RA, Shah N, Wang KC, Kim J, Horlings HM, Wong DJ, Tsai MC, Hung T, Argani P, Rinn JL, Wang Y, Brzoska P, Kong B, Li R, West RB, van de Vijver MJ, Sukumar S, Chang HY: **Long non-coding RNA HOTAIR reprograms chromatin state to promote cancer metastasis.** *Nature* 2010, **464:**1071–1076.

17. Jean D, Thomas E, Manie E, Renier A, de Reynies A, Lecomte C, Andujar P, Fleury-Feith J, Galateau-Salle F, Giovannini M, Zucman-Rossi J, Stern MH, Jaurand MC: **Syntenic relationships between genomic profiles of fiber-induced murine and human malignant mesothelioma.** *Am J Pathol* 2011, **178:**881–894.
18. Smith CM, Steitz JA: **Classification of gas5 as a multi-small-nucleolar-RNA (snoRNA) host gene and a member of the 5′-terminal oligopyrimidine gene family reveals common features of snoRNA host genes.** *Mol Cell Biol* 1998, **18:**6897–6909.
19. Schneider C, King RM, Philipson L: **Genes specifically expressed at growth arrest of mammalian cells.** *Cell* 1988, **54:**787–793.
20. Mourtada-Maarabouni M, Hedge VL, Kirkham L, Farzaneh F, Williams GT: **Growth arrest in human T-cells is controlled by the non-coding RNA growth-arrest-specific transcript 5 (GAS5).** *J Cell Sci* 2008, **121:**939–946.
21. Mourtada-Maarabouni M, Hasan AM, Farzaneh F, Williams GT: **Inhibition of human T-cell proliferation by mammalian target of rapamycin (mTOR) antagonists requires noncoding RNA growth-arrest-specific transcript 5 (GAS5).** *Mol Pharmacol* 2010, **78:**19–28.
22. Kino T, Hurt DE, Ichijo T, Nader N, Chrousos GP: **Noncoding RNA gas5 is a growth arrest- and starvation-associated repressor of the glucocorticoid receptor.** *Sci Signal* 2010, **3:**ra8.
23. Zhang Z, Zhu Z, Watabe K, Zhang X, Bai C, Xu M, Wu F, Mo YY: **Negative regulation of lncRNA GAS5 by miR-21.** *Cell Death Differ* 2013, **20:**1558–1568.
24. Gibb EA, Vucic EA, Enfield KS, Stewart GL, Lonergan KM, Kennett JY, Becker-Santos DD, MacAulay CE, Lam S, Brown CJ, Lam WL: **Human cancer long non-coding RNA transcriptomes.** *PLoS One* 2011, **6:**e25915.
25. Shi Y, Moura U, Opitz I, Soltermann A, Rehrauer H, Thies S, Weder W, Stahel RA, Felley-Bosco E: **Role of hedgehog signaling in malignant pleural mesothelioma.** *Clin Cancer Res* 2012, **18:**4646–4656.
26. Fischer B, Frei C, Moura U, Stahel R, Felley-Bosco E: **Inhibition of phosphoinositide-3 kinase pathway down regulates ABCG2 function and sensitizes malignant pleural mesothelioma to chemotherapy.** *Lung Cancer* 2012, **78:**23–29.
27. Ellis BC, Graham LD, Molloy PL: **CRNDE, a long non-coding RNA responsive to insulin/IGF signaling, regulates genes involved in central metabolism.** *Biochim Biophys Acta* 2014, **1843:**372–386.
28. Connell ND, Rheinwald JG: **Regulation of the cytoskeleton in mesothelial cells: reversible loss of keratin and increase in vimentin during rapid growth in culture.** *Cell* 1983, **34:**245–253.
29. Cohet N, Stewart KM, Mudhasani R, Asirvatham AJ, Mallappa C, Imbalzano KM, Weaver VM, Imbalzano AN, Nickerson JA: **SWI/SNF chromatin remodeling enzyme ATPases promote cell proliferation in normal mammary epithelial cells.** *J Cell Physiol* 2010, **223:**667–678.
30. Sidi R, Pasello G, Opitz I, Soltermann A, Tutic M, Rehrauer H, Weder W, Stahel RA, Felley-Bosco E: **Induction of senescence markers after neo-adjuvant chemotherapy of malignant pleural mesothelioma and association with clinical outcome: an exploratory analysis.** *Eur J Cancer* 2011, **47:**326–332.
31. Aoki K, Adachi S, Homoto M, Kusano H, Koike K, Natsume T: **LARP1 specifically recognizes the 3′ terminus of poly(A) mRNA.** *FEBS Lett* 2013, **587:**2173–2178.
32. Guo G, Huss M, Tong GQ, Wang C, Li Sun L, Clarke ND, Robson P: **Resolution of cell fate decisions revealed by single-cell gene expression analysis from zygote to blastocyst.** *Dev Cell* 2010, **18:**675–685.
33. Kohler PO, Bridson WE, Rayford PL: **Cortisol stimulation of growth hormone production by monkey adenohypophysis in tissue culture.** *Biochem Biophys Res Commun* 1968, **33:**834–840.
34. Bridson WE, Kohler PO: **Cortisol stimulation of growth hormone production by human pituitary tissue in culture.** *J Clin Endocrinol Metab* 1970, **30:**538–540.
35. Bloomfield CD, Smith KA, Peterson BA, Munck A: **Glucocorticoid receptors in adult acute lymphoblastic leukemia.** *Cancer Res* 1981, **41:**4857–4860.
36. Schottelius A, Wedel S, Weltrich R, Rohde W, Buttgereit F, Schreiber S, Lochs H: **Higher expression of glucocorticoid receptor in peripheral mononuclear cells in inflammatory bowel disease.** *Am J Gastroenterol* 2000, **95:**1994–1999.
37. Catts VS, Farnsworth ML, Haber M, Norris MD, Lutze-Mann LH, Lock RB: **High level resistance to glucocorticoids, associated with a dysfunctional glucocorticoid receptor, in childhood acute lymphoblastic leukemia cells selected for methotrexate resistance.** *Leukemia* 2001, **15:**929–935.
38. Marguerat S, Schmidt A, Codlin S, Chen W, Aebersold R, Bahler J: **Quantitative analysis of fission yeast transcriptomes and proteomes in proliferating and quiescent cells.** *Cell* 2012, **151:**671–683.
39. Tripathi V, Shen Z, Chakraborty A, Giri S, Freier SM, Wu X, Zhang Y, Gorospe M, Prasanth SG, Lal A, Prasanth KV: **Long noncoding RNA MALAT1 controls cell cycle progression by regulating the expression of oncogenic transcription factor B-MYB.** *PLoS Genet* 2013, **9:**e1003368.
40. Yang F, Yi F, Han X, Du Q, Liang Z: **MALAT-1 interacts with hnRNP C in cell cycle regulation.** *FEBS Lett* 2013, **587:**3175–3181.
41. Mourtada-Maarabouni M, Pickard MR, Hedge VL, Farzaneh F, Williams GT: **GAS5, a non-protein-coding RNA, controls apoptosis and is downregulated in breast cancer.** *Oncogene* 2009, **28:**195–208.
42. Liu Z, Wang W, Jiang J, Bao E, Xu D, Zeng Y, Tao L, Qiu J: **Downregulation of GAS5 promotes bladder cancer cell proliferation, partly by regulating CDK6.** *PLoS One* 2013, **8:**e73991.
43. Lu X, Fang Y, Wang Z, Xie J, Zhan Q, Deng X, Chen H, Jin J, Peng C, Li H, Shen B: **Downregulation of gas5 increases pancreatic cancer cell proliferation by regulating CDK6.** *Cell Tissue Res* 2013, **354:**891–896.
44. Hruz T, Laule O, Szabo G, Wessendorp F, Bleuler S, Oertle L, Widmayer P, Gruissem W, Zimmermann P: **Genevestigator v3: a reference expression database for the meta-analysis of transcriptomes.** *Adv Bioinformatics* 2008, **2008:**420747.
45. Kimura N, Kimura I: **Podoplanin as a marker for mesothelioma.** *Pathol Int* 2005, **55:**83–86.
46. Tay Y, Rinn J, Pandolfi PP: **The multilayered complexity of ceRNA crosstalk and competition.** *Nature* 2014, **505:**344–352.
47. Cortez MA, Nicoloso MS, Shimizu M, Rossi S, Gopisetty G, Molina JR, Carlotti C Jr, Tirapelli D, Neder L, Brassesco MS, Scrideli CA, Tone LG, Georgescu MM, Zhang W, Puduvalli V, Calin GA: **miR-29b and miR-125a regulate podoplanin and suppress invasion in glioblastoma.** *Genes Chromosomes Cancer* 2010, **49:**981–990.
48. Tsai MC, Spitale RC, Chang HY: **Long intergenic noncoding RNAs: new links in cancer progression.** *Cancer Res* 2011, **71:**3–7.
49. Frei C, Opitz I, Soltermann A, Fischer B, Moura U, Rehrauer H, Weder W, Stahel R, Felley-Bosco E: **Pleural mesothelioma side populations have a precursor phenotype.** *Carcinogenesis* 2011, **32:**1324–1332.
50. Schmitter D, Lauber B, Fagg B, Stahel RA: **Hematopoietic growth factors secreted by seven human pleural mesothelioma cell lines: interleukin-6 production as a common feature.** *Int J Cancer* 1992, **51:**296–301.
51. Thurneysen C, Opitz I, Kurtz S, Weder W, Stahel RA, Felley-Bosco E: **Functional inactivation of NF2/merlin in human mesothelioma.** *Lung Cancer* 2009, **64:**140–147.
52. Bustin SA, Benes V, Garson JA, Hellemans J, Huggett J, Kubista M, Mueller R, Nolan T, Pfaffl MW, Shipley GL, Vandesompele J, Wittwer CT: **The MIQE guidelines: minimum information for publication of quantitative real-time PCR experiments.** *Clin Chem* 2009, **55:**611–622.
53. Knobel PA, Kotov IN, Felley-Bosco E, Stahel RA, Marti TM: **Inhibition of REV3 expression induces persistent DNA damage and growth arrest in cancer cells.** *Neoplasia* 2011, **13:**961–970.
54. Jordan CT, Yamasaki G, Minamoto D: **High-resolution cell cycle analysis of defined phenotypic subsets within primitive human hematopoietic cell populations.** *Exp Hematol* 1996, **24:**1347–1355.

doi:10.1186/1476-4598-13-119
Cite this article as: Renganathan *et al.*: GAS5 long non-coding RNA in malignant pleural mesothelioma. *Molecular Cancer* 2014 **13**:119.

5. CONCLUSIONS AND OUTLOOK

Before these studies, little was known about the mechanisms and molecular factors regulating the expression of calretinin (*CALB2*, CR), a diagnostic marker in malignant pleural mesothelioma (MPM). Therefore, the aim of this PhD study was to focus on investigating transcriptional and post-transcriptional control of calretinin expression in MPM.

Based on the observation that calretinin expression is associated with the epithelioid histotype of MPM, Blum et al. suggested a model in which calretinin expression fluctuates over the time course of mesotheliomagenesis [140]. The model proposed that calretinin expression is absent in healthy human mesothelial cells, is then moderately upregulated in reactive mesothelial cells, is strongly expressed in the epithelioid histotype and is again downregulated in the sarcomatoid mesothelioma histotype. Assuming that the epithelial mesothelioma histotype indeed progresses towards a sarcomatoid one, this fluctuation suggests the existence of molecular mechanisms governing calretinin expression in mesothelioma.

The expression of calretinin in normal human mesothelium is still under debate and questionable. An early study using immunohistochemistry, clearly demonstrated calretinin expression only in certain cuboidal mesothelial cells along with morphologically transformed mesothelial cells (observed pathologically after different stimuli), but not in normal flattened cells of the mesothelium [133]. In a recent study exploiting a proteomic approach, calretinin was ~4-fold overexpressed in MPM tissue samples compared with benign samples (pleural inflammation and hyperplasia what would correspond to the reactive mesothelium) in which mass spectrometry detectable levels of calretinin were also present. However, calretinin could not be detected by Western blot analysis in the benign samples indicating that the amount was below detection level by Western blot analysis in the conditions used in that study [190]. A tissue microarray analysis on 5233 tissue samples from 128 tumor categories and 76 different normal tissues, reported calretinin expression in normal mesothelium, but there was no reported data supporting this statement [131]. In an immunohistochemical analysis of mesothelium kindly provided by Prof. Dr. Alex Soltermann (University Hospital Zurich, data not shown), strong calretinin expression was observed in the mesothelium monolayer. However, it should be noted that these tissue samples were obtained from patients suffering from other thoracic diseases; therefore, it is possible that the investigated tissue microenvironment is not representative of healthy conditions. It is possible that the observed calretinin immunoreactivity in the so-called “normal mesothelium” is rather an indication of the reactive mesothelial cells stimulated by the presence of inflammation, as they appear cuboidal in shape. It should be

emphasized that obtaining normal human mesothelium tissue without any disease indication is rather difficult; hence, in our opinion calretinin is likely either absent, or present at low levels in normal human mesothelium, as demonstrated in the first study [133]. *Calb2*$^{-/-}$ mice form a normal mesothelium without visible abnormal morphology when compared to WT mice [141], indicating that calretinin is not essential for normal mesothelium development. Regardless of the normal mesothelium, the majority of studies demonstrated differential calretinin expression in mesothelioma histotypes, with a strong cytosolic and nuclear calretinin immunoreactivity in the epithelioid type and weak/absent in the sarcomatoid mesothelioma [116, 133, 191, 192]. Based on this obvious dynamic expression of calretinin, our study investigated several molecular levels of regulating calretinin expression and findings from these studies might lead to further directions for deciphering mechanisms driving calretinin expression in mesothelioma.

We began with quantifying protein and mRNA relative expression of calretinin in the panel of eleven mesothelioma cell lines among which five were epithelioid, four biphasic and two sarcomatoid. A strong positive correlation between protein and mRNA levels suggested that calretinin expression is regulated at the mRNA level in mesothelioma.

We defined the minimal calretinin promoter fragment -161bp/+80bp-*CALB2* driving reporter expression in MPM cells, consistent with the previous finding of a minimal mouse *Calb2* promoter (-115bp/+54bp) [193, 194]. In our study, we observed a high correlation between promoter activity of -161bp/+80bp *CALB2*, measured by firefly luciferase assay, with the relative mRNA abundance in 4 mesothelioma cell lines, suggesting a strong contribution of transcription in regulating calretinin expression.

Computational-based predictions revealed numerous transcription factors within the minimal *CALB2* promoter, amongst which NRF-1 and E2F2 were identified to regulate calretinin expression. In our panel of mesothelioma cell lines expressing different levels of calretinin, NRF-1 expression was similar and ubiquitous among cell lines. This indicates that NRF-1 could act as a part of a protein complex, which could be differently assembled and of which all the components remain to be identified. To support this suggestion, the electrophoretic mobility shift assay (EMSA) showed formation of three different DNA-protein complexes. NRF-1 operates through interaction with co-activators e.g. PGC-1-related coactivators (PRC) or peroxisome proliferator-activated receptor γ (PPAR-γ) [195]. Other proteins described to interact with NRF-1 include NRF-2, CREB/ATF family members and histone-acetyltransferase CBR and p300 [196]. Our *in silico* analysis revealed a CREB-putative binding site to bind *CALB2* promoter. Therefore, it is possible that some of these factors are part of the complexes

that we observed using electrophoretic mobility shift assays. In order to further characterize them, it would be necessary to overexpress NRF-1 in cells expressing low levels of calretinin. If increased expression of calretinin would be observed, it would then be of interest to perform NRF-1 immunoprecipitation and mass spectrometry analysis in order to identify the NRF-1-interactors.

The cell-cycle synchronization experiment revealed that calretinin expression is cell cycle dependent, with the strongest expression level observed in the G1 phase, followed by a gradual and slight decrease during S/G2/M phase transitions. Based on this observation, one may raise the question whether calretinin-positive cells in mesothelioma are G1-arrested cells. This would be consistent with a study reporting that growth inhibition induced upon surface binding of galectin-4, strongly increased calretinin protein expression while decreasing Ki-67 (proliferation marker) in colon cancer cell lines [197]. However, this would contradict studies in which *Calb2* silencing resulted in growth arrest [140]. In order to address the question whether calretinin positive-cells are G1-arrested cells, it would be necessary to perform double staining with calretinin and Ki-67 in mesothelioma tumors.

Additionally, we demonstrated that calretinin expression is regulated also at the post-transcriptional level. The calretinin 3'UTR is 573nt in size, and we demonstrated its downregulatory effect utilizing a luciferase reporter assay. *CALB2* 3'UTR also showed a downregulatory effect in a breast cancer cell line, which implies that the effect of the 3'UTR is not cell-type specific. Additionally, luciferase-*CALB2* 3'UTR along with calretinin expression is modulated by *miR-30e-5p* in ONE58 and ACC-MESO-4 MPM cells. The mir-30 family includes five members, *mir-30a* located on chromosome 6, *mir-30b and mir-30d* on chromosome 8, *mir-30c* and *miR-30e* on chromosome 1. Despite testing miR-30 b/c-5p, only miR-30e-5p was capable of modulating expression of the reporter-*CALB2* 3'UTR and calretinin protein levels in our experiments. It might be that indeed only miR-30e-5p is capable of regulating calretinin expression. However, it is also possible that utilizing modified miR-30e-5p mimics, in which the 3' passenger strand is 2'-O-methylation modified, allowing preferential selection of the 5'-strand to bind to the RISC complex and thus avoiding substantial artificial incorporation of passenger strand (3'-strand) [198]. Furthermore, the affinity of the RISC-binding strand can vary between different production batches [199]. Therefore, administration of unmodified miR-30 b/c mimics could have resulted in no observable effect due to overloading of the RISC complex with passenger strand (3' arm) that is not predicted to target the calretinin 3'UTR. From the analysis of differentially expressed genes between MPM and benign tumors and using mRNA-miRNA correlation, enrichment in miR-30e-target gene

was observed in MPM indicating possible downregulation of miR-30e-5p in MPM tumors [200]. This is consistent with the observation that MPM tumors and cell lines have lower expression of miR-30e-5p compared with normal pleural tissue and MET-5A mesothelial immortalized cells, respectively. Therefore, low levels of miR-30e-5p migth contribute to upregulation of calretinin expression in MPM compared to normal mesothelial tissue.

The second functional element in the *CALB2* 3'UTR is a stabilizing adenine/uridine rich element - ARE motif (AUUUA). A 25nt RNA oligo containing the ARE motif, specifically binds a cytosolic protein from ACC-MESO-4, SPC111, and ZL55 cells. Unfortunately, we did not identify the protein-interactor. However, since the mutational approach revealed the stabilization element in the ARE site, we speculate that one of the potential candidates is HuR [201]. We performed one preliminary RNA-protein precipitation experiment, using streptavidin agarose beads and observed an enrichment of a band corresponding to a size of ~37 kDa, which would hint that the bound protein might be indeed HuR; however, the identity of the protein was not confirmed. It would be of interest to perform targeted knockdown of HuR and monitor, whether this would affect calretinin expression. In a resting cell, HuR is located within the nucleus and in response to various stimuli, HuR shuttles to the cytoplasm mainly to stabilize targeted mRNAs [202]. Apparent elevated levels of HuR in all cancer types [203] is associated with poor overall survival, and experimental evidence of a causal role for HuR in tumor development [203, 204] suggests that HuR plays an important role in cancer development and progression [202, 205-207]. The association between elevated cytoplasmic HuR levels and poor overall survival [208-210] could be explained by the observation that HuR affects many mRNAs involved in acquiring malignant phenotypes such as enhanced proliferation, anti-apoptotic effects, angiogenesis, and migration and invasiveness [211, 212]. There has been only one study addressing HuR in mesothelioma tissue, reporting that strong nuclear and cytoplasmic HuR expression correlated with a poor outcome, but no correlation was observed between HuR expression and mesothelioma histotype [213]. If we postulate that it is HuR, which is stabilizing the calretinin transcript, one needed to address how this would be compatible with the observation that HuR increase and calretinin decrease correlate with poor overall survival in MPM [115-117, 213]. One possible explanation would be that HuR binds preferentially to cancer-associated mRNA instead of binding to the calretinin 3'UTR, for example *COX2* 3'UTR, which harbors 14 ARE elements [214]. Another possibility is that mechanisms, which change the affinity of HuR towards targeted mRNA such as phosphorylation or methylation by the methyltransferase CARM1, operate to decrease calretinin expression [215]. While one of the best studied stabilizing AUBP is HuR, there are

other potential candidates: HuD, AUF1, YB1, nucleolin, CUGBP-1, hnRNPC, hnRNPK, hnRNPQ, PAIP1, RNPC1 [216] that might stabilize calretinin mRNA. We could utilize an RNA-protein pull-down assay followed by immunoblotting against HuR or, in case of negative results, mass spectrometry to identify the possible RNA binding partner.

Since the discovery of the pervasive transcription of the non-coding genome, there have been several studies showing a role for noncoding transcripts in regulating gene transcription. Some studies showed that the noncoding RNA (pseudogene transcripts, long noncoding RNA, circular RNA) with unknown functions and containing microRNA-responsive elements could compete for the miRNA pool and therefore decrease availability of miRNA that target and affect specific protein-coding transcripts [217]. Inspired by the work on the *PTEN* pseudogene [218], we discovered a possible role of calretinin alternative transcripts acting as competitive endogenous RNA (ceRNA). Indeed, miR-30e-5p overexpression in ONE58 cells decreased calretinin expression, but we did not observe this effect in ONE58 cells stably overexpressing *CALB2* 3'UTR, likely due to exogenous *CALB2* 3'UTR outcompeting administrated miR-30e-5p mimics. We speculated that the protective role of exogenous *CALB2* 3'UTR was observed in ONE58 cells as they express calretinin weakly and only the full-length protein coding calretinin transcript. In two additional tested mesothelioma cell lines, we observed that the expression of alternative transcripts (*CALB2b* and *CALB2c*) is proportional to the full-length transcript (*CALB2*). Our work demonstrated for the first time the presence of these alternative transcripts in mesothelioma cell lines. *CALB2b* is considered as a candidate for nonsense-mediated RNA decay (NMD) because it has a canonical premature termination codon (PTC) signal [219] and a protein product has never been detected in cells. NMD is an error proofing surveillance or quality control system that targets aberrant and mis-spliced mRNA for degradation and therefore prevent translation of truncated malfunctioning proteins. It is also a mode of regulation of gene transcription. Indeed, specific conditions occurring in the tumor microenvironment, such as nutrition limitation, hypoxia and reactive oxygen species, shutdown the NMD system causing previously suppressed transcripts to become free for translation, and consequently augment tumor formation [220-222]. In order to prove definitively that *CALB2b* is an NMD target, one would need to silence the key factor of the NMD pathway (Ufp1, Ufp2, and Ufp3) and measure if the portion of *CALB2b* increases. Interestingly, calretinin alternative transcripts are neither found in mouse nor in rat tissue and we are not aware of their presence in neuronal human cells, which implies the possibility that they are cancer-specific transcripts. Furthermore, we never detected the 22kDa calretinin isoform at the protein level, even though the antibody that we utilized was produced using the first 119aa of human calretinin, covering

both the canonical and 22kDa sequences. Therefore, based on our experimental findings we postulate that alternative calretinin transcripts may have a role in creating a ceRNA network in order to protect protein-coding calretinin transcripts in mesothelioma. Further experiments of silencing alternative calretinin transcripts would further support the ceRNA hypothesis.

One consideration based on our studies on the promoter and 3'UTR is to mimic calretinin expression more closely to the *in vivo* situation, by adding calretinin 3'UTR downstream of the luciferase gene in pGL3-*CALB2*(-161bp/+80bp). If we would observe a weaker correlation between firefly luciferase signals and calretinin mRNA relative abundance compared to the previous correlation with pGL3-*CALB2*(-161bp/+80bp), this would further support that the post-transcriptional regulation significantly contributes to the regulation of calretinin expression.

As mentioned at the beginning of the discussion, based on the assumption that the epithelial mesothelioma histotype indeed progresses toward the sarcomatoid one, calretinin expression decreases during the transition of the epithelioid towards a sarcomatoid histotype MPM [223]. Transition of the epithelioid towards the sarcomatoid histotype would be an example of the *in vivo* tumor epithelial-mesenchymal transition (EMT) [224, 225], although in the case of the mesothelium this would mostly correspond to shifting the balance in one direction, since mesothelium expresses both, epithelial and mesenchymal markers (cytokeratins and vimentin, respectively). An inducer of "surrogate EMT" in mesothelioma is unknown. EMT is a reversible process, in which alteration of gene expression programs is mainly mediated by epigenetic regulatory mechanisms such as DNA methylation and histones N-tail acetylation/methylation [226]. Based on this, we investigated if calretinin promoter methylation is responsible for the decrease of calretinin expression seen in sarcomatoid mesothelioma. Treatment with the hypomethylating agent 5-aza-2'-deoxycytidine did not upregulate calretinin expression in SPC111 cells (sarcomatoid type) indicating that an increase in DNA methylation is not responsible for calretinin downregulation. Further evidence came from analyzing the TCGA database, in which we observed no difference in methylation status of *CALB2* promoter between the epithelioid and the biphasic MPM. However, it remains to be determined whether histone modification of *CALB2* promoter affects calretinin expression. In the UCSC Genome Browser, we found H3K4Me1 and H3K4me3 marks within *CALB2* promoter (spanning 1kb upstream and 2kb downstream of TSS), indicating the presence of active regulatory elements and promoter, and these marks could undergo modifications that would affect calretinin expression.

In general, TGF-β is a well-known inducer of EMT process. Nevertheless, a hint of a differential effect of TGF-β in sarcomatoid histotype is suggested by the expression of connective tissue growth factor (CTGF) [97, 227]. CTGF is a target of Yes-associated protein (YAP), which is downstream of the dysregulated Hippo pathway often observed in mesothelioma. A strong association between CTGF expression and stroma amount was observed in sarcomatoid mesothelioma. Therefore, one could postulate that continuous TGF-β signaling along with dysregulated *Hippo* pathway might trigger continuous production of extracellular matrix (ECM) components, and stroma buildup in turn creates increased local tissue stiffness [226]. Tissue stiffness is sensed by cells, and affects their activity, motility and differentiation [228]. Tissue matrix stiffness has a very strong effect on the cell lineage specification of naive human mesenchymal stem cell (hMSC) towards osteoblast, myoblast and neurons e.g. the stiffest matrices induced osteoblast formation [229]. In this context, mesothelial cells are peculiar, since similarly to the hMSC, they possess inherited plasticity to differentiate into myofibroblast under certain pathological conditions [230] or into a osteoblast phenotype *in vitro* [76]. Interestingly, mesothelioma sarcomatoid tissues have been reported to contain parts of bone formation, which is suggested to be evidence of the potential for mesothelioma cells to osseously differentiate [77]. It is possible that during mesotheliomagenesis, the ECM undergoes alterations that result in stronger tumor tissue stiffness. Stronger tumor stiffness creates a tumor microenvironment in which mesothelioma cells might undergo osteogenic lineage commitment. Therefore, calretinin downregulation could be the result of mesothelioma cells undergoing osteogenic lineage commitment induced by tumor tissue stiffness.

In conclusion, our data indicate that the calretinin protein level is regulated through both transcriptional (driving) and post-transcriptional (fine-tuning) mechanisms on calretinin mRNA (Figure 13). Using a promoter reporter assay we showed a strong, positive correlation between the minimal *CALB2* -161/+80bp promoter and the endogenous *CALB2* mRNA level, and we identified NRF-1 and E2F2 as two transcription factors driving this expression. Identification of E2F2 led us to further observe that calretinin expression is cell cycle driven with the highest expression in the G1/S transition cell phase. The reporter promoter assay has limitations and can fail to detect epigenetic mechanisms of regulating gene expression. However, DNA hypomethylating treatment demonstrated that calretinin expression is not driven by the change in the promoter DNA methylation status (chapter 4.1). It would be of interest to generate mesothelial cells stably expressing pGL3-*CALB2*-161/+80bp promoter reporter and expose them to the conditions known to increase calretinin levels. Comparison

between variation of the reporter activity and levels of calretinin could serve as a tool to monitor *in vitro* reactivity of mesothelium to novel nanomaterials. If this would prove informative, it would then be possible to generate transgenic mouse models for *in vivo* nanomaterial testing by targeting p*CALB2*(-161/+80)-reporter (luciferase) to mesothelial specific expression using *Cre* expression driven by WT1 promoter/enhancer - $Wt1^{CreERT2/+}$[231, 232].

Demonstrating that the promoter drives calretinin expression does not exclude yet other levels of regulation at mRNA – post-transcriptional regulation (chapter 4.2.). In the second part of the project, utilizing again a reporter assay we showed that the calretinin 3'UTR has a downregulatory effect, which is abolished upon sequence mutation of two mir-30-binding sites. We further demonstrated that calretinin expression is directly downregulated with miR-30e-5p mimic treatment. Interestingly, we observed that constant overexpression of *CALB2* 3'UTR prevented the effect of miR-30e-5p on calretinin expression in ONE58 cells, suggesting that in mesothelioma cells alternatively spliced calretinin transcripts might compete for the trans-regulatory factors such as miRNA or AUBP. The *CALB2* 3'UTR also contains a functional ARE motif and the identification of the AUBP that binds this ARE motif is the focus of our future investigations. These multiple levels of regulation are in line with the view that the genes demonstrating stronger positive mRNA-protein correlation are preferentially regulated by multiple levels of regulation that work together in order to prepare a cell to effectively act upon encountered conditions [233]. Since we observed a strong positive correlation between calretinin protein and mRNA levels, it is of no wonder that we found both levels controlling calretinin protein levels. If we consider that a significant proportion of calretinin primary transcripts is alternatively spliced and thus not translated into protein, the full isoform transcript needs to be post-transcriptionally regulated (e.g. to be stabilized through AUBP or alternative transcripts might also bind AUBP) in order that the final protein levels follow promoter activity and mRNA initially transcribed levels.

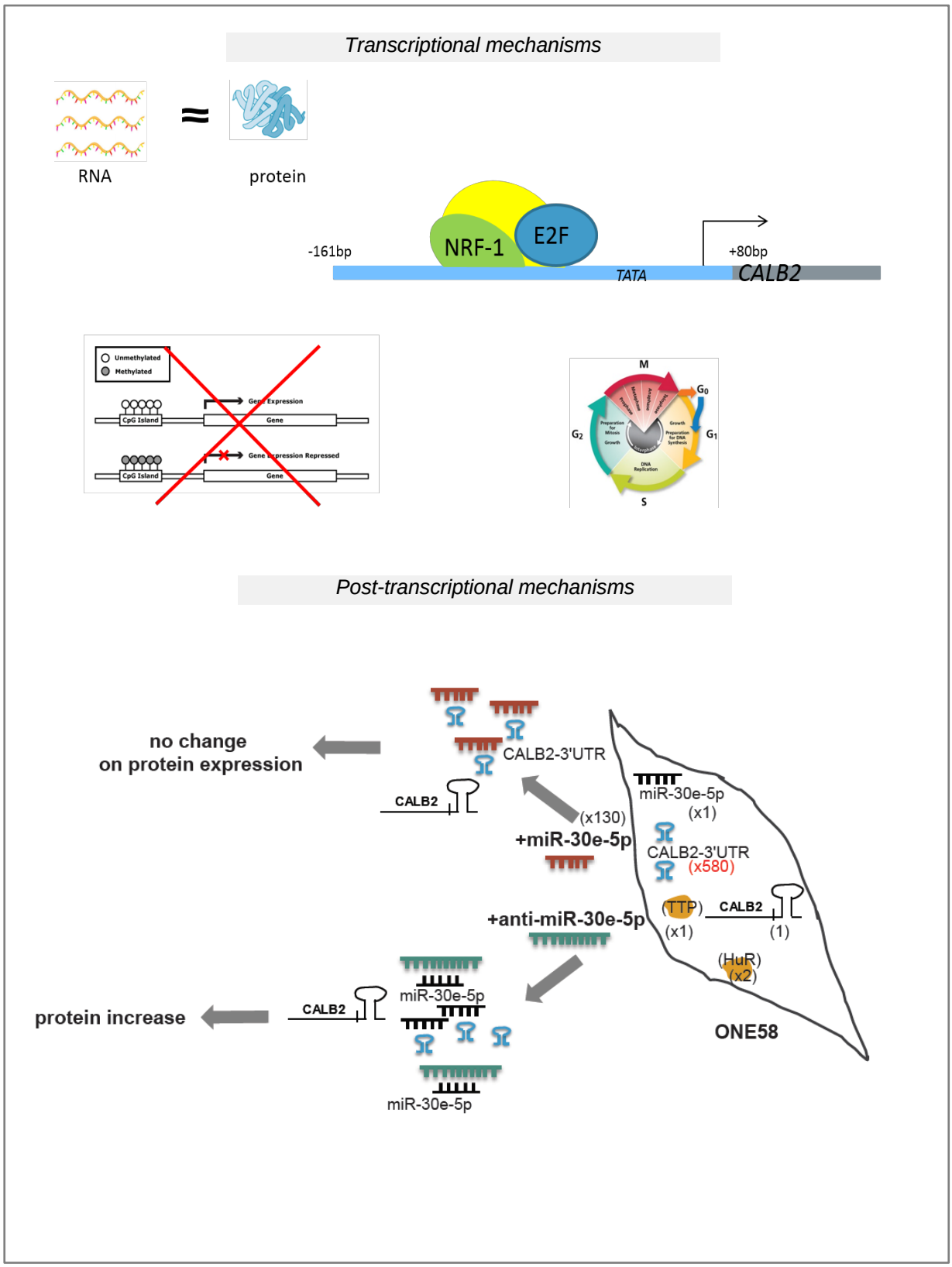

Figure 13. Calretinin expression is mainly driven at the transcriptional level and is fine-tuned at the post-transcriptional level.

6. REFERENCES

1. Schaffner, W., *Enhancers, enhancers - from their discovery to today's universe of transcription enhancers.* Biol Chem, 2015. **396**(4): p. 311-27.
2. Milano, M.T. and H. Zhang, *Malignant pleural mesothelioma: a population-based study of survival.* J Thorac Oncol, 2010. **5**(11): p. 1841-8.
3. van Zandwijk, N., et al., *Guidelines for the diagnosis and treatment of malignant pleural mesothelioma.* J Thorac Dis, 2013. **5**(6): p. E254-307.
4. Faig, J., et al., *Changing pattern in malignant mesothelioma survival.* Transl Oncol, 2015. **8**(1): p. 35-9.
5. Altomare, D.A., et al., *A mouse model recapitulating molecular features of human mesothelioma.* Cancer Res, 2005. **65**(18): p. 8090-5.
6. *IARC Monographs on the Evaluation of Carcinogenic Risks to Humans*. Vol. 100 (C). 2012, Lyons, France: International Agency for Research on Cancer
7. Hendry, N.W., *The geology, occurrences, and major uses of abestos.* Ann N Y Acad Sci, 1965. **132**(1): p. 12-22.
8. *Committee on Biological Effects of Atmospheric Pollutants. Asbestos: The Need for and Feasibility of Air Pollution Controls* 1971, National Academy of Science: Washington, D.C.
9. Skinner HCW, R.M., Frondel C., *Asbestos and other fibrous materials: mineralogy, crystal chemistry and health effects.* . 1988, New York: Oxford University Press.
10. National Toxicology, P., *NTP 12th Report on Carcinogens.* Rep Carcinog, 2011. **12**: p. iii-499.
11. NTP, *13th Report on Carcinogens.* Research Triangle Park, NC: U.S. Department of Health and Human Services, Public Health Service, 2014.
12. 10. June 2016]; Available from: http://www.umt.edu/bioethics/libbyhealth/introduction/background/asbestos_timeline.aspx.
13. Cooke, W.E., *Fibrosis of the Lungs Due to the Inhalation of Asbestos Dust.* Br Med J, 1924. **2**(3317): p. 147-140 2.
14. RA, W., *Pathology of Tumours*. 1967, London: Butterworths.
15. Wagner, J.C., C.A. Sleggs, and P. Marchand, *Diffuse pleural mesothelioma and asbestos exposure in the North Western Cape Province.* Br J Ind Med, 1960. **17**: p. 260-71.

16. Roe, O.D. and G.M. Stella, *Malignant pleural mesothelioma: history, controversy and future of a manmade epidemic.* Eur Respir Rev, 2015. **24**(135): p. 115-31.
17. R.L., V., *Worldwide asbestos supply and consumption trends from 1900 through 2003. U.S. Geological Survey; 2006. Circular 1298*. 2006. p. 80.
18. Corn, J.K., *Environmental Public Health Policy for Asbestos on Schools: Unintended Consequences* 1999: CRC Press
19. Robinson, B.M., *Malignant pleural mesothelioma: an epidemiological perspective.* Ann Cardiothorac Surg, 2012. **1**(4): p. 491-6.
20. Park, E.K., et al., *Global magnitude of reported and unreported mesothelioma.* Environ Health Perspect, 2011. **119**(4): p. 514-8.
21. Prazakova, S., et al., *Asbestos and the lung in the 21st century: an update.* Clin Respir J, 2014. **8**(1): p. 1-10.
22. Pan, X.L., et al., *Residential proximity to naturally occurring asbestos and mesothelioma risk in California.* Am J Respir Crit Care Med, 2005. **172**(8): p. 1019-25.
23. Baris, I., et al., *Epidemiological and environmental evidence of the health effects of exposure to erionite fibres: a four-year study in the Cappadocian region of Turkey.* Int J Cancer, 1987. **39**(1): p. 10-7.
24. Baris, Y.I., et al., *An outbreak of pleural mesothelioma and chronic fibrosing pleurisy in the village of Karain/Urgup in Anatolia.* Thorax, 1978. **33**(2): p. 181-92.
25. Baumann, F., et al., *The Presence of Asbestos in the Natural Environment is Likely Related to Mesothelioma in Young Individuals and Women from Southern Nevada.* J Thorac Oncol, 2015. **10**(5): p. 731-7.
26. Goodman, J.E., M.A. Nascarella, and P.A. Valberg, *Ionizing radiation: a risk factor for mesothelioma.* Cancer Causes Control, 2009. **20**(8): p. 1237-54.
27. Farioli, A., et al., *Risk of mesothelioma following external beam radiotherapy for prostate cancer: a cohort analysis of SEER database.* Cancer Causes Control, 2013. **24**(8): p. 1535-45.
28. Armstrong, B.K., et al., *Mortality in miners and millers of crocidolite in Western Australia.* Br J Ind Med, 1988. **45**(1): p. 5-13.
29. Available from: http://www.swissinfo.ch/eng/development-of-exposure-to-asbestos-fibres-per-capita-and-predicted-cases-of-mesothelioma/32049564.
30. Marinaccio, A., et al., *Analysis of latency time and its determinants in asbestos related malignant mesothelioma cases of the Italian register.* Eur J Cancer, 2007. **43**(18): p. 2722-8.

31. Haber, S.E. and J.M. Haber, *Malignant mesothelioma: a clinical study of 238 cases.* Ind Health, 2011. **49**(2): p. 166-72.
32. Bloom, W. and D. Fawcett, *A textbook of histology*. 10th ed. 1975: Philadelphia, Saunders.
33. CS, M., *The mesoderm and the coelom of vertebrates.* The American Naturalist, 1890. **24**(877-898).
34. Opitz, I., *Management of malignant pleural mesothelioma-The European experience.* J Thorac Dis, 2014. **6 Suppl 2**: p. S238-52.
35. Valle, M.T., et al., *Antigen-presenting function of human peritoneum mesothelial cells.* Clin Exp Immunol, 1995. **101**(1): p. 172-6.
36. Hausmann, M.J., et al., *Accessory role of human peritoneal mesothelial cells in antigen presentation and T-cell growth.* Kidney Int, 2000. **57**(2): p. 476-86.
37. Mutsaers, S.E., *The mesothelial cell.* Int J Biochem Cell Biol, 2004. **36**(1): p. 9-16.
38. Kumar, A., et al., *Expression and assembly of procoagulant complexes by human pleural mesothelial cells.* Thromb Haemost, 1994. **71**(5): p. 587-92.
39. Idell, S., et al., *Pathways of fibrin turnover of human pleural mesothelial cells in vitro.* Am J Respir Cell Mol Biol, 1992. **7**(4): p. 414-26.
40. Mutsaers, S.E., et al., *Mesothelial cells in tissue repair and fibrosis.* Front Pharmacol, 2015. **6**: p. 113.
41. LaRocca, P.J. and J.G. Rheinwald, *Coexpression of simple epithelial keratins and vimentin by human mesothelium and mesothelioma in vivo and in culture.* Cancer Res, 1984. **44**(7): p. 2991-9.
42. Pelin, K., A. Hirvonen, and K. Linnainmaa, *Expression of cell adhesion molecules and connexins in gap junctional intercellular communication deficient human mesothelioma tumour cell lines and communication competent primary mesothelial cells.* Carcinogenesis, 1994. **15**(11): p. 2673-5.
43. Kluge, T. and T. Hovig, *The ultrastructure of human and rat pericardium. II. Intercellular spaces and junctions.* Acta Pathol Microbiol Scand, 1967. **71**(4): p. 547-63.
44. Mutsaers, S.E., *Mesothelial cells: their structure, function and role in serosal repair.* Respirology, 2002. **7**(3): p. 171-91.
45. Li, J., *Ultrastructural study on the pleural stomata in human.* Funct Dev Morphol, 1993. **3**(4): p. 277-80.
46. Yalcin, N.G., C.K. Choong, and N. Eizenberg, *Anatomy and pathophysiology of the pleura and pleural space.* Thorac Surg Clin, 2013. **23**(1): p. 1-10, v.

47. AE., H., *The Peritoneum.* 1919, St. Louis: CV Mosby;.
48. Hubbard, T.B., Jr., et al., *The pathology of peritoneal repair: its relation to the formation of adhesions.* Ann Surg, 1967. **165**(6): p. 908-16.
49. Teranishi, S., M. Sakaguchi, and H. Itaya, *Mesothelial regeneration in the rat and effect of urokinase.* Nihon Geka Hokan, 1977. **46**(4): p. 361-79.
50. Raftery, A.T., *Regeneration of parietal and visceral peritoneum: an electron microscopical study.* J Anat, 1973. **115**(Pt 3): p. 375-92.
51. Raftery, A.T., *Regeneration of parietal and visceral peritoneum. A light microscopical study.* Br J Surg, 1973. **60**(4): p. 293-9.
52. Mutsaers, S.E., et al., *The origin of regenerating mesothelium: a historical perspective.* Int J Artif Organs, 2007. **30**(6): p. 484-94.
53. Ivanova, V.F. and A.A. Puzyrev, *[Autoradiographic study of mesothelial proliferation in white mice under experimental conditions].* Arkh Anat Gistol Embriol, 1977. **72**(2): p. 10-7.
54. Mutsaers, S.E., D. Whitaker, and J.M. Papadimitriou, *Stimulation of mesothelial cell proliferation by exudate macrophages enhances serosal wound healing in a murine model.* Am J Pathol, 2002. **160**(2): p. 681-92.
55. Whitaker, D. and J. Papadimitriou, *Mesothelial healing: morphological and kinetic investigations.* J Pathol, 1985. **145**(2): p. 159-75.
56. Mutsaers, S.E., D. Whitaker, and J.M. Papadimitriou, *Mesothelial regeneration is not dependent on subserosal cells.* J Pathol, 2000. **190**(1): p. 86-92.
57. Foley-Comer, A.J., et al., *Evidence for incorporation of free-floating mesothelial cells as a mechanism of serosal healing.* J Cell Sci, 2002. **115**(Pt 7): p. 1383-9.
58. S.N.;, C.G.R.H.S.M.D., *Repair of Glisson's capsule after tangential wounds of the liver.* Journal of Pathology Bacteriology, 1957. **73**: p. 1-10.
59. Cleaver C.L.; Hopkins A.D., N.N.K.K.C.R.A., *The effect of postoperative peritoneal lavage on survival, peritoneal wound healing and adhesion formation following fecal peritonitis: An experimental study in the rat. .* British Journal of Surgery, 1974(61): p. 601-604.
60. Wagner, J.C., et al., *Histology and ultrastructure of serially transplanted rat mesotheliomas.* Br J Cancer, 1982. **46**(2): p. 294-9.
61. Herrick, S.E. and S.E. Mutsaers, *Mesothelial progenitor cells and their potential in tissue engineering.* Int J Biochem Cell Biol, 2004. **36**(4): p. 621-42.

62. Perez-Pomares, J.M., et al., *Contribution of mesothelium-derived cells to liver sinusoids in avian embryos.* Dev Dyn, 2004. **229**(3): p. 465-74.
63. Perez-Pomares, J.M., et al., *Origin of coronary endothelial cells from epicardial mesothelium in avian embryos.* Int J Dev Biol, 2002. **46**(8): p. 1005-13.
64. Munoz-Chapuli, R., et al., *Differentiation of hemangioblasts from embryonic mesothelial cells? A model on the origin of the vertebrate cardiovascular system.* Differentiation, 1999. **64**(3): p. 133-41.
65. Chau, Y.Y., et al., *Visceral and subcutaneous fat have different origins and evidence supports a mesothelial source.* Nat Cell Biol, 2014. **16**(4): p. 367-75.
66. Asahina, K., et al., *Septum transversum-derived mesothelium gives rise to hepatic stellate cells and perivascular mesenchymal cells in developing mouse liver.* Hepatology, 2011. **53**(3): p. 983-95.
67. Que, J., et al., *Mesothelium contributes to vascular smooth muscle and mesenchyme during lung development.* Proc Natl Acad Sci U S A, 2008. **105**(43): p. 16626-30.
68. Wilm, B., et al., *The serosal mesothelium is a major source of smooth muscle cells of the gut vasculature.* Development, 2005. **132**(23): p. 5317-28.
69. Yang, A.H., J.Y. Chen, and J.K. Lin, *Myofibroblastic conversion of mesothelial cells.* Kidney Int, 2003. **63**(4): p. 1530-9.
70. Lachaud, C.C., et al., *Functional vascular smooth muscle-like cells derived from adult mouse uterine mesothelial cells.* PLoS One, 2013. **8**(2): p. e55181.
71. Rinkevich, Y., et al., *Identification and prospective isolation of a mesothelial precursor lineage giving rise to smooth muscle cells and fibroblasts for mammalian internal organs, and their vasculature.* Nat Cell Biol, 2012. **14**(12): p. 1251-60.
72. Klebe, S., et al., *Malignant mesothelioma with heterologous elements: clinicopathological correlation of 27 cases and literature review.* Mod Pathol, 2008. **21**(9): p. 1084-94.
73. Yousem, S.A. and L. Hochholzer, *Malignant mesotheliomas with osseous and cartilaginous differentiation.* Arch Pathol Lab Med, 1987. **111**(1): p. 62-6.
74. Rittinghausen, S., et al., *Atypical malignant mesotheliomas with osseous and cartilaginous differentiation after intraperitoneal injection of various types of mineral fibres in rats.* Exp Toxicol Pathol, 1992. **44**(1): p. 55-8.

75. Kiyozuka, Y., et al., *An autopsy case of malignant mesothelioma with osseous and cartilaginous differentiation: bone morphogenetic protein-2 in mesothelial cells and its tumor.* Dig Dis Sci, 1999. **44**(8): p. 1626-31.
76. Lansley, S.M., et al., *Mesothelial Cell Differention into Osteoblast- and Adipocyte-Like Cells.* J Cell Mol Med, 2010. **15**: p. 2095-105.
77. Lansley, S.M., et al., *A Subset of Malignant Mesothelioma Tumors Retain Osteogenic Potential.* Sci Rep, 2016. **6**: p. 36349.
78. Sebastien, P., et al., *Asbestos retention in human respiratory tissues: comparative measurements in lung parenchyma and in parietal pleura.* IARC Sci Publ, 1980(30): p. 237-46.
79. Stanton, M.F., et al., *Relation of particle dimension to carcinogenicity in amphibole asbestoses and other fibrous minerals.* J Natl Cancer Inst, 1981. **67**(5): p. 965-75.
80. Choe, N., et al., *Pleural macrophage recruitment and activation in asbestos-induced pleural injury.* Environ Health Perspect, 1997. **105 Suppl 5**: p. 1257-60.
81. Beachy, P.A., S.S. Karhadkar, and D.M. Berman, *Tissue repair and stem cell renewal in carcinogenesis.* Nature, 2004. **432**(7015): p. 324-31.
82. Ault, J.G., et al., *Behavior of crocidolite asbestos during mitosis in living vertebrate lung epithelial cells.* Cancer Res, 1995. **55**(4): p. 792-8.
83. Benedetti, S., et al., *Reactive oxygen species a double-edged sword for mesothelioma.* Oncotarget, 2015. **6**(19): p. 16848-65.
84. Bueno, R., et al., *Comprehensive genomic analysis of malignant pleural mesothelioma identifies recurrent mutations, gene fusions and splicing alterations.* Nat Genet, 2016. **48**(4): p. 407-16.
85. Murthy, S.S. and J.R. Testa, *Asbestos, chromosomal deletions, and tumor suppressor gene alterations in human malignant mesothelioma.* J Cell Physiol, 1999. **180**(2): p. 150-7.
86. Bjorkqvist, A.M., et al., *Recurrent DNA copy number changes in 1q, 4q, 6q, 9p, 13q, 14q and 22q detected by comparative genomic hybridization in malignant mesothelioma.* Br J Cancer, 1997. **75**(4): p. 523-7.
87. Forbes, S.A., et al., *COSMIC: mining complete cancer genomes in the Catalogue of Somatic Mutations in Cancer.* Nucleic Acids Res, 2011. **39**(Database issue): p. D945-50.
88. Felley-Bosco, E. and R. Stahel, *Hippo/YAP pathway for targeted therapy.* Translational Lung cancer Research
2014. **3**: p. 75-83.

89. Cheng, J.Q., et al., *p16 alterations and deletion mapping of 9p21-p22 in malignant mesothelioma.* Cancer Res, 1994. **54**(21): p. 5547-51.
90. Xio, S., et al., *Codeletion of p15 and p16 in primary malignant mesothelioma.* Oncogene, 1995. **11**(3): p. 511-5.
91. Prins, J.B., et al., *The gene for the cyclin-dependent-kinase-4 inhibitor, CDKN2A, is preferentially deleted in malignant mesothelioma.* Int J Cancer, 1998. **75**(4): p. 649-53.
92. Toyooka, S., et al., *Aberrant methylation and simian virus 40 tag sequences in malignant mesothelioma.* Cancer Res, 2001. **61**(15): p. 5727-30.
93. Wong, L., et al., *Inactivation of p16INK4a expression in malignant mesothelioma by methylation.* Lung Cancer, 2002. **38**(2): p. 131-6.
94. Badouel, C., A. Garg, and H. McNeill, *Herding Hippos: regulating growth in flies and man.* Curr Opin Cell Biol, 2009. **21**(6): p. 837-43.
95. Bianchi, A.B., et al., *High frequency of inactivating mutations in the neurofibromatosis type 2 gene (NF2) in primary malignant mesotheliomas.* Proc Natl Acad Sci U S A, 1995. **92**(24): p. 10854-8.
96. Zhao, B., et al., *Inactivation of YAP oncoprotein by the Hippo pathway is involved in cell contact inhibition and tissue growth control.* Genes Dev, 2007. **21**(21): p. 2747-61.
97. Murakami, H., et al., *LATS2 Is a Tumor Suppressor Gene of Malignant Mesothelioma.* Cancer Res, 2011. **71**(3): p. 873-83.
98. Sekido, Y., *Inactivation of Merlin in malignant mesothelioma cells and the Hippo signaling cascade dysregulation.* Pathol Int, 2011. **61**(6): p. 331-44.
99. Bott, M., et al., *The nuclear deubiquitinase BAP1 is commonly inactivated by somatic mutations and 3p21.1 losses in malignant pleural mesothelioma.* Nat Genet, 2011. **43**(7): p. 668-72.
100. Yoshikawa, Y., et al., *Frequent inactivation of the BAP1 gene in epithelioid-type malignant mesothelioma.* Cancer Sci, 2012. **103**(5): p. 868-74.
101. Kadariya, Y., et al., *Bap1 Is a Bona Fide Tumor Suppressor: Genetic Evidence from Mouse Models Carrying Heterozygous Germline Bap1 Mutations.* Cancer Res, 2016. **76**(9): p. 2836-44.
102. Ventii, K.H., et al., *BRCA1-associated protein-1 is a tumor suppressor that requires deubiquitinating activity and nuclear localization.* Cancer Res, 2008. **68**(17): p. 6953-62.
103. Testa, J.R., et al., *Germline BAP1 mutations predispose to malignant mesothelioma.* Nat Genet, 2011. **43**: p. 1022-5.

104. Baumann, F., et al., *Mesothelioma patients with germline BAP1 mutations have 7-fold improved long-term survival.* Carcinogenesis, 2015. **36**(1): p. 76-81.
105. Fleury-Feith, J., et al., *Hemizygosity of Nf2 is associated with increased susceptibility to asbestos-induced peritoneal tumours.* Oncogene, 2003. **22**(24): p. 3799-805.
106. Xu, J., et al., *Germline mutation of Bap1 accelerates development of asbestos-induced malignant mesothelioma.* Cancer Res, 2014. **74**(16): p. 4388-97.
107. Napolitano, A., et al., *Minimal asbestos exposure in germline BAP1 heterozygous mice is associated with deregulated inflammatory response and increased risk of mesothelioma.* Oncogene, 2015.
108. Jongsma, J., et al., *A conditional mouse model for malignant mesothelioma.* Cancer Cell, 2008. **13**(3): p. 261-71.
109. Ordonez, N.G., *The diagnostic utility of immunohistochemistry in distinguishing between epithelioid mesotheliomas and squamous carcinomas of the lung: a comparative study.* Mod Pathol, 2006. **19**(3): p. 417-28.
110. D., T.W., et al., *Histological Typing of Lung and Pleural Tumours* 3rd ed. 1999: World Health Organization
111. Flores, R.M., et al., *Prognostic factors in the treatment of malignant pleural mesothelioma at a large tertiary referral center.* J Thorac Oncol, 2007. **2**(10): p. 957-65.
112. Borasio, P., et al., *Malignant pleural mesothelioma: clinicopathologic and survival characteristics in a consecutive series of 394 patients.* Eur J Cardiothorac Surg, 2008. **33**(2): p. 307-13.
113. Ceresoli, G.L., et al., *Therapeutic outcome according to histologic subtype in 121 patients with malignant pleural mesothelioma.* Lung Cancer, 2001. **34**(2): p. 279-87.
114. Ordóñez, N.G., *Value of calretinin immunostaining in diagnostic pathology: a review and update.* Appl Immunohistochem Mol Morphol, 2014. **22**(6): p. 401-15.
115. Kao, S.C., et al., *Low calretinin expression and high neutrophil-to-lymphocyte ratio are poor prognostic factors in patients with malignant mesothelioma undergoing extrapleural pneumonectomy.* J Thorac Oncol, 2011. **6**(11): p. 1923-9.
116. Otterstrom, C., et al., *CD74: a new prognostic factor for patients with malignant pleural mesothelioma.* Br J Cancer, 2014. **110**(8): p. 2040-6.
117. Linton, A., et al., *Factors associated with survival in a large series of patients with malignant pleural mesothelioma in New South Wales.* Br J Cancer, 2014. **111**(9): p. 1860-9.

118. Rogers, J.H., *Calretinin: a gene for a novel calcium-binding protein expressed principally in neurons.* J Cell Biol, 1987. **105**(3): p. 1343-53.
119. Camp, A.J. and R. Wijesinghe, *Calretinin: modulator of neuronal excitability.* Int J Biochem Cell Biol, 2009. **41**(11): p. 2118-21.
120. Reifegerste, R., et al., *An invertebrate calcium-binding protein of the calbindin subfamily: protein structure, genomic organization, and expression pattern of the calbindin-32 gene of Drosophila.* J Neurosci, 1993. **13**(5): p. 2186-98.
121. Schwaller, B., *The continuing disappearance of "pure" Ca2+ buffers.* Cell Mol Life Sci, 2009. **66**(2): p. 275-300.
122. Lewit-Bentley, A. and S. Rety, *EF-hand calcium-binding proteins.* Curr Opin Struct Biol, 2000. **10**(6): p. 637-43.
123. Schwaller, B., et al., *Comparison of the Ca^{2+}-binding properties of human recombinant calretinin-22k and calretinin.* J Biol Chem, 1997. **272**(47): p. 29663-29671.
124. Faas, G.C., et al., *Resolving the fast kinetics of cooperative binding: Ca2+ buffering by calretinin.* PLoS Biol, 2007. **5**(11): p. e311.
125. Palczewska, M., et al., *Structural and biochemical characterization of neuronal calretinin domain I-II (residues 1-100). Comparison to homologous calbindin D28k domain I-II (residues 1-93).* Eur J Biochem, 2001. **268**(23): p. 6229-37.
126. Schwaller, B., et al., *The calcium-binding protein calretinin-22k is detectable in the serum and specific cells of cancer patients.* Anticancer Res, 1998. **18**(5B): p. 3661-7.
127. Schwaller, B., M.R. Celio, and W. Hunziker, *Alternative splicing of calretinin mRNA leads to different forms of calretinin.* Eur J Biochem, 1995. **230**: p. 424-430.
128. Gander, J.-C., et al., *The calcium-binding protein calretinin-22k, an alternative splicing product of the calretinin gene is expressed in several colon adenocarcinoma cell lines.* Cell Calcium, 1996. **20**(1): p. 63-72.
129. Rogers, J., M. Khan, and J. Ellis, *Calretinin and other CaBPs in the nervous system.* Adv Exp Med Biol, 1990. **269**: p. 195-203.
130. Andressen, C., I. Blumcke, and M.R. Celio, *Calcium-binding proteins: selective markers of nerve cells.* Cell Tissue Res, 1993. **271**(2): p. 181-208.
131. Lugli, A., et al., *Calretinin expression in human normal and neoplastic tissues: a tissue microarray analysis on 5233 tissue samples.* Hum Pathol, 2003. **34**(10): p. 994-1000.
132. Doglioni, C., et al., *Calretinin: a novel immunocytochemical marker for mesothelioma.* Am J Surg Pathol, 1996. **20**(9): p. 1037-46.

133. Gotzos, V., P. Vogt, and M.R. Celio, *The calcium binding protein calretinin is a selective marker for malignant pleural mesotheliomas of the epithelial type.* Pathology Research and Practice, 1996. **192**(2): p. 137-147.
134. Shield, P.W. and K. Koivurinne, *The value of calretinin and cytokeratin 5/6 as markers for mesothelioma in cell block preparations of serous effusions.* Cytopathology, 2008. **19**(4): p. 218-23.
135. Dargan, S.L., B. Schwaller, and I. Parker, *Spatiotemporal patterning of IP3-mediated Ca2+ signals in Xenopus oocytes by Ca2+-binding proteins.* J Physiol, 2004. **556**(Pt 2): p. 447-61.
136. Schurmans, S., et al., *Impaired long-term potentiation induction in dentate gyrus of calretinin-deficient mice.* Proc Natl Acad Sci U S A, 1997. **94**(19): p. 10415-20.
137. Kuznicki, J., et al., *Localization of Ca(2+)-dependent conformational changes of calretinin by limited tryptic proteolysis.* Biochem J, 1995. **308 (Pt 2)**: p. 607-12.
138. Christel, C.J., et al., *Calretinin regulates Ca2+-dependent inactivation and facilitation of Cav2.1 Ca2+ channels through a direct interaction with the α12.1 subunit.* J Biol Chem, 2012. **287**(47): p. 39766-75.
139. Dong, G., et al., *Calretinin interacts with huntingtin and reduces mutant huntingtin-caused cytotoxicity.* J Neurochem, 2012. **123**(3): p. 437-46.
140. Blum, W. and B. Schwaller, *Calretinin is essential for mesothelioma cell growth/survival in vitro: a potential new target for malignant mesothelioma therapy?* Int J Cancer, 2013. **133**(9): p. 2077-88.
141. Blum, W., et al., *Overexpression or absence of calretinin in mouse primary mesothelial cells inversely affects proliferation and cell migration.* Respir Res, 2015. **16**: p. 153.
142. Alberts, B., et al., *Essential Cell Biology*. 4th ed. 2013. 864p.
143. Butler, J.E. and J.T. Kadonaga, *The RNA polymerase II core promoter: a key component in the regulation of gene expression.* Genes Dev, 2002. **16**(20): p. 2583-92.
144. Smale, S.T. and J.T. Kadonaga, *The RNA polymerase II core promoter.* Annu Rev Biochem, 2003. **72**: p. 449-79.
145. Thomas, M.C. and C.M. Chiang, *The general transcription machinery and general cofactors.* Crit Rev Biochem Mol Biol, 2006. **41**(3): p. 105-78.
146. Danino, Y.M., et al., *The core promoter: At the heart of gene expression.* Biochim Biophys Acta, 2015. **1849**(8): p. 1116-31.

147. Latchman, D., *Transcriptional Gene Regulation in Eukaryotes.* eLS. John Wiley & Sons, Ltd: Chichester, 2011.
148. Deaton, A.M. and A. Bird, *CpG islands and the regulation of transcription.* Genes Dev, 2011. **25**(10): p. 1010-22.
149. Mattick, J.S., *RNA regulation: a new genetics?* Nat Rev Genet, 2004. **5**(4): p. 316-23.
150. Mayr, C., *Evolution and Biological Roles of Alternative 3'UTRs.* Trends Cell Biol, 2016. **26**(3): p. 227-37.
151. Barrett, L.W., S. Fletcher, and S.D. Wilton, *Regulation of eukaryotic gene expression by the untranslated gene regions and other non-coding elements.* Cell Mol Life Sci, 2012. **69**(21): p. 3613-34.
152. Berkovits, B.D. and C. Mayr, *Alternative 3' UTRs act as scaffolds to regulate membrane protein localization.* Nature, 2015. **522**(7556): p. 363-7.
153. An, J.J., et al., *Distinct role of long 3' UTR BDNF mRNA in spine morphology and synaptic plasticity in hippocampal neurons.* Cell, 2008. **134**(1): p. 175-87.
154. Beaudoing, E. and D. Gautheret, *Identification of alternate polyadenylation sites and analysis of their tissue distribution using EST data.* Genome Res, 2001. **11**(9): p. 1520-6.
155. Tian, B., et al., *A large-scale analysis of mRNA polyadenylation of human and mouse genes.* Nucleic Acids Res, 2005. **33**(1): p. 201-12.
156. Matoulkova, E., et al., *The role of the 3' untranslated region in post-transcriptional regulation of protein expression in mammalian cells.* RNA Biol, 2012. **9**(5): p. 563-76.
157. Tanguay, R.L. and D.R. Gallie, *Translational efficiency is regulated by the length of the 3' untranslated region.* Mol Cell Biol, 1996. **16**(1): p. 146-56.
158. Sandberg, R., et al., *Proliferating cells express mRNAs with shortened 3' untranslated regions and fewer microRNA target sites.* Science, 2008. **320**(5883): p. 1643-7.
159. Sarnowska, E., et al., *Hairpin structure within the 3'UTR of DNA polymerase beta mRNA acts as a post-transcriptional regulatory element and interacts with Hax-1.* Nucleic Acids Res, 2007. **35**(16): p. 5499-510.
160. Di Liegro, C.M., G. Schiera, and I. Di Liegro, *Regulation of mRNA transport, localization and translation in the nervous system of mammals (Review).* Int J Mol Med, 2014. **33**(4): p. 747-62.
161. Kedde, M., et al., *A Pumilio-induced RNA structure switch in p27-3' UTR controls miR-221 and miR-222 accessibility.* Nat Cell Biol, 2010. **12**(10): p. 1014-20.

162. Xie, X., et al., *Systematic discovery of regulatory motifs in human promoters and 3' UTRs by comparison of several mammals.* Nature, 2005. **434**(7031): p. 338-45.
163. Lee, R.C., R.L. Feinbaum, and V. Ambros, *The C. elegans heterochronic gene lin-4 encodes small RNAs with antisense complementarity to lin-14.* Cell, 1993. **75**(5): p. 843-54.
164. *miRBase*. [cited 2016 22.12.]; Available from: ftp://mirbase.org/pub/mirbase/CURRENT/README.
165. Olena, A.F. and J.G. Patton, *Genomic organization of microRNAs.* J Cell Physiol, 2010. **222**(3): p. 540-5.
166. Miska, E.A., et al., *Most Caenorhabditis elegans microRNAs are individually not essential for development or viability.* PLoS Genet, 2007. **3**(12): p. e215.
167. Kim, V.N., J. Han, and M.C. Siomi, *Biogenesis of small RNAs in animals.* Nat Rev Mol Cell Biol, 2009. **10**(2): p. 126-39.
168. Lee, Y., et al., *MicroRNA maturation: stepwise processing and subcellular localization.* EMBO J, 2002. **21**(17): p. 4663-70.
169. Bartel, D.P., *MicroRNAs: target recognition and regulatory functions.* Cell, 2009. **136**(2): p. 215-33.
170. Kwak, P.B., S. Iwasaki, and Y. Tomari, *The microRNA pathway and cancer.* Cancer Sci, 2010. **101**(11): p. 2309-15.
171. Bartel, D.P., *MicroRNAs: genomics, biogenesis, mechanism, and function.* Cell, 2004. **116**(2): p. 281-97.
172. Gu, S., et al., *Biological basis for restriction of microRNA targets to the 3' untranslated region in mammalian mRNAs.* Nat Struct Mol Biol, 2009. **16**(2): p. 144-50.
173. Landgraf, P., et al., *A mammalian microRNA expression atlas based on small RNA library sequencing.* Cell, 2007. **129**(7): p. 1401-14.
174. Lee, Y., et al., *MicroRNA genes are transcribed by RNA polymerase II.* EMBO J, 2004. **23**(20): p. 4051-60.
175. Borchert, G.M., W. Lanier, and B.L. Davidson, *RNA polymerase III transcribes human microRNAs.* Nat Struct Mol Biol, 2006. **13**(12): p. 1097-101.
176. Corcoran, D.L., et al., *Features of mammalian microRNA promoters emerge from polymerase II chromatin immunoprecipitation data.* PLoS One, 2009. **4**(4): p. e5279.
177. Ozsolak, F., et al., *Chromatin structure analyses identify miRNA promoters.* Genes Dev, 2008. **22**(22): p. 3172-83.
178. Ramalingam, P., et al., *Biogenesis of intronic miRNAs located in clusters by independent transcription and alternative splicing.* RNA, 2014. **20**(1): p. 76-87.

179. Calin, G.A. and C.M. Croce, *MicroRNA signatures in human cancers.* Nat Rev Cancer, 2006. **6**(11): p. 857-66.
180. Thomson, J.M., et al., *Extensive post-transcriptional regulation of microRNAs and its implications for cancer.* Genes Dev, 2006. **20**(16): p. 2202-7.
181. Melo, S.A., et al., *A genetic defect in exportin-5 traps precursor microRNAs in the nucleus of cancer cells.* Cancer Cell, 2010. **18**(4): p. 303-15.
182. Kumar, M.S., et al., *Impaired microRNA processing enhances cellular transformation and tumorigenesis.* Nat Genet, 2007. **39**(5): p. 673-7.
183. Kim, M.S., et al., *Somatic mutations and losses of expression of microRNA regulation-related genes AGO2 and TNRC6A in gastric and colorectal cancers.* J Pathol, 2010. **221**(2): p. 139-46.
184. Chang, T.C., et al., *Widespread microRNA repression by Myc contributes to tumorigenesis.* Nat Genet, 2008. **40**(1): p. 43-50.
185. Barreau, C., L. Paillard, and H.B. Osborne, *AU-rich elements and associated factors: are there unifying principles?* Nucleic Acids Res, 2005. **33**(22): p. 7138-50.
186. Elkon, R., A.P. Ugalde, and R. Agami, *Alternative cleavage and polyadenylation: extent, regulation and function.* Nat Rev Genet, 2013. **14**(7): p. 496-506.
187. Mignone, F., et al., *Untranslated regions of mRNAs.* Genome Biol, 2002. **3**(3): p. REVIEWS0004.
188. Wu, X. and G. Brewer, *The regulation of mRNA stability in mammalian cells: 2.0.* Gene, 2012. **500**(1): p. 10-21.
189. Reznik, B. and J. Lykke-Andersen, *Regulated and quality-control mRNA turnover pathways in eukaryotes.* Biochem Soc Trans, 2010. **38**(6): p. 1506-10.
190. Giusti, L., et al., *Comparative proteomic analysis of malignant pleural mesothelioma evidences an altered expression of nuclear lamin and filament-related proteins.* Proteomics Clin Appl, 2014. **8**(3-4): p. 258-68.
191. Klebe, S., et al., *Sarcomatoid mesothelioma: a clinical-pathologic correlation of 326 cases.* Mod Pathol, 2010. **23**(3): p. 470-9.
192. Chirieac, L.R., et al., *The immunohistochemical characterization of sarcomatoid malignant mesothelioma of the pleura.* Am J Cancer Res, 2011. **1**(1): p. 14-24.
193. Billing-Marczak, K., et al., *AP2-like cis element is required for calretinin gene promoter activity in cells of neuronal phenotype differentiated from multipotent human cell line DEV.* Biochim Biophys Acta, 2002. **1577**(3): p. 412-20.

194. Billing-Marczak, K., et al., *Calretinin gene promoter activity is differently regulated in neurons and cancer cells. Role of AP2-like cis element and zinc ions.* Biochim Biophys Acta, 2004. **1678**(1): p. 14-21.
195. Andersson, U. and R.C. Scarpulla, *Pgc-1-related coactivator, a novel, serum-inducible coactivator of nuclear respiratory factor 1-dependent transcription in mammalian cells.* Mol Cell Biol, 2001. **21**(11): p. 3738-49.
196. Smith, K.T., R.D. Nicholls, and D. Reines, *The gene encoding the fragile X RNA-binding protein is controlled by nuclear respiratory factor 2 and the CREB family of transcription factors.* Nucleic Acids Res, 2006. **34**(4): p. 1205-15.
197. Cao, Z.Q. and X.L. Guo, *The role of galectin-4 in physiology and diseases.* Protein Cell, 2016. **7**(5): p. 314-24.
198. Thomson, D.W., et al., *On measuring miRNAs after transient transfection of mimics or antisense inhibitors.* PLoS One, 2013. **8**(1): p. e55214.
199. Sokilde, R., et al., *Passenger strand loading in overexpression experiments using microRNA mimics.* RNA Biol, 2015. **12**(8): p. 787-91.
200. Cheng, Y.Y., et al., *KCa1.1, a calcium-activated potassium channel subunit alpha 1, is targeted by miR-17-5p and modulates cell migration in malignant pleural mesothelioma.* Mol Cancer, 2016. **15**(1): p. 44.
201. Ma, W.J., et al., *Cloning and characterization of HuR, a ubiquitously expressed Elav-like protein.* J Biol Chem, 1996. **271**(14): p. 8144-51.
202. Wang, J., et al., *Multiple functions of the RNA-binding protein HuR in cancer progression, treatment responses and prognosis.* Int J Mol Sci, 2013. **14**(5): p. 10015-41.
203. Lopez de Silanes, I., et al., *Role of the RNA-binding protein HuR in colon carcinogenesis.* Oncogene, 2003. **22**(46): p. 7146-54.
204. Abdelmohsen, K., et al., *miR-519 suppresses tumor growth by reducing HuR levels.* Cell Cycle, 2010. **9**(7): p. 1354-9.
205. Meisner, N.C., et al., *Identification and mechanistic characterization of low-molecular-weight inhibitors for HuR.* Nat Chem Biol, 2007. **3**(8): p. 508-15.
206. Jimbo, M., et al., *Targeting the mRNA-binding protein HuR impairs malignant characteristics of pancreatic ductal adenocarcinoma cells.* Oncotarget, 2015. **6**(29): p. 27312-31.
207. *Correction: Delivery of Therapeutics Targeting the mRNA-Binding Protein HuR Using 3DNA Nanocarriers Suppresses Ovarian Tumor Growth.* Cancer Res, 2016. **76**(11): p. 3437.

208. Heinonen, M., et al., *Cytoplasmic HuR expression is a prognostic factor in invasive ductal breast carcinoma.* Cancer Res, 2005. **65**(6): p. 2157-61.
209. Erkinheimo, T.L., et al., *Cytoplasmic HuR expression correlates with poor outcome and with cyclooxygenase 2 expression in serous ovarian carcinoma.* Cancer Res, 2003. **63**(22): p. 7591-4.
210. Yoo, P.S., et al., *Tissue microarray analysis of 560 patients with colorectal adenocarcinoma: high expression of HuR predicts poor survival.* Ann Surg Oncol, 2009. **16**(1): p. 200-7.
211. Dixon, D.A., et al., *Altered expression of the mRNA stability factor HuR promotes cyclooxygenase-2 expression in colon cancer cells.* J Clin Invest, 2001. **108**(11): p. 1657-65.
212. Nabors, L.B., et al., *HuR, a RNA stability factor, is expressed in malignant brain tumors and binds to adenine- and uridine-rich elements within the 3' untranslated regions of cytokine and angiogenic factor mRNAs.* Cancer Res, 2001. **61**(5): p. 2154-61.
213. Stoppoloni, D., et al., *Expression of the embryonic lethal abnormal vision-like protein HuR in human mesothelioma: association with cyclooxygenase-2 and prognosis.* Cancer, 2008. **113**(10): p. 2761-9.
214. Sheng, H., et al., *Transforming growth factor-beta1 enhances Ha-ras-induced expression of cyclooxygenase-2 in intestinal epithelial cells via stabilization of mRNA.* J Biol Chem, 2000. **275**(9): p. 6628-35.
215. Srikantan, S. and M. Gorospe, *HuR function in disease.* Front Biosci (Landmark Ed), 2012. **17**: p. 189-205.
216. von Roretz, C., et al., *Turnover of AU-rich-containing mRNAs during stress: a matter of survival.* Wiley Interdiscip Rev RNA, 2011. **2**(3): p. 336-47.
217. Salmena, L., et al., *A ceRNA hypothesis: the Rosetta Stone of a hidden RNA language?* Cell, 2011. **146**(3): p. 353-8.
218. Poliseno, L., et al., *A coding-independent function of gene and pseudogene mRNAs regulates tumour biology.* Nature, 2010. **465**(7301): p. 1033-8.
219. Hug, N., D. Longman, and J.F. Caceres, *Mechanism and regulation of the nonsense-mediated decay pathway.* Nucleic Acids Res, 2016. **44**(4): p. 1483-95.
220. Mendell, J.T., et al., *Nonsense surveillance regulates expression of diverse classes of mammalian transcripts and mutes genomic noise.* Nat Genet, 2004. **36**(10): p. 1073-8.
221. Gardner, L.B., *Hypoxic inhibition of nonsense-mediated RNA decay regulates gene expression and the integrated stress response.* Mol Cell Biol, 2008. **28**(11): p. 3729-41.

222. Wang, D., et al., *Inhibition of nonsense-mediated RNA decay by the tumor microenvironment promotes tumorigenesis.* Mol Cell Biol, 2011. **31**(17): p. 3670-80.
223. Thies, S., et al., *Expression of the Stem Cell Factor Nestin in Malignant Pleural Mesothelioma Is Associated with Poor Prognosis.* PLoS One, 2015. **10**(9): p. e0139312.
224. Fassina, A., et al., *Epithelial-mesenchymal transition in malignant mesothelioma.* Mod Pathol, 2012. **25**(1): p. 86-99.
225. Schramm, A., et al., *Prognostic significance of epithelial-mesenchymal transition in malignant pleural mesothelioma.* Eur J Cardiothorac Surg, 2010. **37**(3): p. 566-72.
226. Li, L. and W. Li, *Epithelial-mesenchymal transition in human cancer: comprehensive reprogramming of metabolism, epigenetics, and differentiation.* Pharmacol Ther, 2015. **150**: p. 33-46.
227. Fujii, M., et al., *TGF-beta synergizes with defects in the Hippo pathway to stimulate human malignant mesothelioma growth.* J Exp Med, 2012. **209**(3): p. 479-94.
228. Handorf, A.M., et al., *Tissue stiffness dictates development, homeostasis, and disease progression.* Organogenesis, 2015. **11**(1): p. 1-15.
229. Engler, A.J., et al., *Matrix elasticity directs stem cell lineage specification.* Cell, 2006. **126**(4): p. 677-89.
230. Yanez-Mo, M., et al., *Peritoneal dialysis and epithelial-to-mesenchymal transition of mesothelial cells.* N Engl J Med, 2003. **348**(5): p. 403-13.
231. [cited 2017 February 10]; Available from: https://www.jax.org/strain/010912.
232. Firth, A. and J.X.J. Yuan, *Lung Stem Cells in the Epithelium and Vasculature*. Stem cell biology and regenerative medicine. 2015, Cham: Springer International Publishing. Online-Ressource.
233. Koussounadis, A., et al., *Relationship between differentially expressed mRNA and mRNA-protein correlations in a xenograft model system.* Sci Rep, 2015. **5**: p. 10775.

7. ACKNOWLEDGMENTS

This was an amazing experience, a tremendous journey, hard but joyful.

I am happy to take further challenges in research.

I would not be able to bring up this work without a number of people who supported me.

I would like to thank to Prof. Rolf Stahel and Prof. Walter Weder who gave me opportunity to be a part of their laboratory.

My special thanks to Dr. Emanuela Felley-Bosco, my supervisor, who carefully followed, guided my work and had an endless patience to answer all my questions and doubts. I am grateful that you invested your energy and time for taking care of my development. I am also thankful that you supported my participations in conferences as well as my wishes and plans. I am happy that I learned from such a hardworking, diligent, motivating and goal-focused supervisor, always carrying optimistic-driven spirit. I would like to thank you for all those moments that gave me wings when it was hard to stay up.

I would like to express my gratitude to Prof. Beat Schäfer who agreed to be my faculty supervisor, who closely followed my work, gave me the essential inputs and critically supported my work and my ambitions.

I am very grateful to Prof. Beat Schwaller who also followed the work and shared his vast scientific knowledge and experience that I was always carefully listening.

I thank to Prof. Lukas Sommer for accepting to be a member of my thesis committee and his useful suggestions for my project.

I thank also to Agata, Manuel, Nohemy and Gabriela for great time and support in the lab.

I would specially thank to Sonja Hemmi and Marina Tusup for an amazing friend support and understanding, thanks to whom I kept my childish (and creative!) part of my personality.

To my mom, dad and sister who mentally supported me with their wisdom throughout all those rough periods.

Finally, the big thanks to my husband Sasha, who supported me on this way and understood all those days when I said, “I will come home later, I need to finish-up”.

8. CURRICULUM VITAE

Name: Jelena Kresoja

Date of Birth: 26.10.1985

Nationality: Serbia

Email: jrakicmb@gmail.com

Education

2010-2012	Master of Science in Genetics, Faculty of Science, University of Zurich, Switzerland
2004-2009	Diploma in Molecular Biology Faculty of Science, University of Novi Sad, Serbia

Research experience

2013 – present	Laboratory of Molecular Oncology, Division of Thoracic Surgery University Hospital Zurich
2011 – 2012	Laboratory of Oncology, Children's Hospital Zurich, Zurich

Publications

Kresoja-Rakic J, Sulemani M, Kirschner MB, Ronner M, Reid G, Kao S, Schwaller B, Weder W, Stahel RA, Felley-Bosco E. Post-transcriptional regulation controls calretinin expression in malignant pleural mesothelioma. Submitted.

Kresoja-Rakic J, Kapaklikaya E, Ziltener G, Dalcher D, Santoro R, Christensen BC, Johnson K, Schwaller B, Weder W, Stahel R, Felley-Bosco E. Identification of cis- and trans-acting elements regulating calretinin expression in mesothelioma. Oncotarget 2016, 7(16), 21272-21286.

Renganathan A, **Kresoja-Rakic** J, Echeverry N, Ziltener G, Vrugt B, Opitz I, Stahel RA, Felley-Bosco E. GAS5 long non-coding RNA in malignant pleural mesothelioma. Molecular cancer 2014, 13(1): 119.

Wachtel M, **Rakic J**, Okoniewski M, Bode P, Niggli F, Schafer BW. FGFR4 signaling couples to Bim and not Bmf to discriminate subsets of alveolar rhabdomyosarcoma cells. International Journal of Cancer 2014, 135(7)**:** 1543-1552

Languages

English	C2 (Cambridge Certificate of Proficiency, London)
German	B2 (Telc exam, Zurich)
Serbian	mother tongue